2020

CHRONIC EXPOSURE TO OPIOIDS DOWN-REGULATES GENOMIC HISTONE MODIFICATIONS AND DISRUPTS STAT3 GENE EXPRESSION IN HUMAN INDUCED PLURIPOTENT STEM CELLS

Anirudh Jagannadh Chintalapati
Saint John's University, Jamaica New York

CHRONIC EXPOSURE TO OPIOIDS DOWN-REGULATES GENOMIC HISTONE MODIFICATIONS AND DISRUPTS *STAT3* GENE EXPRESSION IN HUMAN INDUCED PLURIPOTENT STEM CELLS

A dissertation submitted in partial fulfillment
of the requirements for the degree of

DOCTOR OF PHILOSOPHY

to the faculty of the

DEPARTMENT OF GRADUATE DIVISION

of

COLLEGE OF PHARMACY AND HEALTH SCIENCES

at

ST. JOHN'S UNIVERSITY

New York

by

Anirudh J. Chintalapati

Date Submitted: _____ Date Approved: _____

_____ _____

Anirudh J. Chintalapati Frank A. Barile, Ph.D.

ABSTRACT

CHRONIC EXPOSURE TO OPIOIDS DOWN-REGULATES GENOMIC HISTONE MODIFICATIONS AND DISRUPTS *STAT3* GENE EXPRESSION IN HUMAN INDUCED PLURIPOTENT STEM CELLS

Anirudh Jagannadh Chintalapati

Examining epigenetic (EG) manifestations and genomic heterogeneity is a novel perspective to understand opioid induced toxicity. Aberrations in histone protein post-translational modifications (HP-PTM) induce perturbations in chromatin integrity resulting in consequences for genomic expression patterns. In the current study, we hypothesize that chronic exposure to morphine sulfate (MS) alters histone-3-protein (H3)-PTM and disrupts *STAT3* gene expression in human induced pluripotent stem cells (iPSC). We analyzed 21 genomic H3-PTM following exposure to 1 and 10 μM MS for 2 and 5 days. The results showed decreases in levels of repressive H3-PTM, namely H3K9me1 (2 day) and H3K27me3 (5 day). To confirm if these changes were reversible, cells were allowed to recover for 3 days in the absence of MS; genomic levels of both H3K9me1 and H3K27me3 rebounded to control levels, suggesting that MS induced EG effects are reversible and not heritable. Additionally, decreases in levels of H3K9me1 and H3K27me3 were concentration dependent and were not antagonized by pre-exposure of iPSC to naltrexone indicating that EG effects are independent of opioid receptor antagonism. Continuous chronic MS exposure for through 10 passages rendered the levels of histone modifications to increase by day 26. In addition, exposure for 2 days resulted in significant up-regulation of *STAT3* gene expression which plunged with continuing MS exposure. This characteristic transcriptional up-regulation coupled with

translational downregulation of STAT3 demonstrates the ability of MS mediated gene expression disruption. Interestingly, STAT3 protein levels remained at control levels when iPSC were pretreated with naltrexone prior to MS exposure. Controlled regulation of STAT3 signaling pathway is pivotal in sustaining and propagating pluripotency phenotype in stem cells. Furthermore, the levels of phosphorylated STAT3 at residues – tyrosine705 (STAT3-pTyr-705) and –serine727 (STAT3-pSer-727) were down-regulated on day 5 and day 2, correspondingly, following MS exposure. Together, the results indicate that MS alters pre-programmed genomic H3-PTM and induces *STAT3* gene expression perturbations in iPSC.

DEDICATION

To my parents,

Prabhakara Raju and Visala Chintalapati,

for their infinite sacrifices, profound patience and unconditional love.

ACKNOWLEDGEMENTS

I would like to express my deepest gratitude to my mentor, Dr. Frank A. Barile for accepting me as his student, and for providing adequate resources, tremendous support and advice throughout my graduate research. For all the years as his student, he always encouraged me to think independently by applying scientific logic, and to pursue my research project without any objections. I'm very grateful for his knowledgeable teaching of scientific writing and analytical thinking skills that are my valuable assets for a lifetime. Undoubtedly, the guidance and invaluable lessons learnt from Dr. Barile as his student will forever serve as foundation stones to my future endeavors: I thank you for being a great and inspirational mentor.

I would like to thank Dr. Sandra E. Reznik to serve as Chair of my defense committee. I would also like to thank my thesis committee members, Dr. Blase C. Billack, Dr. Sue M. Ford, Dr. Jeanette C. Perron, and Dr. Francis A. Schanne. I am indebted to each of them for their insightful questions and suggestions at my thesis committee meetings.

I thank the Department of Pharmaceutical Sciences, St John's University for the academic and financial support throughout my graduate studies. I am thankful to the department Chair, Dr. Vijaya Korlipara and the Associate Dean, Dr. Marc E. Gillespie for their invaluable support in the completion of this work. I have to thank Dr. Felicia Carvalho, Joyce, Susana, and Velda for providing me the opportunity to instruct undergraduate students which was an incredible opportunity to learn and develop my teaching and mentoring skills. I thank Arlene and Mery for providing me administrative information and support vital to the completion of my degree. I am extremely thankful to all the members of "Barile-lab-family", both past and present in providing me with necessary knowledge to initiate and carryon my research in the lab.

A very special thank you to Dr. Angela Aliberti, for her immense support, constructive criticism, advice, and encouragement that constantly boosted my confidence to complete this project.

I thank my friends Igor, Silpa, and Trishaal for making my journey as a graduate student a wonderful experience with their cheerfulness, insight, and support.

I thank my father- and mother-in-law, Haranadha and Gayatri Vegesna, for their blessings, love, guidance, and constant encouragement to do best in all my accomplishments.

I thank my mom, dad, baby brother, and my uncle, Raj Shekar Varma; I owe them the completion of my degree with their encouragement, guidance, patience, inspiration, and endless love: Thank you for believing in me, I love you, and hope I make you proud.

Finally, I am especially indebted to my wife, Sindhura Chintalapati. I am very thankful and blessed to have her by my side at every instance. She sacrificed her life's comfort and shared the million ups and downs associated with my research work and patiently dealt with my idiosyncrasies: I love you and words are not enough to express my gratitude towards your unwavering support, kindness, and faith in me.

TABLE OF CONTENTS

LIST OF TABLES

LIST OF FIGURES

LIST OF ABBREVIATIONS

BCA	Bicinchoninic acid
d	Days
DAPI	4,6-diamidino-2-phenylindole
DMEM	Dulbecco's modified eagle medium
EG	Epigenetic
ELISA	Enzyme-linked immunosorbent assay
F12	Ham's F-12 medium
FC	Flow cytometry
h	Hours
H3	Histone-3-protein
H3K27me3	Trimethyl histone H3 lysine 27
H3K9me1	Monomethyl histone H3 lysine 9
HP-PTM	Histone protein post-translational modifications
iPSC	Induced pluripotent stem cells
K	Lysine
LDEV	Lactate dehydrogenase elevating virus
mES	Mouse embryonic stem cells
MS	Morphine Sulfate
N	Naltrexone
OCT4	Octamer-binding transcription factor 4
OPRD1	Opioid receptor delta 1
OPRK1	Opioid receptor kappa 1
OPRM1	Opioid receptor mu 1
OR	Opioid receptor
p-Ser-727	Phosphorylated serine 727
PTM	Post-translational modification
p-Tyr-705	Phosphorylated tyrosine 727
R	Recovery
ROCK	Rho kinase
SFCA	Surfactant free cellulose acetate
SSEA4	Stage-specific embryonic antigen-4
STAT3	Signal transducer and activator of transcription 3
THP	Total histone protein
TRA-1-60	T-cell receptor alpha locus

1. INTRODUCTION

1.1. Opioids, Opioid Abuse and Addiction, and Morphine Sulfate

1.1.1. Opioids

Opiates and Opioids are a class of chemically related compounds that elicit their effects by binding to endogenous opioid receptors on the cell membrane. Opiates are naturally produced opium alkaloids obtained from poppy plant, *Papaver somniferum*; these include morphine, codeine, narcotine, thebaine, papaverine and narceine. The opium latex is generally present in differential quantities throughout the plant, but, it is concentrated in the developing fruit, serving an evolutionary purpose of protecting seeds (Kreek, 1996). The term opioid in general encompass all semi-synthetic and fully synthetic opioid drugs such as fentanyl, oxycodone, hydrocodone etc. Endogenous opioids produced naturally in the body are classified into 3 families: β-endorphin, enkephelin, and dynorphin families, that regulate the pathways for autonomic control, pain sensitivity and modulation, reward, and stress responses in central and peripheral nervous system (Table 1) (Shenoy & Lui, 2019).

1.1.2. Opioid Abuse and Addiction

The advent of malicious opioid crisis inflicts a burden on mankind, often rendering clinicians an intractable challenge to mitigate the exponential spread of the opioid epidemic (Skolnick, 2018). Abuse and addiction to a prescription opioid pain reliever stems from its potential to cause immediate dependency upon short-term use and misuse. In addition, illicit and clandestine circulation of heroin, an illegal semi-synthetic prodrug of morphine, significantly synergizes the opioid crisis. The purest form of heroin typically sold in the

form of white or brown powder, can be snorted or smoked, thus eliminating the injection drug abuse stigma to new users. Prescription opioid use and heroin abuse are inextricably related; data pooled from 2002 to 2012 suggests the incidence of heroin abuse being 19 times higher in population with prior opioid pain reliever use (Powell *et al*., 2020). Furthermore, results from a study conducted among young, injection drug users during years 2008 and 2009 demonstrate that 86% of heroin abusers had a usage history of non-medical opioid pain relievers (Lankenau *et al*., 2012). The primary factors contributing to rapid spread of the opioid epidemic in the U.S. is increased and the ease in availability of prescription opioid and under the table heroin. The rate of opioid prescriptions dispensed from U.S. pharmacies have increased from 76 to 219 million prescriptions from 1991 to 2011 (Toth *et al*., 2016). The Mexican heroin production increased from an estimated 8 metric tons to 50 metric tons from 2005 to 2009. In order to address such progressive and swift spread of opioid epidemic and its associated detrimental consequences to human health, it is important to understand the sub-cellular perturbations induced following opioid administration.

1.1.3. Morphine

Archeological evidence demonstrates the cultivation of opium poppies during the Neolithic and Bronze eras for its medicinal and pleasuring properties; pointing its likely origination to northeastern part of the Mediterranean in Asia minor and Turkey. Evidence also indicates that opium was brought into India and China by Arab traders from which it travelled all the way to Europe and flourished throughout the world. Morphine, opium's active ingredient was first isolated in 1806 by Wilhelm Serturner, who named it "morphine" after *Morpheus* the Greek god of dreams (Kritikos *et al*., 1967). Subsequently,

morphine's chemical formula was elucidated by Sir Robert Robinson, for which he was awarded the 1947 Noble Prize in Chemistry.

Morphine is an alkaloid and a weak base that exerts its pharmacological effect primarily through activation opioid receptors (ORs), mu-, kappa-, and delta-opioid receptors (*OPRM1*, *OPRK1*, and *OPRD1*, respectively), which are members of the G_i protein-coupled receptor (GPCR) superfamily (Kieffer, 1995). However, morphine's analgesic effect is mediated predominantly via *OPRM1*. After binding to an agonist, the ORs activate intracellular signaling through inhibitory G proteins, which affect several downstream signaling pathways, including inhibition of adenylyl cyclase and voltage-gated calcium channels, and activation of receptor-regulated potassium channels (Law *et al.*, 2000). These intracellular changes cause hyperpolarization in cells, inhibiting both transmission of nerve impulses and release of excitatory neurotransmitters. Although morphine and other opioids are used for management of chronic pain conditions, they have an enormous potential for abuse. Predisposition to morphine abuse and its addictive potential are a direct consequence of its ability to induce tolerance, desensitization, and withdrawal (Hyman *et al.* 2001). In this study, morphine sulfate pentahydrate was used to study the effects of opioids when exposed to stem cells (Figure 1).

1.2. Epigenetics

Epigenetic (EG) mechanistic changes comprise any and all reversible changes in gene expression pattern without any modification to the DNA sequence. It is well established that EG regulation along with genetic regulation is fundamental to establish, maintain, and alter cellular identity of all mammalian cells (Chintalapati & Barile, 2019). Importantly,

EG modulations are associated with regulation of cellular plasticity during the processes of cellular proliferation, de-differentiation, and homeostasis. EG mechanisms at the interface of environment and genome, translate the environmental cues to controlled phenotypic changes by altering the dynamic states of chromatin integrity (Mohn & Schübeler, 2009). Perturbations in the chromatin landscape results in alterations of gene expression pattern in the form of transcriptional activation or repression. EG-mediated changes in chromatin structure occurs by 3 distinct yet interrelated pathways: (1) post-translational modifications (PTM) of histone proteins (HP), (2) covalent addition of methyl group to carbon-5 (C-5) of cytosine molecule, referred to as DNA methylation, and (3) non-coding RNAs (ncRNAs). It is important to note that EG alterations are not always isolated and independent molecular events, but are interrelated, interact, and influence (the "3i's) each other to variable magnitude. For instance, the methyl-C_pG binding domain (MBD) that binds to CpG regions on DNA containing methyl groups is dependent on the chromatin microenvironment regulated by PTM to HP (HP-PTM). Another example of such EG pathway dependency is when methylation of the lysine (K)-4 residue of histone 3 (H3) serves as a docking site for DNA methyltransferases (DNMTs), causing transcriptionally repressive DNA methylation to occur (Li *et al*., 2011). Interestingly, EG pathways demonstrate differential tissue specificity due to differences in expression of EG modifiers between tissues (Eckmann-Scholz *et al*., 2012). EG "modifiers" are the group of transcription factors and enzymes that regulate induction or repression of specific EG modification. "Readers" are EG modifiers that recognize an EG change in the genome. Enzyme modifiers that induce molecular EG changes are referred to as "writers" and modifiers that remove such changes are called "erasers" (Chintalapati & Barile, 2019).

1.2.1. DNA methylation

DNA methylation is a transcriptionally repressive EG modification that switches euchromatin to heterochromatin making DNA unavailable for transcriptional machinery binding. Cytosine-guanine dinucleotide (C_PG) islands are primary targets for this EG modification. DNA methyl transferases (DNMTs) are the enzymes that catalyze this reaction by substituting the hydrogen with a methyl group on position 5' of the pyrimidine ring of the cytosine molecule (Chintalapati & Barile, 2019). DNA methyltransferase-1 (DNMT1), DNA methyltransferase-2 (DNMT2), DNA methyltransferase-3a (DNMT3a) and DNA methyltransferase-3b (DNMT3b) are the most commonly recognized mammalian DNA methyltransferases. Hemi-methylated DNA is the target of DNMT1, known as maintenance methyltransferase and DNMT3a/3b are responsible for *de novo* methylation called *de novo* methyltransferases. In mammals, the most aggressive modulation in DNA methylation associated chromatin dynamics occurs at early stages of life. Case in point, the embryonic stage of fetal development is characterized by excessive *de novo* methylation followed by progressive demethylation in the latter stages (Smith & Meissner, 2013). This phenomenon of variable methylation is supported by studies showing over expression of DNMT3a and 3b at early post-implantation stage of fetal development, followed by their immediate decrease in expression in the later stages of growth (Chen *et al*., 2003).

1.2.2. Post-translational Modifications of Histone Protein

HP-PTM are one of the EG mechanistic subtypes involved in modulating the dynamic states of chromatin and consequent gene expression aberrations. PTM alter stability of nucleosomal framework in chromatin by modifying the chemical interactions between DNA and HP via chemical modifications of several amino acid residues, specifically lysine (K) in HP. HP-PTM include wide array of functional group additions and deletions on K-residues; the most commonly studied K-modifications include methylation, acetylation, phosphorylation, ubiquitination, sumoylation and ADP-ribosylation (Gadhia *et al*., 2015; Chintalapati & Barile, 2019). Despite possible occurrence of PTM on one, few or all HPs, H2A, H2B, H3 and H4, H3 modifications are widely supported to have substantial impact on gene expression regulation (Herz *et al*., 2014; Yang *et al*., 2012). Furthermore, methylation of K-residues 4, 9, 27 and 79, and acetylation of K-residues 9, 14, 18, and 56, are considered to be of considerable importance in transcriptional initiation, maintenance, and termination, collectively called gene activation, and transcriptional repression that functionally results in gene inactivation (Kaliman *et al*., 2014; Lawrence *et al*., 2016; Schvartzman *et al*., 2018). Evidence suggests acetylation at H3K4 and methylation at H3K4, H3K36 and H3K79 are predominantly localized in vicinity of genes undergoing active transcription. Conversely, methylation at H3K9, H3K20 and H3K27 are confined to regions of transcriptional repression (Hyun *et al*., 2017; Nguyen *et al*., 2015; Siveen *et al*., 2014; Zhang & Liu, 2015). However, emerging studies indicate the paradoxical presence of HP-PTM such as methylated H3K9 in both active and inactive gene expression sites (Chintalapati & Barile, 2019; Lawrence *et al*., 2016). It is important to note that HP-PTM are regulated by complex interplay of their respective writers-enzymes that add a PTM,

and erasers-enzymes that remove a PTM (Biswas & Rao, 2018; Yang *et al.*, 2016; Gadhia *et al.*, 2015). Hence, HP-PTM and their influence on genomic expression are the determinants of active/inactive gene expression which is in turn influenced by PTM localized at the writer and eraser gene regions.

1.2.3. Non-coding RNA

Approximately 2% of human genome constitutes the functional protein coding region; the remaining genomic region, historically considered to be superfluous information that code non-translatable RNA are referred to as ncRNAs (Wu *et al.*, 2013). However, recent studies demonstrate biological significance of ncRNAs which are categorized as small and long ncRNAs based on their sequence length. Furthermore, small ncRNAs are further classified as microRNAs (miRNAs), ribosomal RNAs (rRNAs), small nuclear RNAs (snRNAs), piwi-interacting RNAs (piRNAs), transfer RNAs (tRNAs), and small interfering RNAs (siRNAs). miRNAs and long ncRNAs are the ncRNAs most studied for their genomic and epigenomic influence in living organisms, especially mammals (Chintalapati & Barile, 2019; Quinn & Chang, 2016). The regulatory function of ncRNAs involve their interaction and complex formation to functional mRNA or other proteins that belong to transcriptional machinery causing perturbations in genomic expression. The mature miRNA elicits its influence on functional protein synthesis by recognizing, targeting and complex formation with functional mRNA, rendering it ineffective to undergo translation (Kumarswamy *et al.*, 2011).

1.2.4. Significance of EG modifications as biomarkers in Current Study

The field of EG is now associated with an abundance of biomarkers, and the mechanisms of diseases have been correlated to them. Consequently, such EG biomarkers offers significant opportunities to understand the progression of pathologies and disease states. The role of biomarkers thus encourages appreciation of the mechanisms associated with the disease states, aids in the diagnosis of pathologies, and is involved in identifying therapeutic modalities with pathological consequences. *In vitro* and *in vivo* laboratory studies pertaining to opioid induced EG mechanistic perturbations will help identify and validate molecular EG biomarkers associated to opioid abuse, addiction, and other associated pathological states (Heard & Martienssen, 2014; Sharma, 2017).Recently, abuse of opioids and other drugs and their associated molecular EG changes are proving to be vital in addiction research (Cadet *et al*., 2016). However, most of the past and current studies pertaining EG's of opioid addiction were specifically targeted to opioid induced cellular changes at the level of developing and/or mature central nervous system circuitry and physiology *in vivo* (Lester *et al*., 2011) . Consequently, our current study intends to address the potential of opioids to cause aberrations in genomic HP-PTM in induced pluripotent stem cells (iPSC) *in vitro*. Identification and validation of changes in biologically significant H3-PTM in response to opioid exposure can serve as valuable EG biomarkers for opioid abuse and addiction disease. The genotypic and phenotypic characteristics of iPSC involving substantial EG reprogramming with dynamic chromatin remodeling guiding their ability to differentiate into any or all cells of the three embryonic layers, ectoderm, endoderm, and mesoderm, render them ideal for EG mechanistic studies *(*Goodnight *et al., 2019;* Ming-Tao *et al.*, 2017). In this study, we aim to observe

aberrations in genomic levels of one or multiple H3-PTM in iPSC following acute and chronic exposure to MS.

1.3. Signal Transducers and Activators of Transcription

The signal transducers and activators of transcription (STAT) are a class of transcriptional factors comprising STAT proteins-1,2,3,4,5a,5b and 6 which participate in cytokine-mediated cellular signaling (Yu *et al*., 2014). Among other STAT sub-types, STAT3, an acute phase response factor, is considered to be a key biological regulator of cellular proliferation, survival, and angiogenesis (Haghikia *et al*., 2014; Siveen *et al*., 2014). Activation of STAT3 is mediated primarily by IL-6 family of cytokines via janus kinases (JAKs), and receptor or non-receptor tyrosine kinases. The kinase-mediated phosphorylation of –tyrosine705 (STAT3-pTyr-705) at C-terminal domain, results in formation of homodimers or heterodimers with STAT1 resulting in consequent nuclear translocation and transcriptional regulation. Additionally, phosphorylation of STAT3 at another residue in C-terminal domain –serine727 (STAT3-pSer-727), further strengthens STAT3 activation and increases its retention time in nucleus extending the influence on genomic transcription (Betts *et al.*, 2015; Zhang *et al*., 2020). In addition to opioid associated G-protein coupled receptor (GPCR) pathway, studies show morphine induced stimulation of STAT3 signaling pathway. Evidence suggests that morphine induced stimulation to STAT3 signaling is linked to increased proliferation of mesangial cells in the kidney and retinal endothelial cells (Weber *et al.*, 2013).

1.4. Induced Pluripotent Stem Cells (iPSC)

Stem cells generated from mature somatic cells by introducing defined set of transcription factors that render pluripotency, self-renewal, and undifferentiated phenotype, are called induced pluripotent stem cells (iPSC). IPSC have an *in vitro* significance unparalleled to any mammalian cell line, considering their ability to propagate undifferentiated for several passages and can be stimulated to differentiate into many cell types. Mouse iPSC were discovered and developed in 2006 by Japanese stem cell researchers Shinya Yamanaka and Kazutoshi Takahashi using retrovirus-mediated delivery of four reprogramming transcription factors, Oct 3/4 (Octamer-binding transcription factor-3/4), Sox2 (Sex-determining region Y)-box 2, Klf4 (Kruppel Like Factor-4), and c-Myc, into mouse fibroblast cells. Consequently, in 2007, Yamanaka and his team applied a similar reprogramming method to adult human fibroblasts to generate human iPSC. IPSC are used for a range of applications including, but not limited to, regenerative medicine, *in vitro* disease modeling, and pharmacological and toxicological screening (Takahashi *et al.*, 2007).

1.5. Current Study

In mouse embryonic stem cells (mES cells), we previously demonstrated that exposure of morphine sulfate (MS) at early and late stages of differentiation leads to down-regulation of neuronal phenotype and expression of opioid receptors (Dholakiya *et al*., 2016). Also, we established the occurrence in mitotic inheritance of HP-PTM H3K27me1, and resulting chromatin instability following cadmium exposure to mES cells (Gadhia *et al*., 2015). In

the current study we hypothesize that short- and long-term exposure of iPSC to MS induces heritable EG aberrations to genomic H3-PTM, H3K9me1 and H3K27me3, and disrupts gene expression of critical cell signaling molecule STAT3. This study includes, investigating the effects of MS exposure on the levels of genomic H3-PTM, H3K9me1 and H3K27me3-; gene expression and protein level aberrations of STAT3, STAT3-pSer-727 and STAT3-pTyr-705; gene expression changes of OR's, *OPRM1*; *OPRD1*; *OPRK1*- in iPSC. In addition, we concurrently monitored the levels of stem cell specific nuclear transcription factor, OCT4 and cell surface marker TRA-1-60 to investigate the influence of MS on pluripotency expression.

2. MATERIALS AND METHODS

2.1. Cell Culture

Undifferentiated episomal human iPSC line derived from CD34+ cord blood (Gibco) was maintained on Geltrex LDEV-free reduced growth factor basement membrane matrix in serum-free Essential 8^{TM} (E-8) medium (Life Technologies Corporation, Carlsbad, CA, USA). The E-8 kit constituted E-8 basal medium and E-8 supplement, serum free, to maintain iPSC in undifferentiated state. Media were replenished every 24h. Geltrex concentrate was diluted with DMEM/F-12 (Thermo Fisher Scientific,Waltham, MA, USA), and stored at -20^{0}C; solution was thawed at 4^{0}C overnight prior to thawing or sub-culturing iPSC as per manufacturer's protocol. Tissue culture treated plates from Corning (Corning, NY, USA) were coated with diluted geltrex solution thawed at 4^{o}C overnight prior to thawing or sub-culturing iPSC as per manufacturer's instructions. Cell suspension was supplemented with RevitaCell^{TM} (Life Technologies Corporation, Carlsbad, CA, USA) post-thaw, for duration of 12h after which media was replaced with regular E-8. RevitaCell^{TM} is a combination of Rho Kinase (ROCK) inhibitor and antioxidants to enhance post-thaw cellular recovery and survival (Baust *et al.*, 2017). Cells were sub-cultured at a ratio of 1:4 on day 3 following the previous sub-culture or post-thaw.

Table 2 illustrates the durations of MS exposure to iPSC after which the cell samples were collected for downstream analyses.

Note- The day on which the cells were initially passaged, seeded, and designated to initiate MS or naltrexone (N) exposure was referred to as day 0. Prior to initiation of MS

exposure, cells were given a duration of 24h to settle and acclimatize to E-8 medium and the Geltrex matrix environment after which MS or N exposure was initiated.

2.2. Stock and working concentrations of MS and N

Stock solutions of 100 µM MS and 200 µM N were freshly prepared during every sub-culture in E-8 medium with vortexing and a brief 1-minute sonication followed by sterilization using 0.2-micron SFCA membrane filter. Working concentration solutions were prepared every 24h by serial dilution of stock solutions with E-8. For cells designated to be exposed to both MS and N, cells were initially exposed to 10 µM N for 2h followed by aspiration and addition of E-8 media to a final concentration of 10 µM MS and 10 µM N. Figure 2 illustrates the iPSC viability data following 24h MS and N exposure.

2.3. Cell viability by MTT assay (Mosmann, 1983)

Approximately 48h after passage, iPSC were treated with MS and N. Treatment concentrations 0-, 50-, 100-, 200-, 400- and 800-µM MS and N exposure to iPSC for a duration of 24h was used to assess their effects on cell viability. 5 mg/mL MTT reagent (Sigma-Aldrich Corp) was added 2h prior to end of exposure period (22^{nd}h) to each well (10% v/v) without the removal of respective treatment media and plates were kept in an incubator for 2h. At the end of the exposure period (total exposure time: 24h), treatment solutions containing MTT reagent were removed and replaced by spectrophotometric grade dimethyl sulfoxide (DMSO; Alfa Aesar, Ward Hill, MA, USA). The plates were then shaken for 15 minutes on a reciprocal shaker and absorbance was measured at 550nm using Synergy H1 microplate reader (BioTek, Winooski, Vermont, USA). Cell viability was determined by comparing average absorbance readings of respective treatment concentrations minus average blank absorbance (DMSO only) to average control absorbance readings minus average blank absorbance (DMSO only) and reported as percentage viability of control.

2.4. Total Histone Protein Extraction and Quantification

Total histone protein (THP) extraction from 4 X 10^6 iPSC of MS unexposed and exposed cell samples was performed using EpiQuik™ total histone extraction kit (Epigentek, Farmingdale, NY, USA), as per manufacturer's instructions. The histone extracts were further diluted using balance buffer and stored at -80^0C. Diluted THP extracts were quantified using the bicinchoninic acid (BCA) protein assay (Thermo Fisher Scientific, Waltham, MA, USA) using bovine serum albumin (BSA) as the standard.

2.5. Histone H3 Modification Multiplex Assay

Quantification of 21 genomic H3-PTM was performed using an ELISA-based calorimetric assay (Epigentek, Farmingdale, NY, USA). THP extracts from unexposed, 10 µM MS, 10 µM nicotine, and 1% ethanol exposed iPSC were added to designated wells pre-coated with antibodies specific to each H3-PTM and incubated for 1.5h at 37^0C. Wells were washed and incubated with diluted detection antibody for 1h at room temperature. Following incubation, wells were sequentially incubated with color developer and stop solutions, and the absorbance of the developed color was measured at 450nm using Synergy H1 microplate reader (BioTek, Winooski, VT, USA). The amount of H3-PTM was calculated according to the following formula:

$$\text{H3-PTM modification (ng/µg)} = \frac{(\text{Sample OD- BLANK OD})/ S}{(\text{Assay control OD- BLANK OD})/P}$$

where OD is optical density, S is amount of input sample protein (ng), and P is amount of input assay control (ng).

2.6. Global Histone H3K9 mono-methyl (H3K9me1) and H3K27 tri-methyl (H3K27me3) quantification

Quantification of H3K9me1 and H3K27me3 modifications was performed using an ELISA-based calorimetric assay (Epigentek, Farmingdale, NY, USA), similar to as described in section 2.5. The amount of histone modification was quantified according to the following formula:

$$\text{H3K9me1/H3K27me3 (ng/mg protein)} = \frac{OD_{(SAMPLE-BLANK)}}{\text{Input protein (µg) x slope}}$$

Note- Slope was computed from the change in OD/ng of standard control

2.7. Characterization of iPSC by Immunocytochemistry

All solutions for immunocytochemistry (ICC) were obtained from Life Technologies Corporation (Carlsbad, CA, USA). iPSC were cultured for 2d and then fixed with 4% paraformaldehyde solution for 15 min after which they were permeabilized for 15 min with permeabilization solution S. Cells were then incubated with blocking solution for 30mins. Primary antibodies, rabbit anti-OCT4 and mouse anti-SSEA4, were added directly to the blocking solution and incubated for 3h, after which cells were washed and incubated with secondary antibodies, Alexa-Fluor 594 donkey anti-rabbit for OCT-4, and Alexa-Fluor 488 goat anti-mouse for SSEA4 for 1h. DNA-binding fluorescent dye 4,6-diamidino-2-phenylindole (DAPI; Santa Cruz Biotechnology, Santa Cruz, CA, USA) was used as counter stain to detect cell nuclei. The cells were then washed, air-dried and mounted with coverslip and imaged with EVOS FL microscope (Figures 3A-3E) (Thermo Fisher Scientific, Waltham, MA, USA).

2.8. Flow cytometry analyses - Measuring intra-cellular levels of STAT-3, STAT3-pTyr-705, STAT3-pSer-727, OCT4, and TRA-1-60 in iPSC

Cells at required density were condensed into single cell suspensions using 0.48 mM Gibco® Versene Solution 0.48 mM (Thermo Fisher Scientific, Waltham, MA, USA). Cells were re-suspended in stain buffer containing 0.2% BSA and 0.09% sodium azide (BD Biosciences, San Jose, CA, USA) and fixed to a final concentration of 2% paraformaldehyde for 10min. Following fixation, cells were permeabilized with ice-cold 90% v/v methanol for 15min, and then washed and incubated with respective

fluorochrome-conjugated monoclonal antibody for 30mins in the dark at room temperature. Antibodies, Phycoerythrin (PE) conjugated anti-STAT3, Alexa-Fluor 647 conjugated anti-STAT3-pSer-727, and PE conjugated anti-STAT3-pTyr-705 were obtained from BD Biosciences (San Jose, CA, USA); antibodies FITC conjugated anti-TRA-1-60 and alexa-fluor 647 conjugated anti-OCT4 were procured from Millipore Sigma (Burlington, MA, USA). After staining, cells were washed twice with stain buffer and ready for flow cytometry (FC) analysis. Appropriate isotype controls were conducted simultaneously with each antibody (Figure 4). All samples were run in Luminex FlowSight® (Luminex Corporation, Austin, TX, USA) with an acquisition count of 10,000 events per sample.

2.9. Real-time quantitative PCR

Total RNA extractions were performed using the RNeasy Mini Kit (Qiagen, Germantown, MD, USA) including an on-column DNase digestion using RNase-free DNase Set (Qiagen, Germantown, MD, USA). Extracts were collected and quantified using NanoDrop One (Thermo Scientific, Waltham, MA, USA) and stored at -80^{0}C. Real time quantitative polymerase chain reaction (RT-qPCR) was performed using a two-step method; cDNA synthesis from total RNA extracts was performed using SuperScript IV VILO master mix (Thermo Fisher Scientific, Waltham, MA, USA) according to the manufacturer's protocol using a Techne TC-412 Thermal Cycler (Vernon Hills, IL, USA). RT-qPCR of cDNA templates was performed using Taqman gene expression assays (Thermo Scientific, Waltham, MA, USA) in Quant Studio 3 Real-Time PCR system (Applied Biosystems, Carlsbad, CA, USA). Results for RT-qPCR were calculated by the

relative gene expression method ($\Delta\Delta C_t$). Threshold cycle (C_t) value of all the target genes were normalized using the C_t value 18S rRNA as endogenous control.

2.10. Statistical and data analysis

All data were analyzed using GraphPad Prism 6.0 (La Jolla, CA, USA). All experiments were repeated at least 3 times and performed with at least 2 replicates per sample group. One-way or two-way ANOVA followed by Bonferroni's post-hoc test was used to determine statistical significance. Data for genomic H3-PTM were either expressed in terms of percent modification relative to control or as time versus quantity of H3-PTM.

Results for RT-qPCR were calculated by the relative gene expression method ($\Delta\Delta$Ct). The Ct value of all the target genes were normalized using the Ct value 18S rRNA as endogenous control using SABiosciences statistical software (Rao *et al*., 2013). Manual gating for all the experiments involving FC analyses was performed with IDEAS software (Luminex Corporation, Austin, TX, USA) by identifying single cell populations followed by establishing positive (+) and negative (-) gates. Scatter plots for the gating procedure were obtained by plotting fluorescence intensity (FI) on X-axis and aspect ratio intensity on Y-axis. Negative gate is the single cell region of unstained and isotype control samples in the scatter plot representing cell population as FI versus aspect ratio intensity. The FI region succeeding the negative gate was labelled positive. In this study, FC data is expressed in terms of concentration or time versus percentage cell population in the positive gate labelled as "% Gated."

3. RESULTS

3.1 Cell viability of iPSC exposed to Morphine Sulfate and Naltrexone

The MTT assay is used to measure the mitochondrial activity of cells, which indirectly serves as a measure of cell viability in proportion with changes to mitochondrial metabolism. The cell viability of iPSC was unaltered following 24h exposure to various concentrations of MS and N (Figure 2) as discussed in section 2.3.

3.2. Suppression of H3K9me1 and H3K27me3

Analyses of 21 genomic H3-PTM (Table 3) following exposure to 10 μM MS for 2d (Figures 5A-5F) and 5d (Figures 5G-5L) suggest decreased levels of gene expression repressive H3-PTM, H3K9me1 (Fig.5C) and H3K27me3 (Fig. 5J). To further understand the specificity of MS-induced down-regulation of H3-PTM, we analyzed the changes of H3-PTM by exposing 10 μM nicotine (Figures 6A-6F) and 1% ethanol (Figures 6G-6L) to iPSC for 5 days. Transcriptionally repressive H3K9me1 and H3K27me3 are predominantly associated with heterochromatin. Our data demonstrates suppression of genomic H3K9me1 and H3K27me3 with MS exposure but neither with nicotine nor ethanol. Interestingly, exposure to nicotine resulted in increased genomic levels of H3K18ac, H3ser10P, and H3K79me2 and a decrease in genomic H3ser28P. However, the decrease in H3K9me1 (Figure 7A) preceded H3K27me3 (Figure 7B) suggesting MS-mediated suppression is linked to the duration of MS exposure. Furthermore, the effect was not antagonized by pre-exposure to N but was reversible following a 3d recovery (R) period (Figures 7C and 7D). Furthermore, prolonged durations of MS exposure suggest

progressive decrease in the genomic levels of both H3K9me1 (Figures 8A-8C) and H3K27me3 (Figures 9A-9C) with another increase on day 26 signifying compensatory mechanisms in stem cells to stabilize MS-induced chromatin aberrations (Figures 8D and 9D). These results support the idea that EG insult induced by MS is reversible but neither mitotically heritable nor antagonized by N.

3.3. Gene expression disruption of *STAT3*

Gene expression analyses of 44 genes (Table 4) controlling transcriptional regulatory networks in stem cells show an approximate 12-fold transcriptional up-regulation of STAT3 mRNA following 2d MS exposure (Figure 10A). Interestingly, STAT3 mRNA levels were unchanged following 2d-nicotine and -ethanol exposure, suggesting an MS specific *STAT3* gene expression perturbation (Figures 10B and 10C). However, the transcriptional stimulation started to plunge on day 11 and 20 and were not different from control on day 29 (Figure 11; Table 5). In contrast to the transcriptional stimulation of *STAT3* gene expression, levels of STAT3 protein were suppressed suggesting translational down-regulation. Also, both pre-exposure to N and recovery effectively antagonized and reversed the MS-induced effect on STAT3 protein levels, respectively, with 2d and 5d MS exposure (Figures 12A-12C). Upon continuous MS exposure, protein levels exhibited considerable decrease relative to control on day 2 and day 11 respectively but were not different on day 29 (Figure 12D; Table 6). Thus, we conclude that MS targets and disrupts gene expression of critical cell signaling molecule STAT3 in an opioid receptor dependent mechanism.

3.4. Differences in STAT3-pTyr-705 and STAT3-pSer-727 following MS exposure

Phosphorylation at tyrosine-705 residue in STAT3 protein is deemed as pre-requisite for nuclear translocation of STAT3 and its consequent genomic transcriptional influence. STAT3-pTyr-705 was unchanged after 2d (Figures 13A and 13C), yet down-regulated with 5d MS exposure (Figures 13B and 13D); downregulation was observed in iPSC exposed to 10 μM but not 1 μM MS, and was not antagonized by N. Results obtained from prolonged MS exposure show no significant changes in STAT3-pTyr-705 levels relative to control on days 2, 11, 20 and 29, respectively (Figure 13E; Table 7). In addition to STAT3-pTyr-705, phosphorylation at serine-727 in STAT3 protein is linked to an increase in stability and intra-nuclear retention time of previously translocated STAT3 protein.

Our data demonstrates a statistically significant reduction in STAT3-pSer-727, with 1 and 10 μM MS on day 2 (Figure 14A and 14C) but not on day 5 (Figures 14B and 14D); the MS-induced effect was effectively antagonized in iPSC pre-exposed to N. Furthermore, unlike STAT3-pTyr-705, prolonged MS exposure demonstrated significant downregulation of STAT3-pSer-727 levels relative to control on days 11 and 20, but not on day 29 (Figure 14E; Table 8).

3.5. MS-induced transcriptional repression of *OPRM1*, *OPRD1*, and *OPRK1*

MS induced down-regulation in OR gene-expression is a well-established phenomenon. All 3 OR, *OPRM1* (Figure 15A), *OPRD1* (Figure 15B) and *OPRK1* (Figure 15C), are known to be expressed in all types of stem cells. Our data illustrates transcriptional downregulation of OR's in iPSC due to MS exposure. Moreover, the magnitude of transcriptional downregulation was proportional to the concentration of MS. Furthermore,

duration of exposure to MS positively correlated to transcriptional repression of OR up to day 20. MS exposed iPSC on day 29, however show no change in OR mRNA levels, except for *OPRD1*, relative to control (Table 9).

3.6. Effects of MS on stem cell pluripotency expression in iPSC

OCT4 is a critical nuclear transcription factor protein essential for pluripotency maintenance of stem cells. Also, expression of cell surface antigen TRA-1-60 reflects the stem cell phenotype in iPSC. Thus, steady or increased expression of these factors maintains pluripotency. Shorter durations of MS exposure induced these markers as determined by FC analyses of OCT4 (Figure 16A; Table 10) and TRA-1-60 (Figure 16B; Table 11) expression in cells. Pluripotency markers stimulation was effectively inhibited when iPSC were exposed to 10 μM N prior to MS exposure. However, except for a small MS-induced decrease in TRA-1-60 marker following MS exposure on day 29, protein levels of both stem cell markers did not significantly differ from control following prolonged MS.

Figure 1. Structure of morphine sulfate pentahydrate.

(ChemDraw version 16, PerkinElmer informatics, MA, USA)

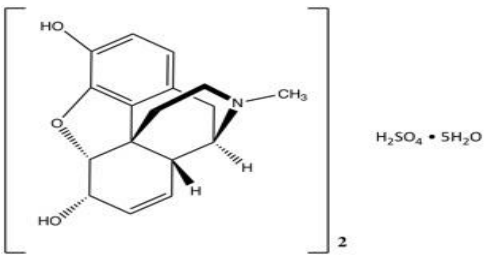

Figure 2. Effect of MS and N exposure on viability of iPSC following 24h exposure as determined by MTT assay.
iPSC were cultured for 48h post-passage and then exposed to 50, 100, 200, 400, and 800 μM of both MS and N for 24h. Unpaired t test was used to compare groups. Data represents mean ± SEM of 3 independent experiments with ≥ 3 replicates.

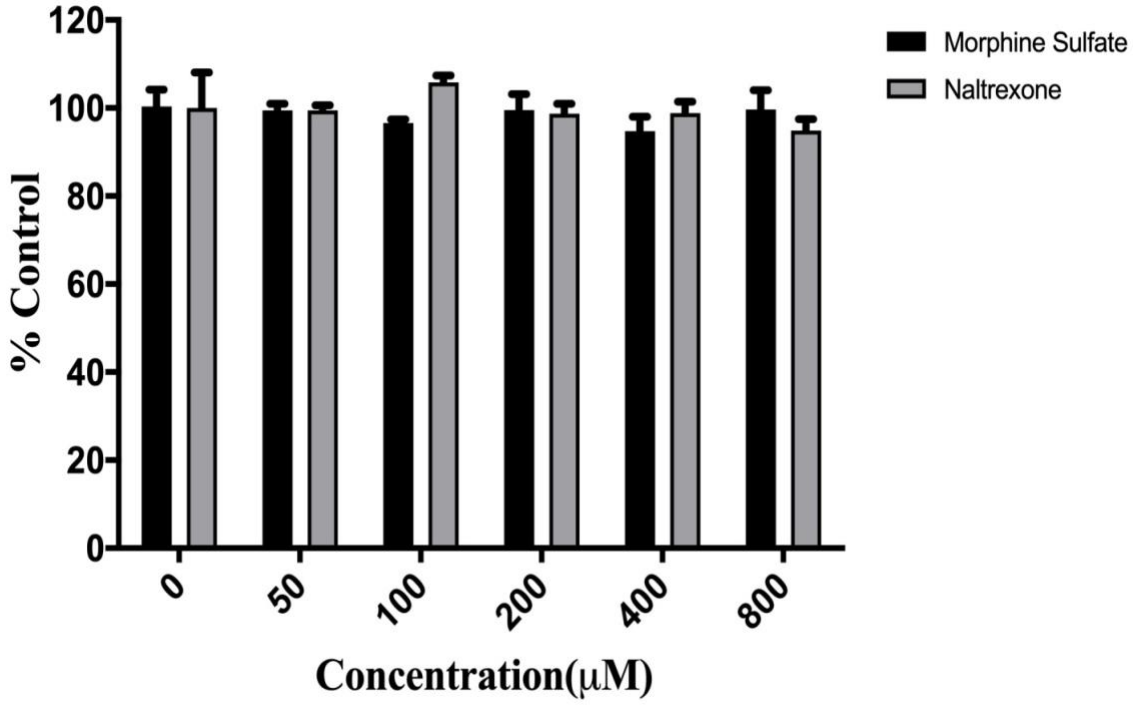

Figure 3. Expression of pluripotent stem cell specific markers in iPSC as observed by immunocytochemistry.
(A) Bright field. (B) DAPI. (C) Cell surface marker SSEA4. (D) Nuclear transcription factor Oct4. (E) Merge image- DAPI+SSEA4+Oct4; Magnification: 200X.

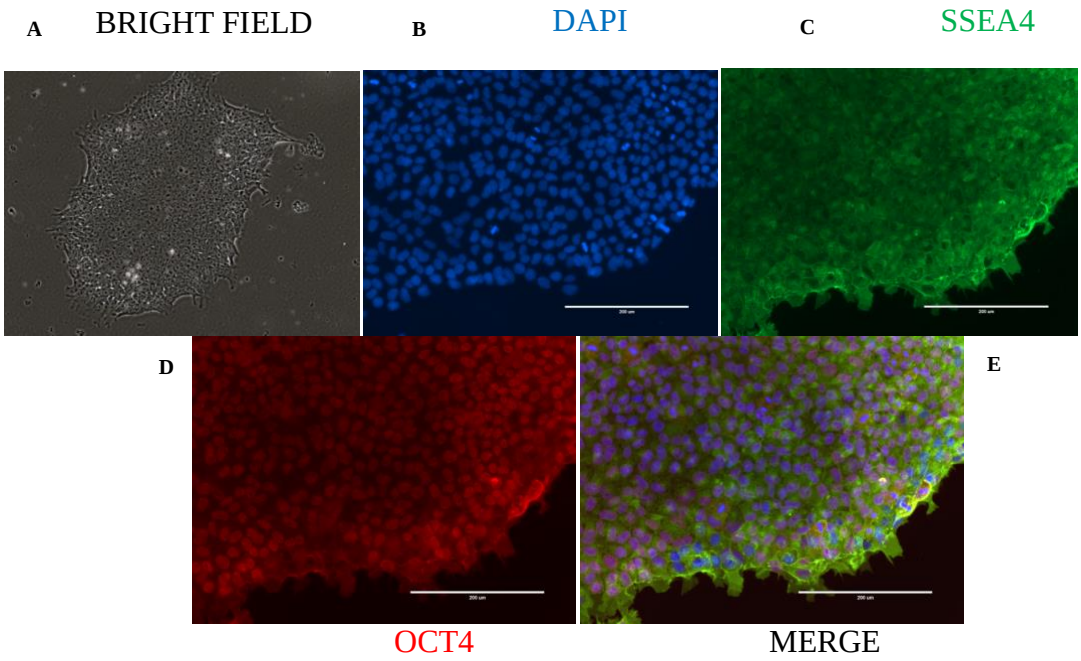

Figure 4. Isotype controls for markers OCT4, SSEA1, STAT3, STAT3-pTyr-705, and STAT3-pSer-727 in iPSC as determined by flow cytometry.

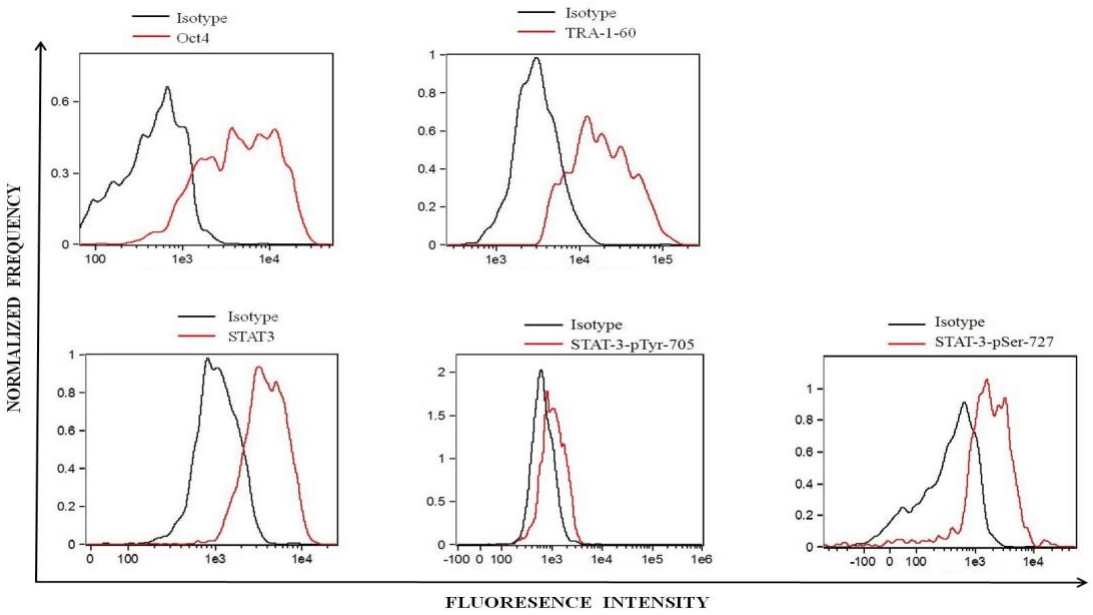

Figure 5. Effect of 2d and 5d MS exposure on genomic levels of 21 different H3-PTM.

Genomic H3-modification ELISA base calorimetric assay following 2 days- (A-F) and 5 days- (G-L) MS exposure. Two-way ANOVA followed by Bonferroni's post-hoc test. Experiment was performed 3 independent times with 2 replicates. * $p<0.05$ relative to control. Data represented as percent control in mean ± SEM of specific H3-modification per input mg protein.

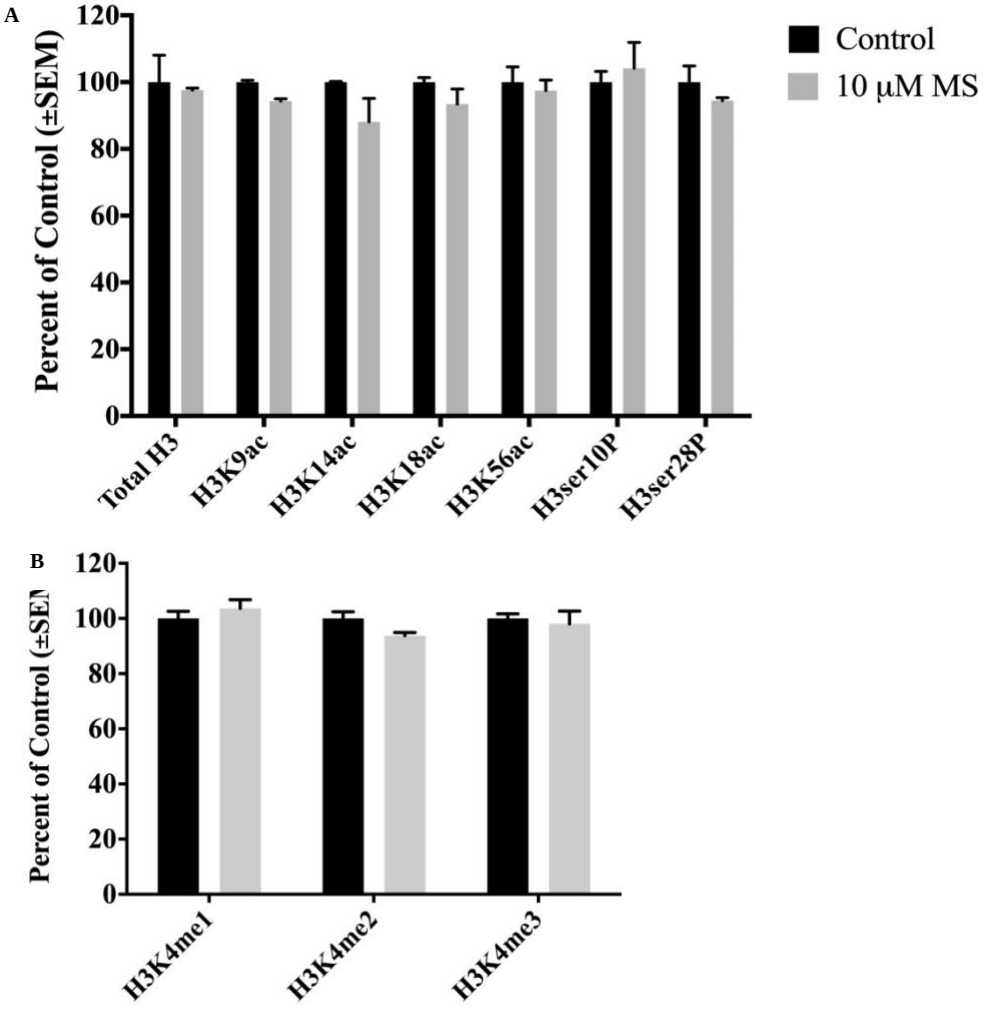

C

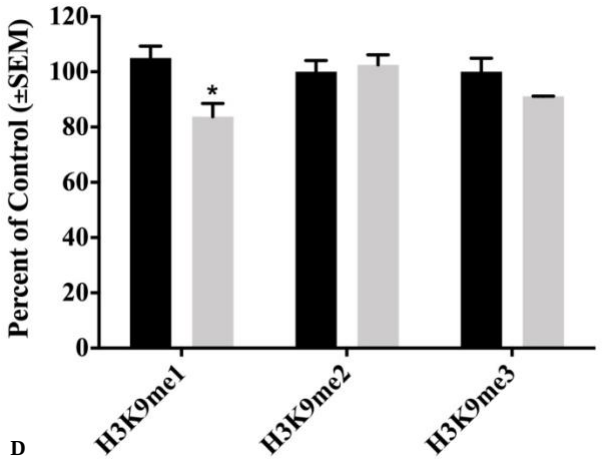

D

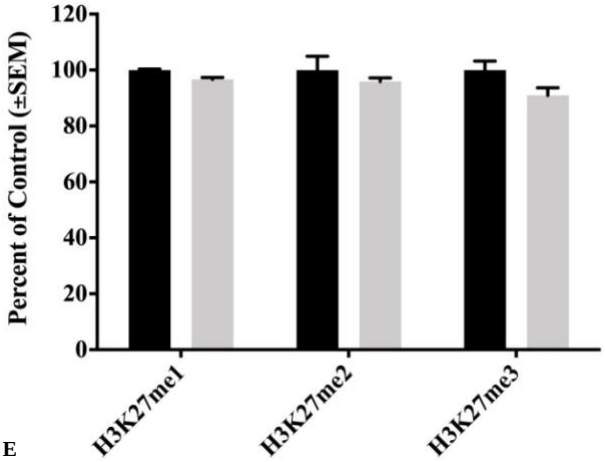

E

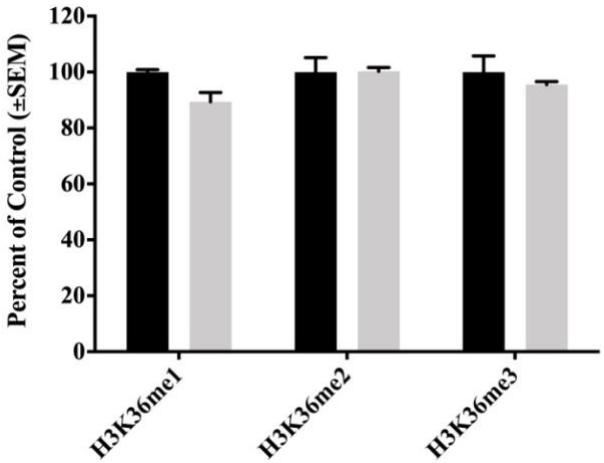

F

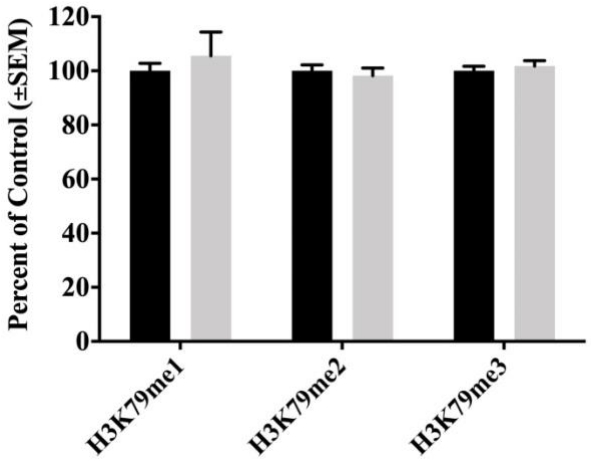

G

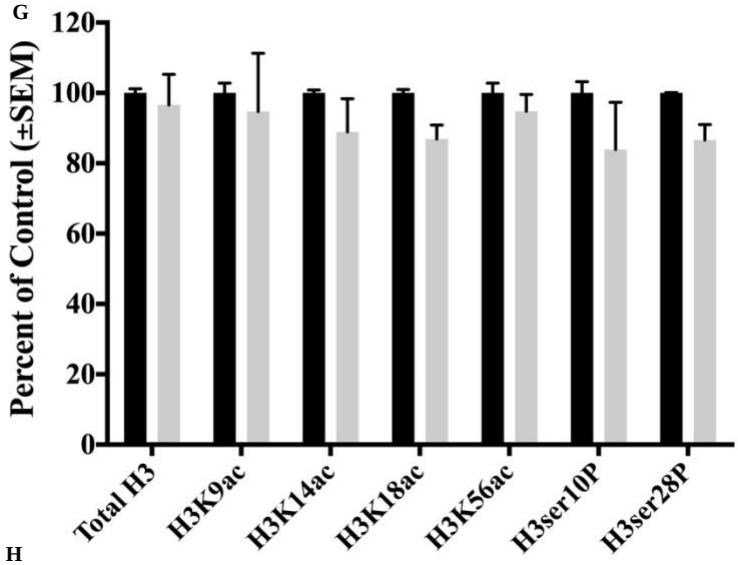

H

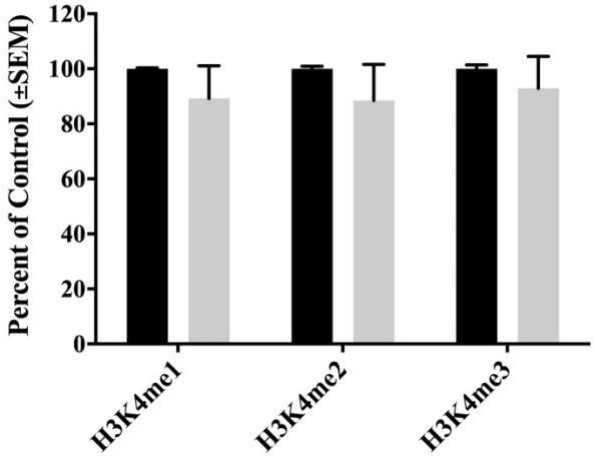

I

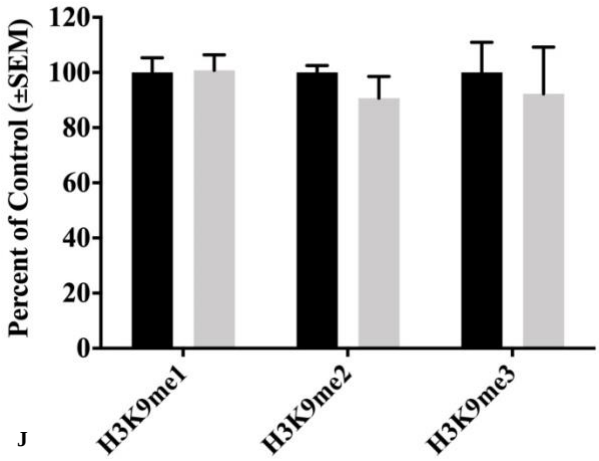

J

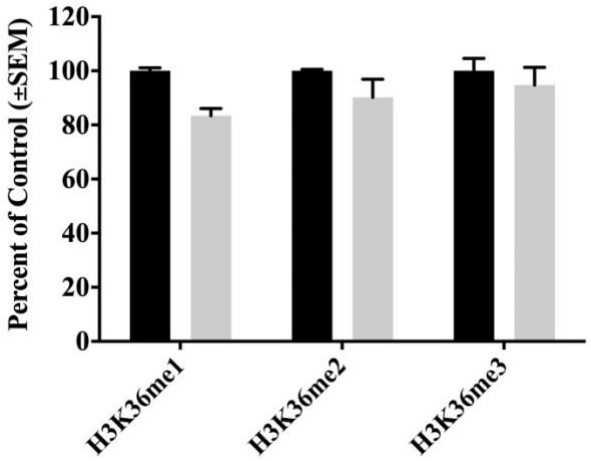

K

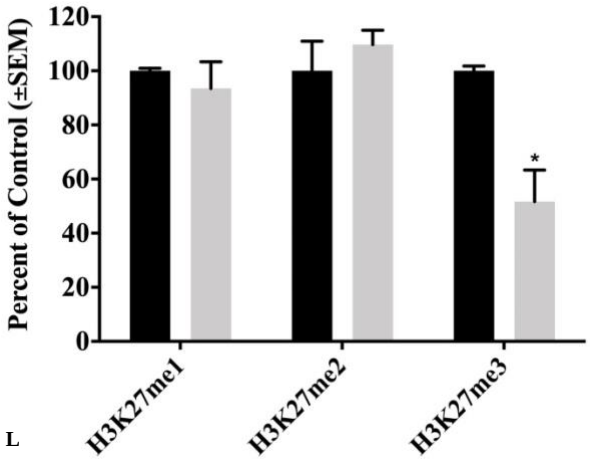

L

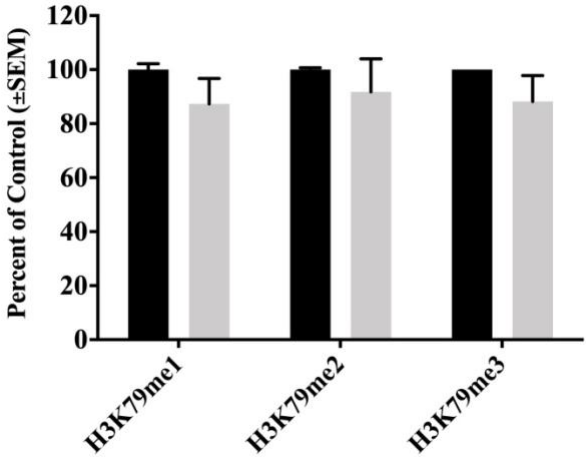

Figure 6. Effects of 5d nicotine and ethanol exposure on genomic levels of 21 different H3-PTM.

Genomic H3-modification ELISA base calorimetric assay following 5d exposure to nicotine (A-F) and ethanol (G-L). Two-way ANOVA followed by Bonferroni's post-hoc test. Experiment was performed 3 independent times with 2 replicates. $^{***}p<0.001$ relative to control. Data represented as percent control in mean ± SEM of specific H3-modification per input mg protein.

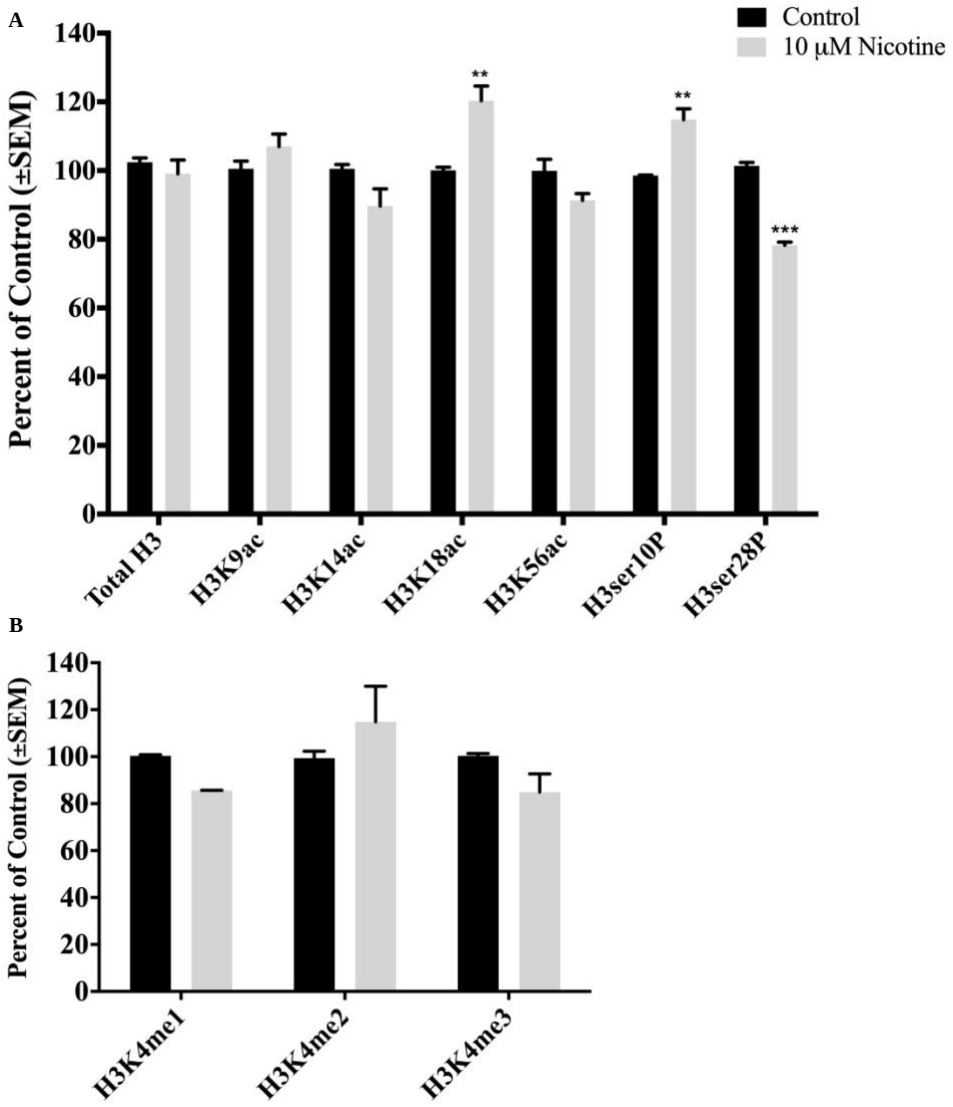

C

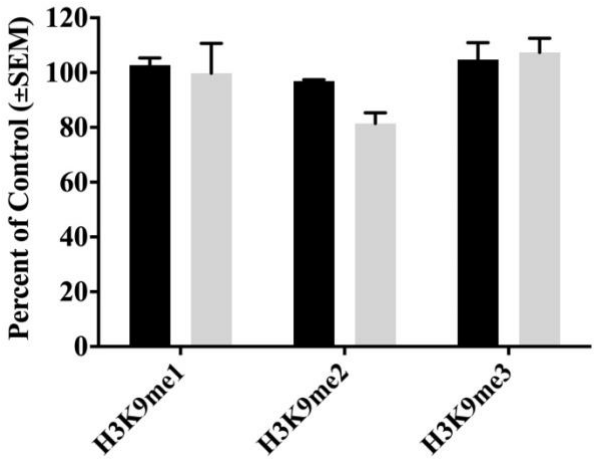

D

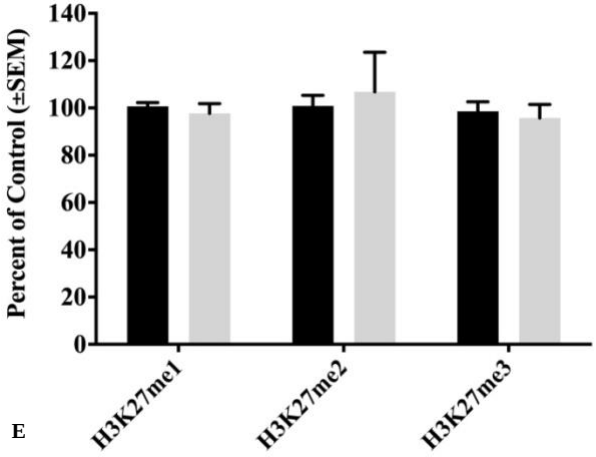

E

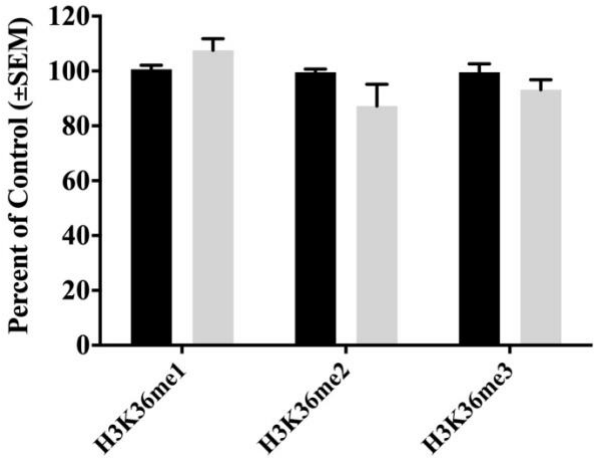

F

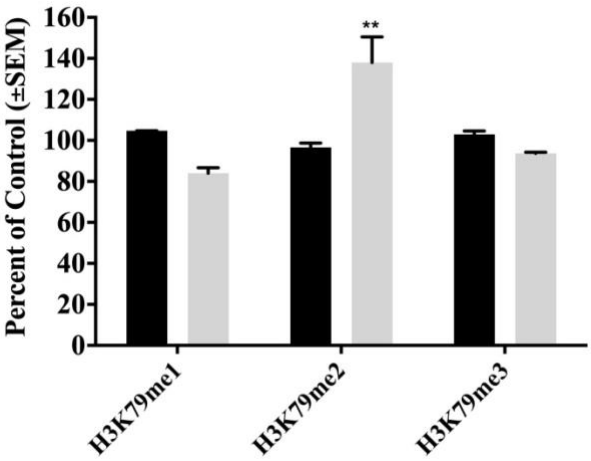

G

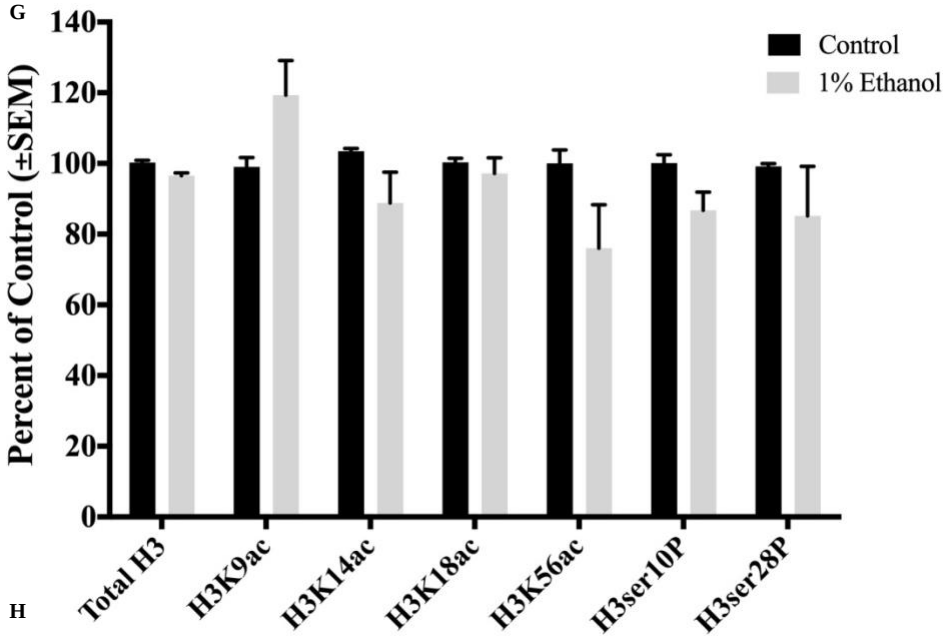

H

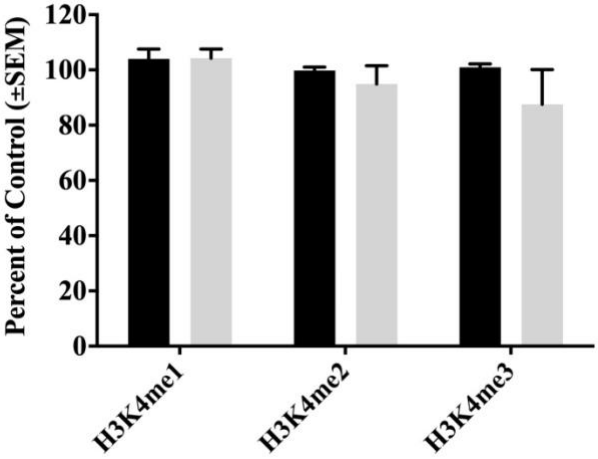

I

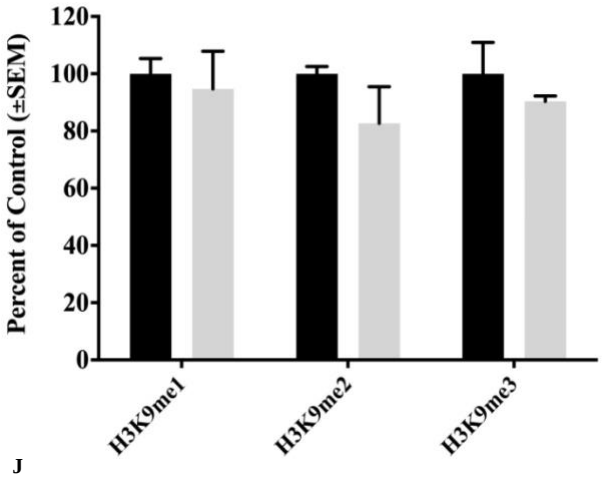

J

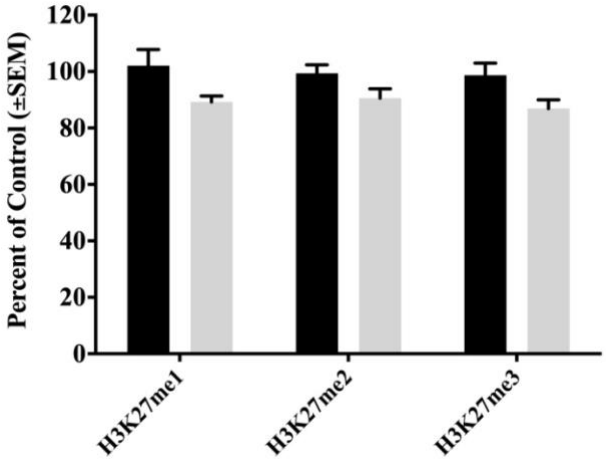

K

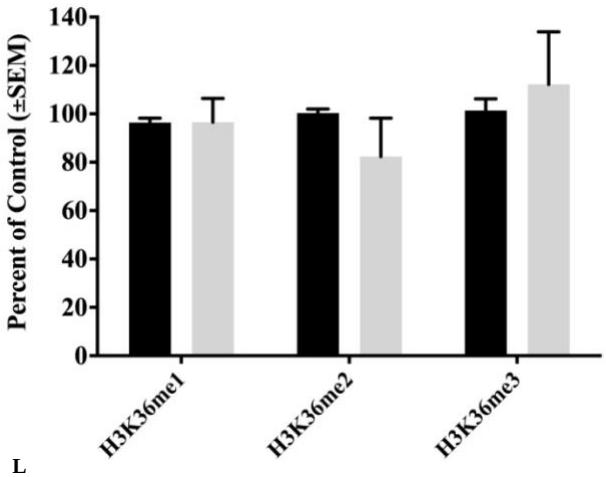

L

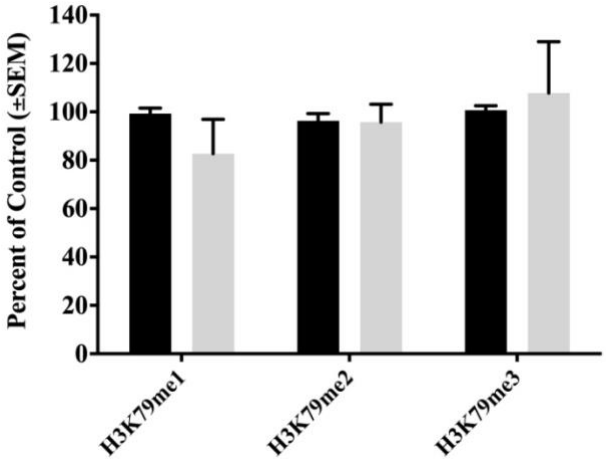

Figure 7. Suppression of genomic H3K9me1 and H3K27me3 levels in shorter and longer-term culture passages following MS exposure.
iPSC were collected following 2d and 5d MS exposure for histone protein extraction, and extracts were subjected to ELISA based analyses of genomic H3K9me1 and H3K27me3. Two-way ANOVA followed by Bonferroni's post-hoc test. Experiment was performed 3 independent times with 2 replicates. * $p<0.05$ relative to control. Data represented as percent control in mean ± SEM of specific H3-modification per input mg protein. Figures 7A through 7D represent calculated histone modifications (ng/mg of total protein), expressed as mean percent control ± SEM of 3 independent experiments, each with ≥ 2 replicates. Panels represent ELISA based assays of genomic (A) H3K9me1, (B) H3K27me3, (C) H3K9me1 on day 2, and (D) H3K27me3 on day 5. To deduce the pattern of MS induced alterations in H3K9me1 and H3K27me3, iPSC were collected during every passage, and analyzed similarly on days 8, 11, 14, 17, 20, 23, 26, and 29 respectively. (E) H3K9me1 and (F) H3K27me3 data are expressed as days in cell culture versus quantity of histone modification in ng/mg total protein (representative image from 3 independent experiments with 3 replicates; * $p<0.05$ relative to control; two-way ANOVA followed by Bonferroni's post-hoc test was used for statistical analyses.

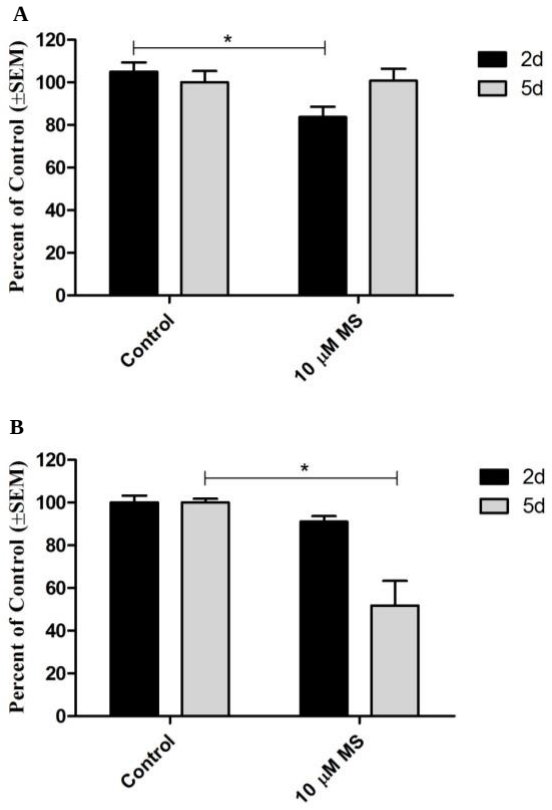

C

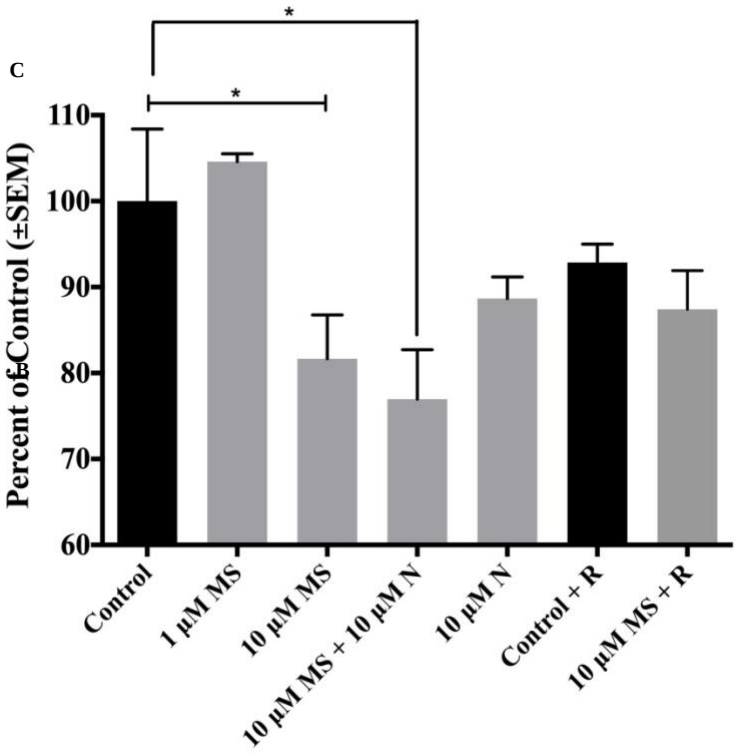

D

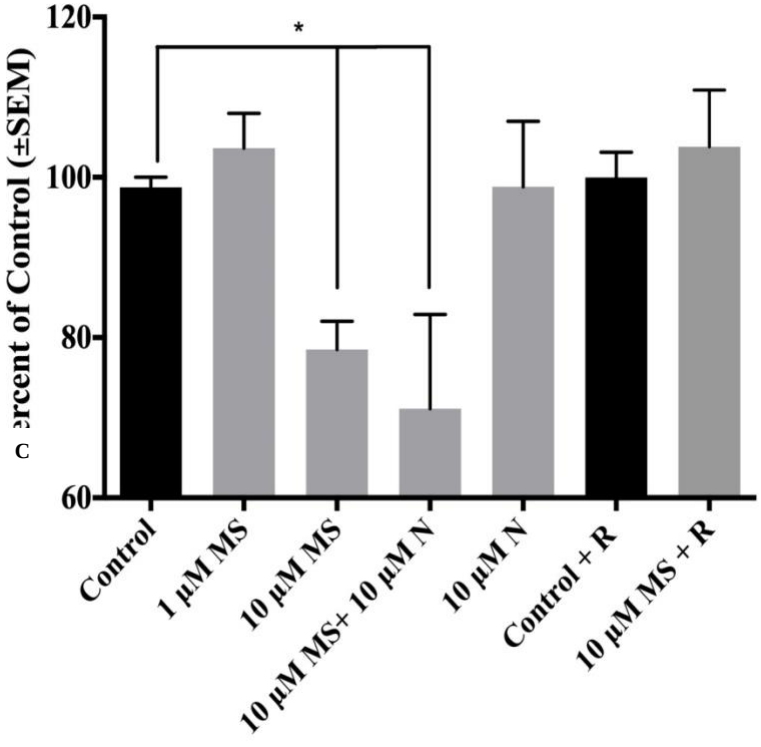

C

Figure 8. Effect of chronic MS exposure on genomic levels of H3K9me1.
iPSC were collected during every passage, and analyzed similarly on days 8, 11, 14, 17, 20, 23, 26, and 29 respectively. Data are expressed as days in cell culture versus quantity of histone modification in ng/mg total protein. Figures 8A, 8B, and 8C show one representative independent experiment each (n=1) with 3 biological replicates. Figure 8D represents the genomic H3K9me1 data following 8d, 17d, and 29d MS exposure compiled from 3 independent experiments; Two-way ANOVA followed by Bonferroni's post-hoc test where $^{*}p<0.05$, $^{**}p<0.01$ and $^{***}p<0.001$ relative to control. Data represented as %Control ± SEM.

A

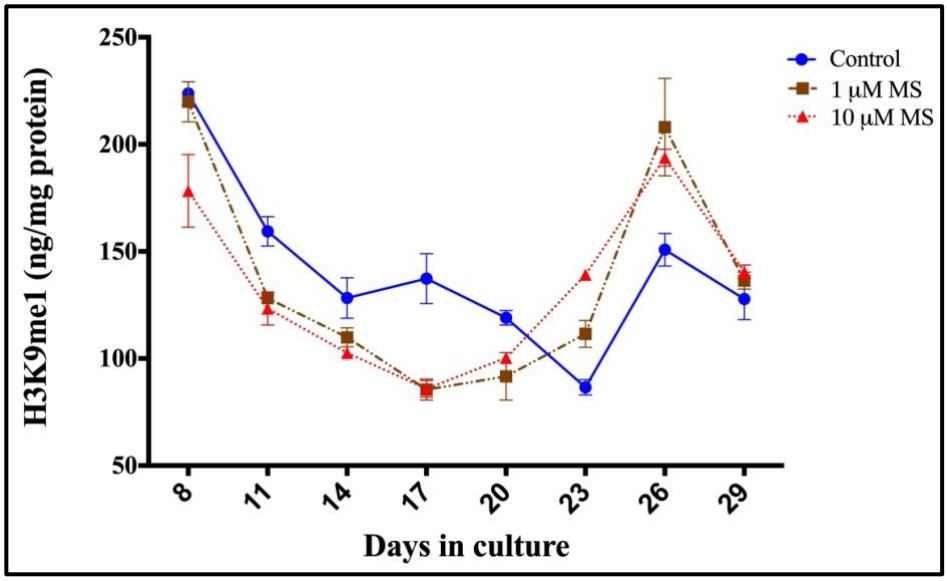

B

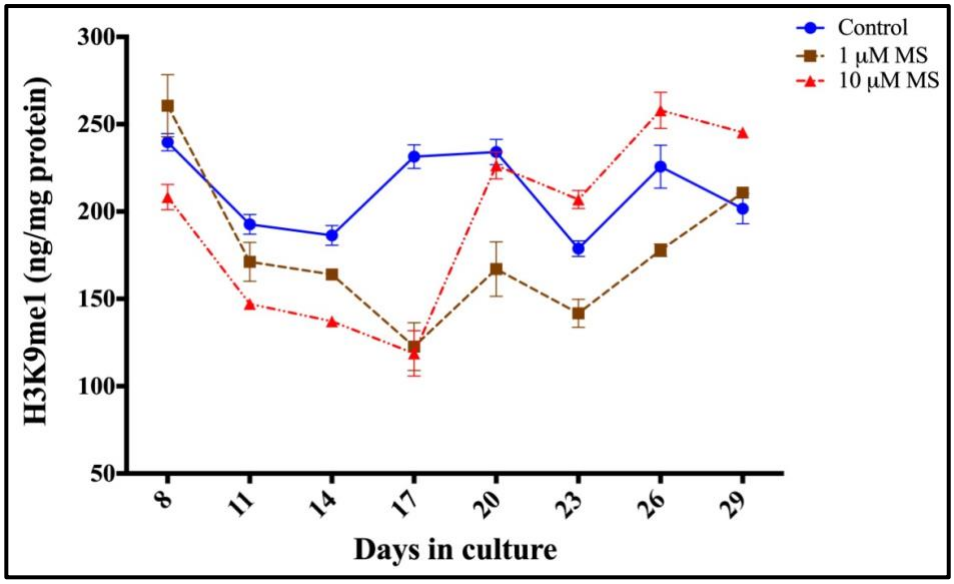

C

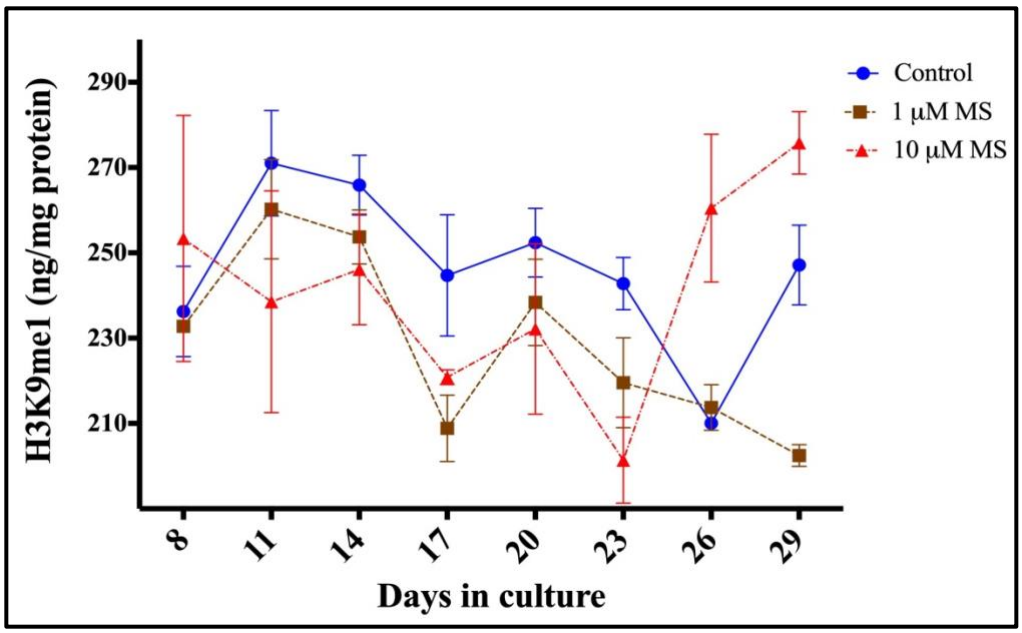

D

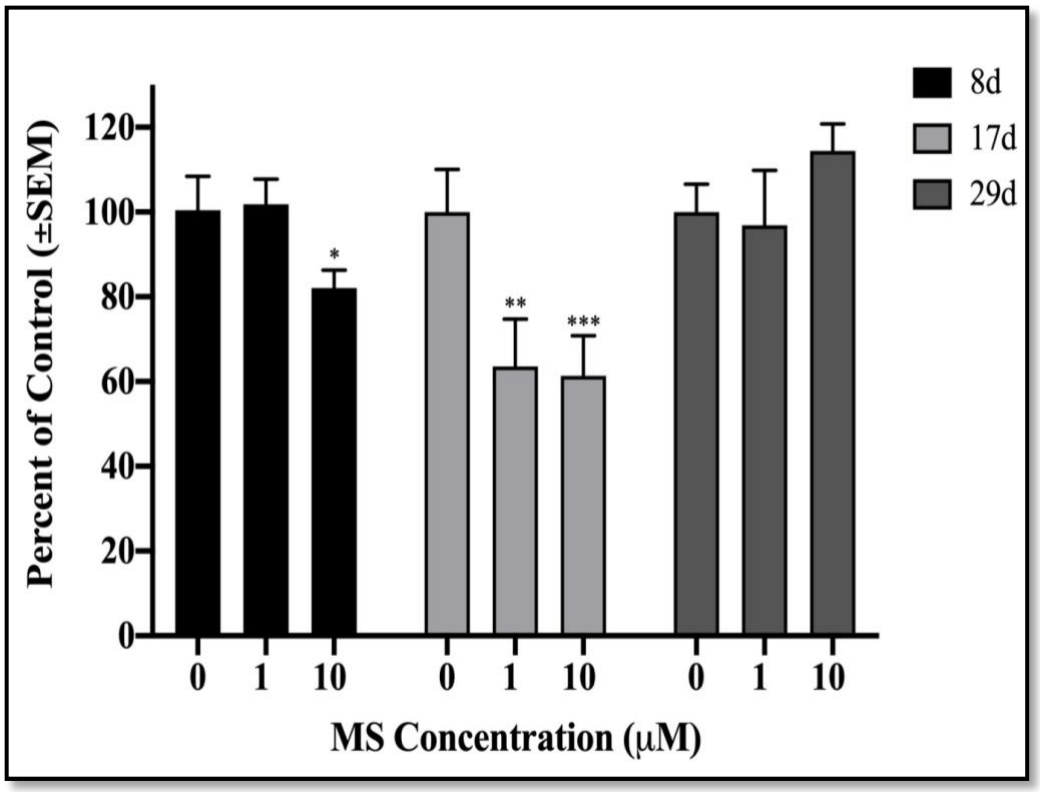

Figure 9. Effect of chronic MS exposure on genomic levels of H3K27me3.
iPSC were collected during every passage, and analyzed similarly on days 8, 11, 14, 17, 20, 23, 26, and 29 respectively. Data are expressed as days in cell culture versus quantity of histone modification in ng/mg total protein. Figures 9A, 9B, and 9C show one independent experiment each (n=1) with 3 biological replicates. Figure 9D represents the genomic H3K27me3 data following 8d, 17d, and 29d MS exposure compiled from 3 independent experiments; Two-way ANOVA followed by Bonferroni's post-hoc test where $^{*}p<0.05$ and $^{***}p<0.001$ relative to control. Data represented as %Control ± SEM.

A

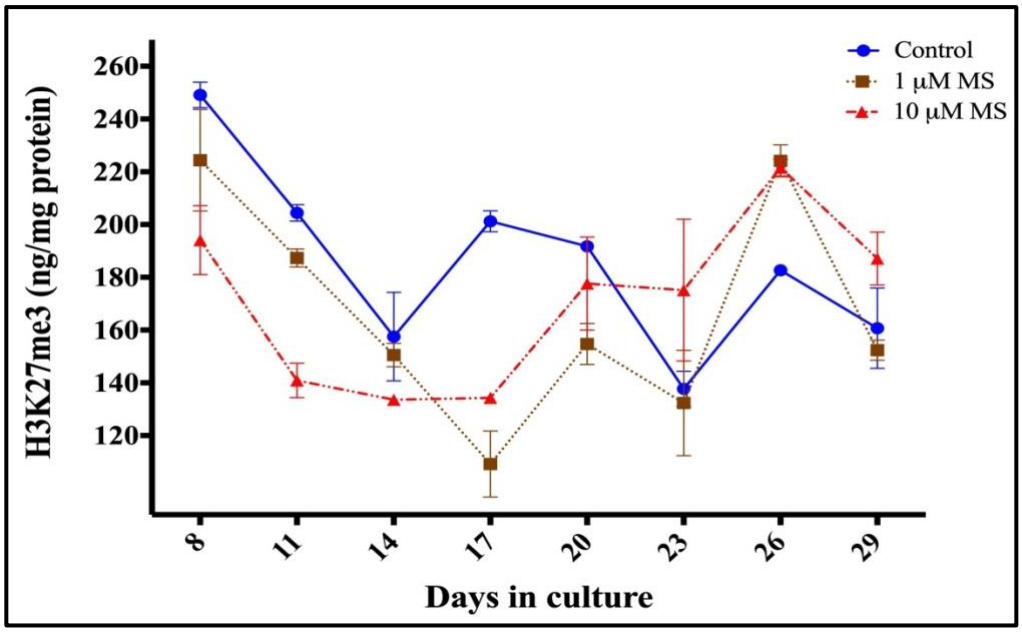

B

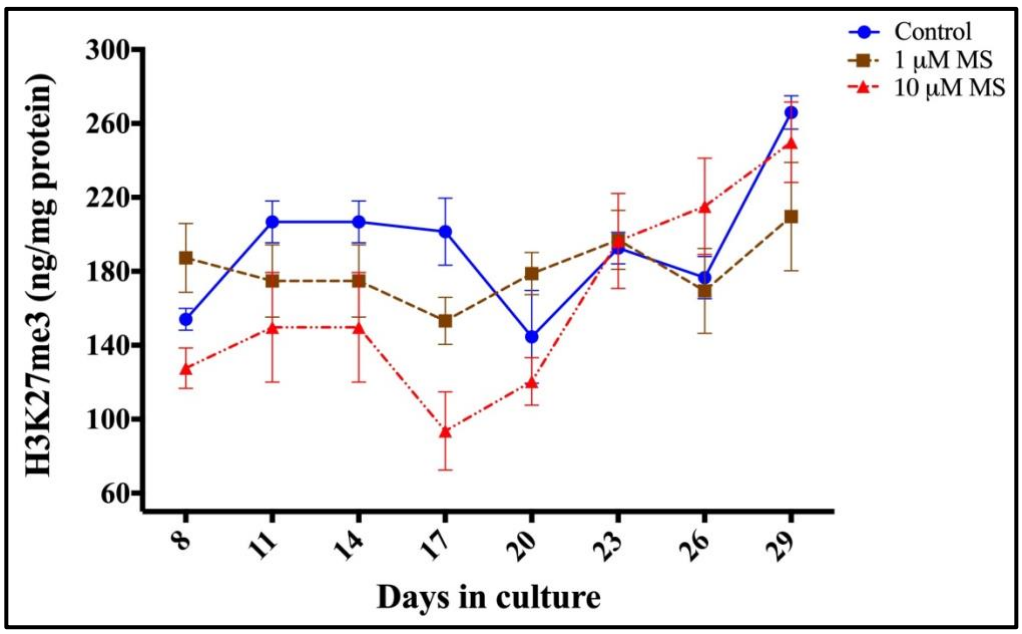

C

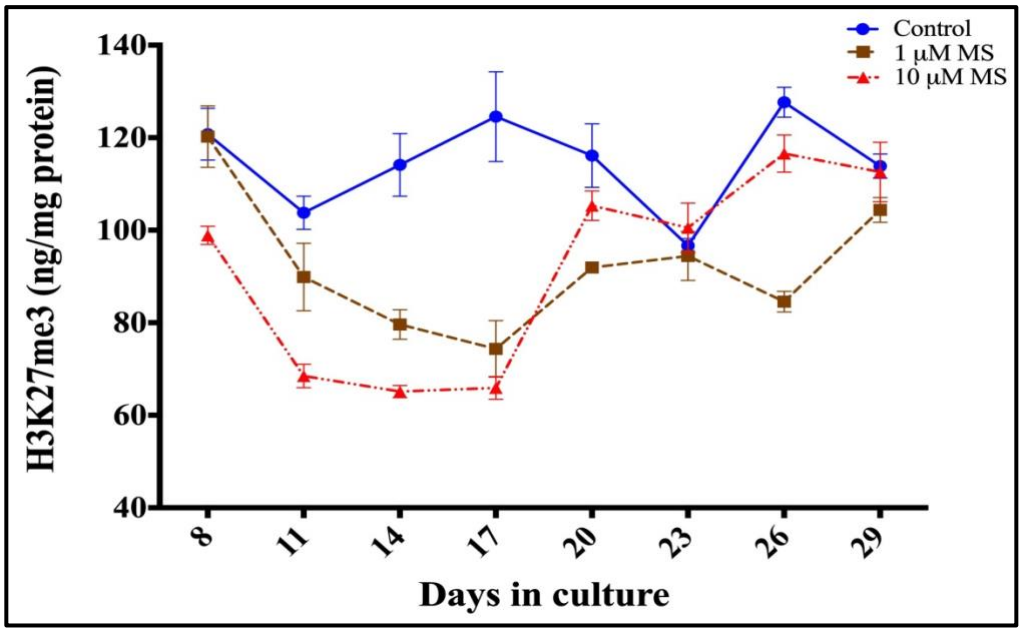

D

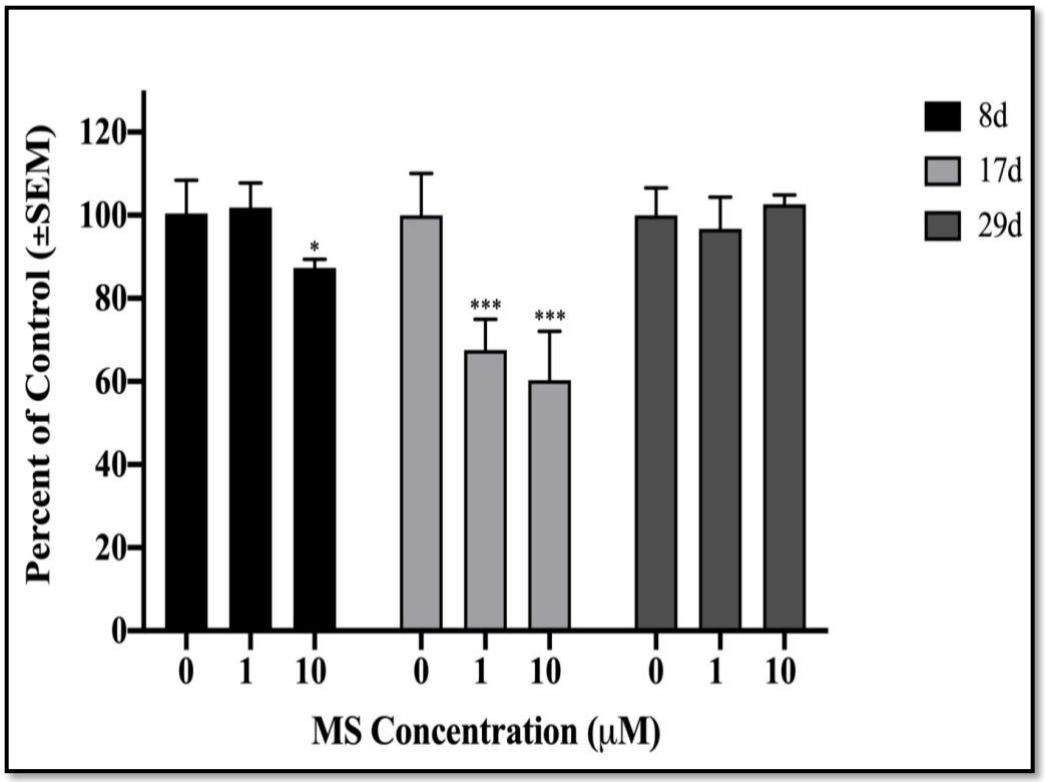

Figure 10. Volcano plot representing stem cell transcription regulating gene expression changes following 2d exposure to (A)MS, (B) nicotine, and (C) ethanol. Figures represent mean fold change in gene expressions relative to untreated mRNA samples, normalized by 18s rRNA's mRNA expression. Fold change data was analyzed using SAbiosciences statistical software. Experiment was performed 3 independent times with 3 replicates.

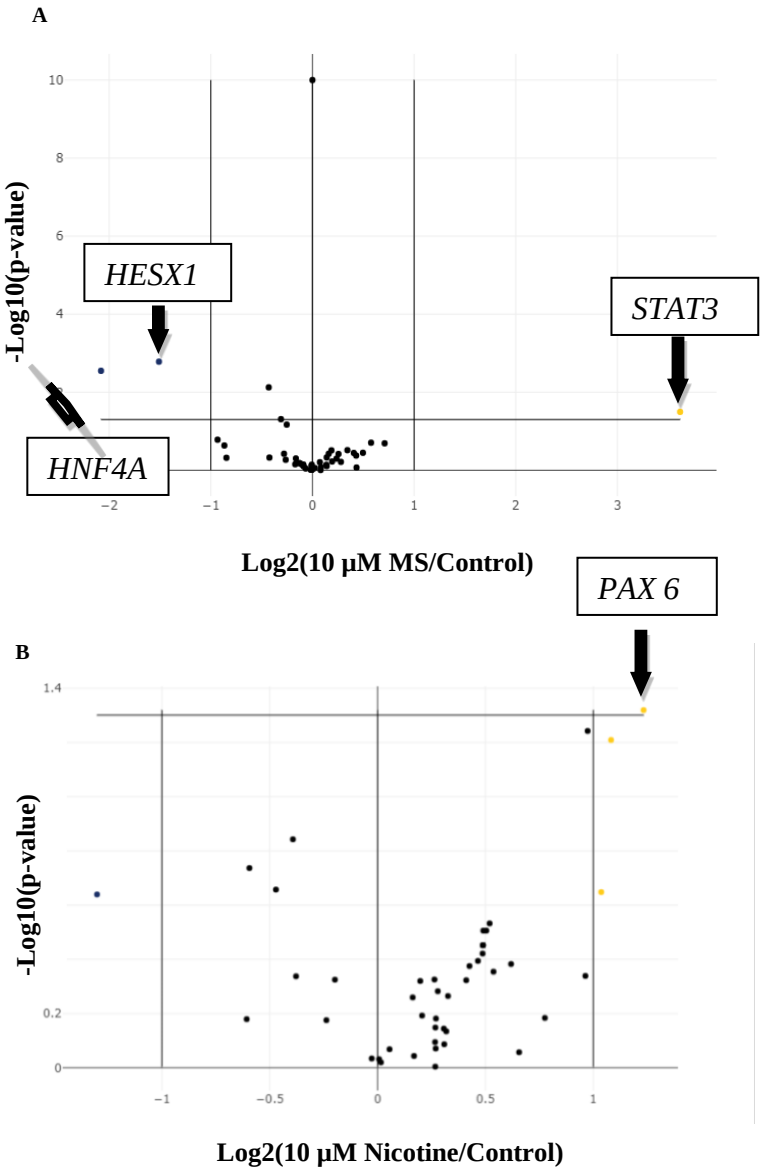

C

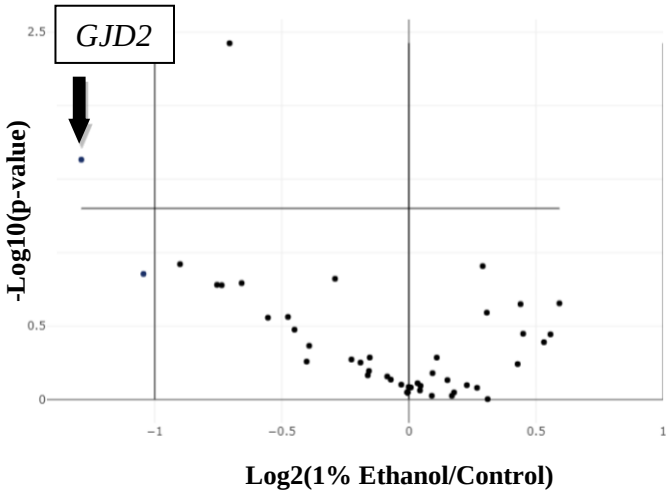

Figure 11. Gene expression changes of *STAT3* gene following continuous MS exposure.

Transcriptional up-regulation (UR) followed by down-regulation (DR) of *STAT3* gene as determined by qPCR. Data represent up/down-regulation ± SEM of normalized fold change mean relative to 18s rRNA mRNA levels followed by one-way ANOVA and Tukey's multiple comparisons post-hoc test. Experiment was performed 3 independent times with 3 replicates.

Refer table 5.

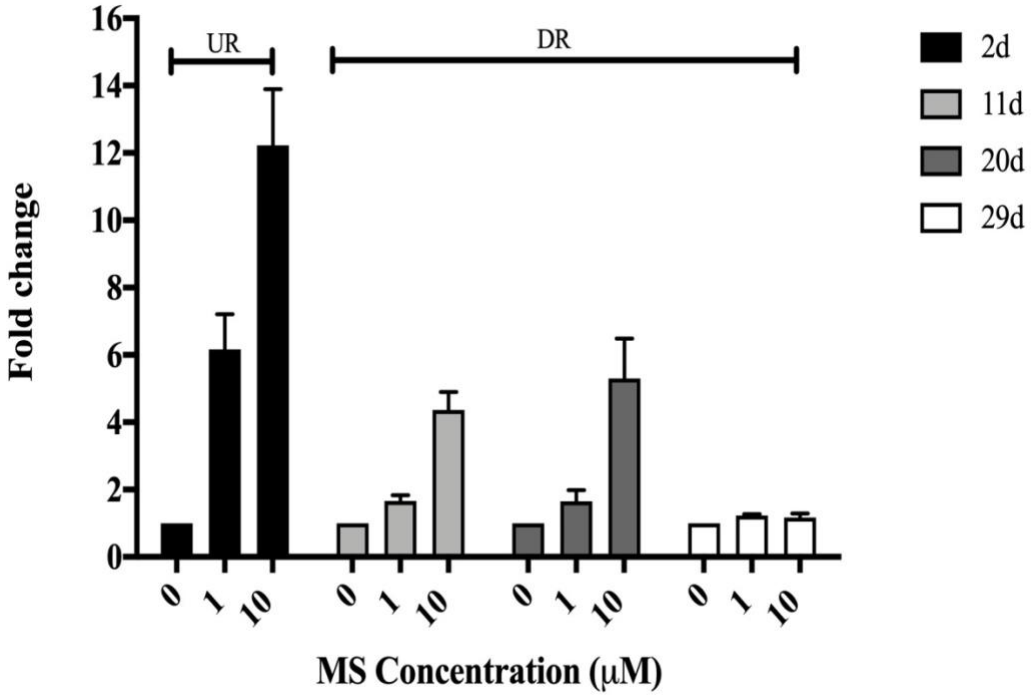

Figure 12. Effect of MS on STAT3 protein expression followed by 2d, 5d, and continuous exposure as determined by flow cytometry.
Percentage values obtained post-gating from 3 independent experiments with ≥ 2 replicates were further analyzed by two-way ANOVA and Bonferroni's post-hoc test where $^{*}p<0.05$ and $^{***}p<0.001$ relative to control. Data represented as %Gated ± SEM. (A) FC analysis of STAT3 protein levels in control-, MS exposed-, MS exposed and recovered-, pre-exposed to N followed by exposure to equimolar concentrations of MS and N -, and naltrexone exposed- iPSC; data expressed as percentage gated, where the lower gate limit was applied to the region excluding fluorescent positive population of unstained, and isotype control. PE-STAT3-2d (Panel 12B) and PE-STAT3-5d (Panel 12C). Panel's 12B and 12C show one representative FC scatter plot of each sample following 2- and 5-days MS exposure respectively. (D) FC analyses of changes in STAT3 protein levels on days 2, 11, 20 and 29 respectively (Refer table 6).

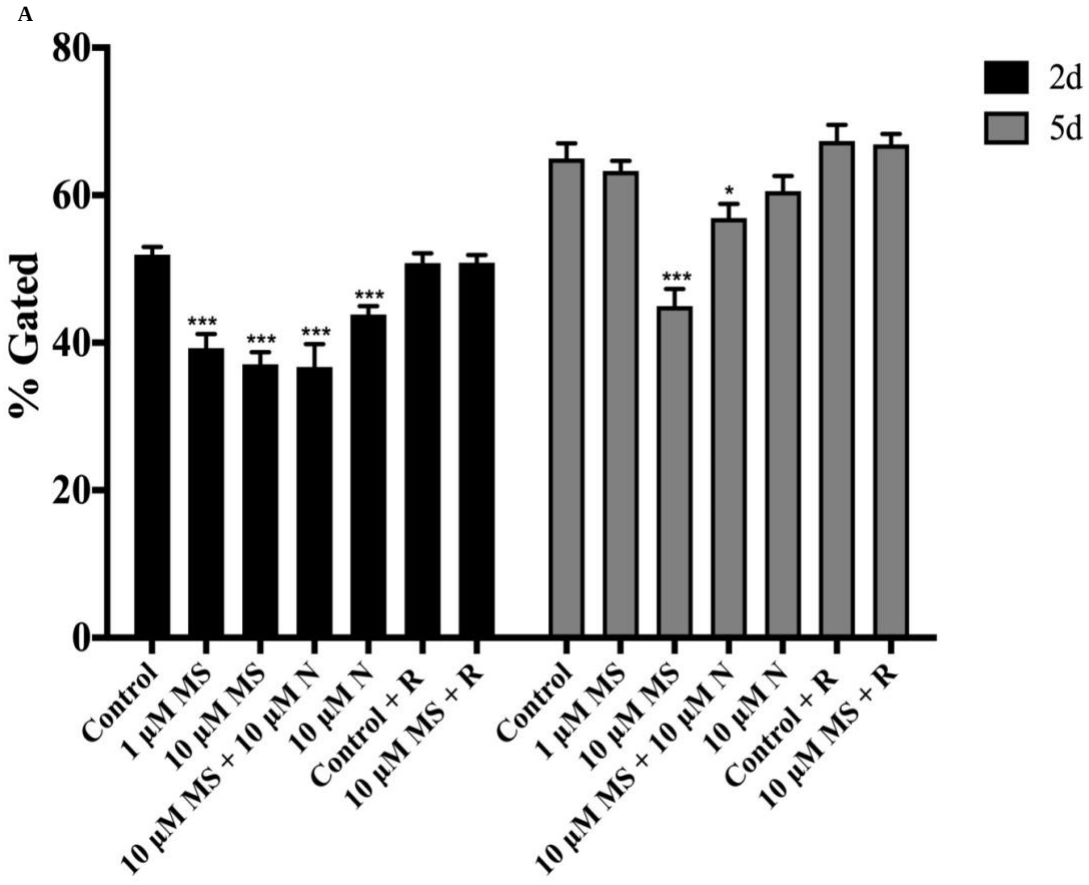

B

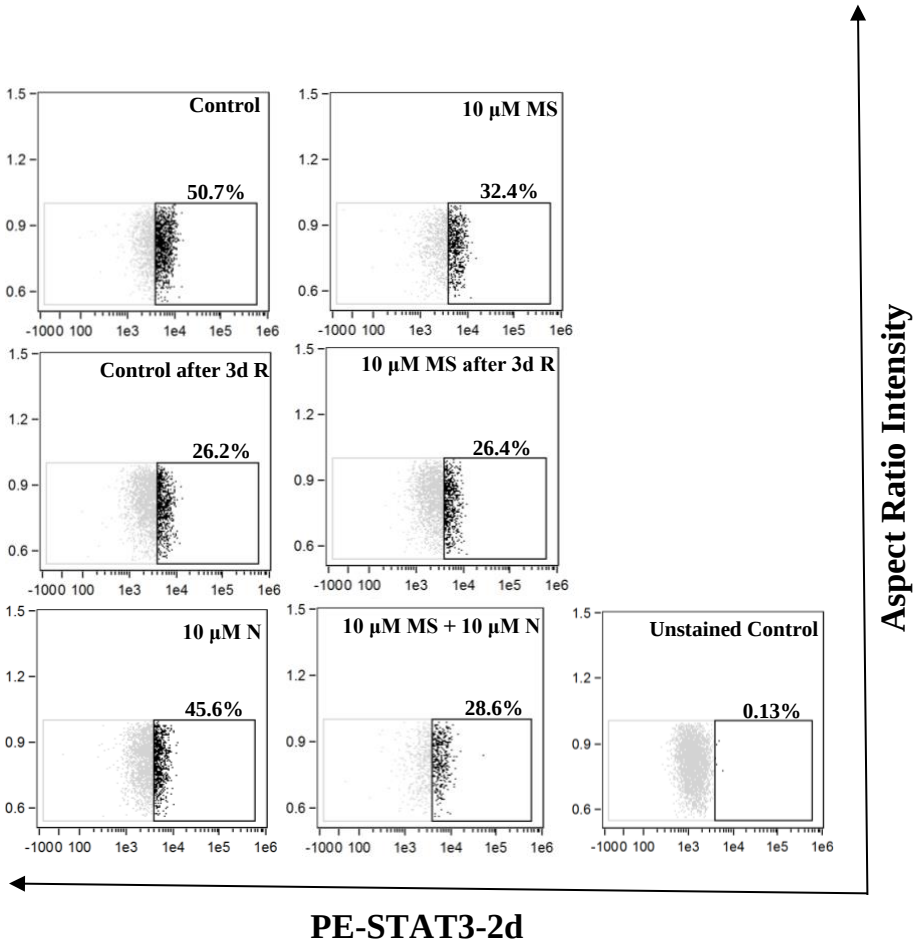

C

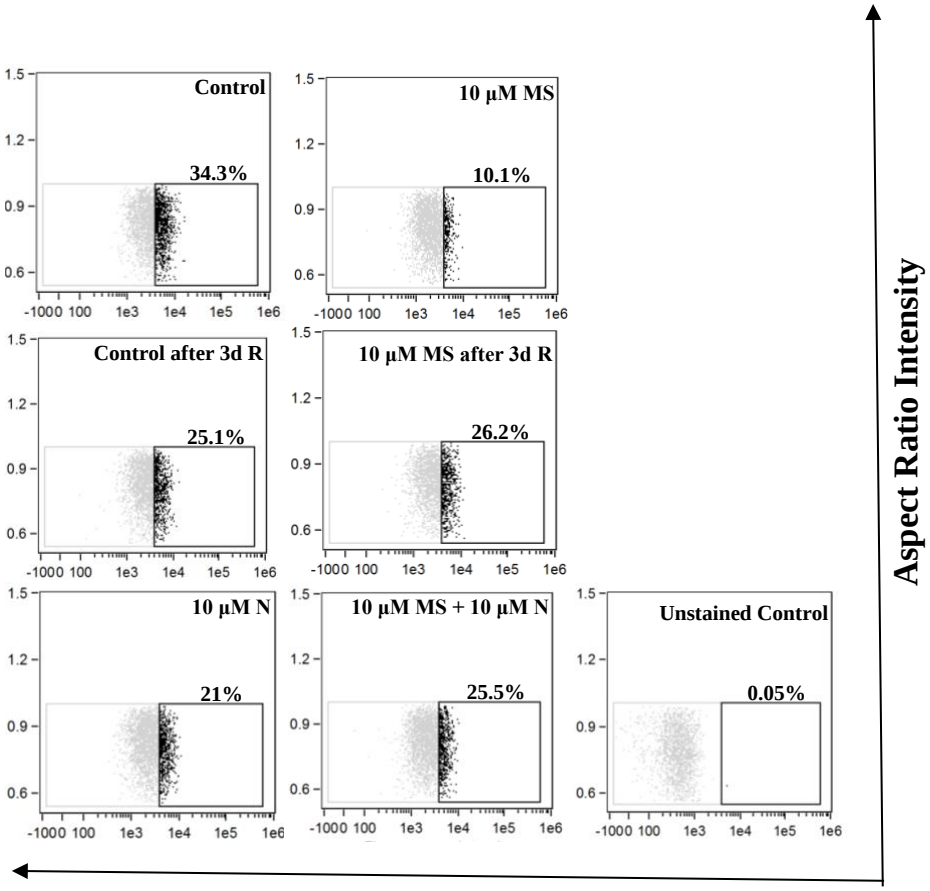

D

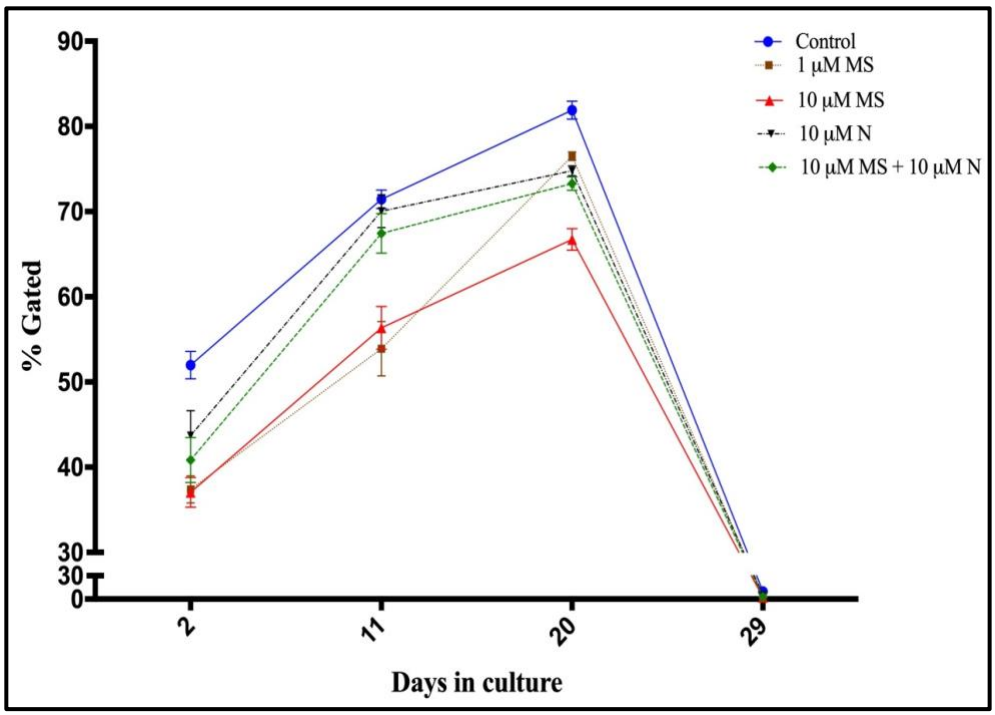

Figure 13. MS induced suppression in levels of STAT3-pTyr-705.
Figures A and B show FC mediated analysis of STAT3 protein levels from control-, MS exposed-, MS exposed and recovered-, pre-exposed to N followed by exposure to equimolar concentrations of MS and N-, and N exposed- samples of iPSC. Two-way ANOVA followed by Bonferroni's post-hoc test. Experiment was performed 3 independent times with 3 replicates. $^{*}p<0.05$, $^{**}p<0.01$, and $^{***}p<0.001$ relative to control. Data represented as %Gated ± SEM. (A) STAT3-pTyr-705, 2d MS exposure (B) STAT3-pTyr-705, 5d MS exposure. PE-STAT3-pSer-727-2d (Panel 13C) and PE-647-STAT3-pSer-727-5d (Panel 13D). Panel's 13C and 13D show one representative FC scatter plot of each sample following 2- and 5-day MS exposure, respectively. FC aided pattern analyses of changes in phosphorylated protein levels of STAT3-pSer-727 (E) protein levels on days 2, 11, 20 and 29, respectively. Experiment was performed 3 independent times with 3 replicates.; two-way ANOVA followed by Bonferroni's post-hoc test was used for statistical analyses (Refer table 7).

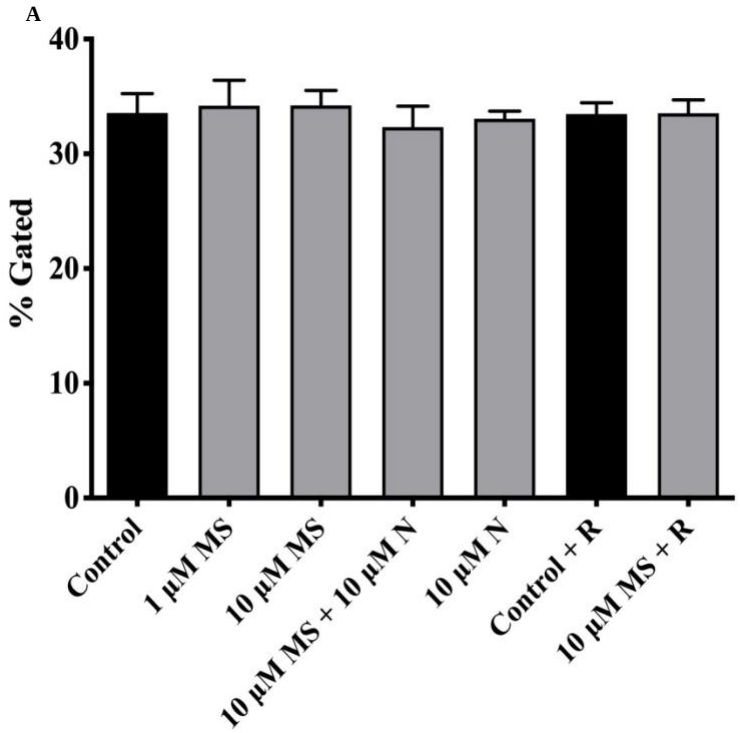

B

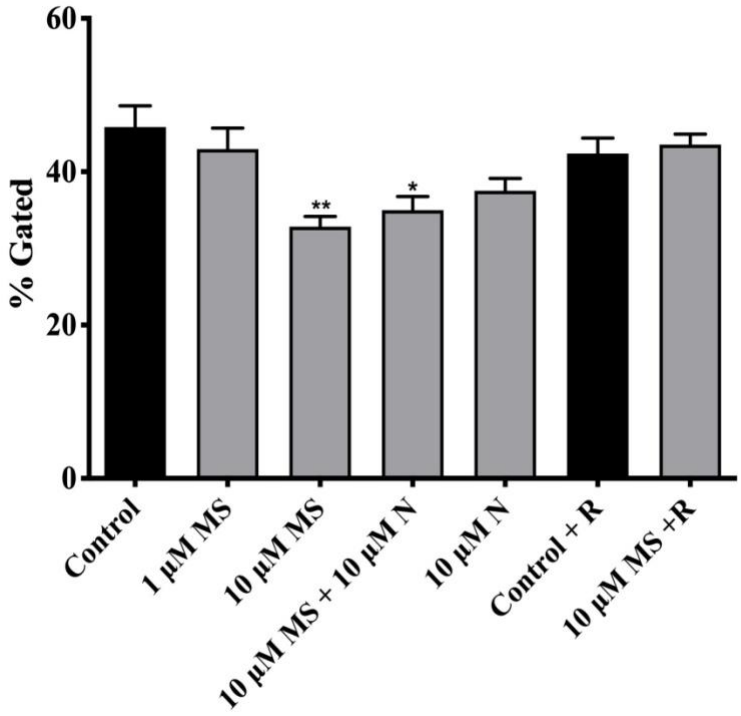

C

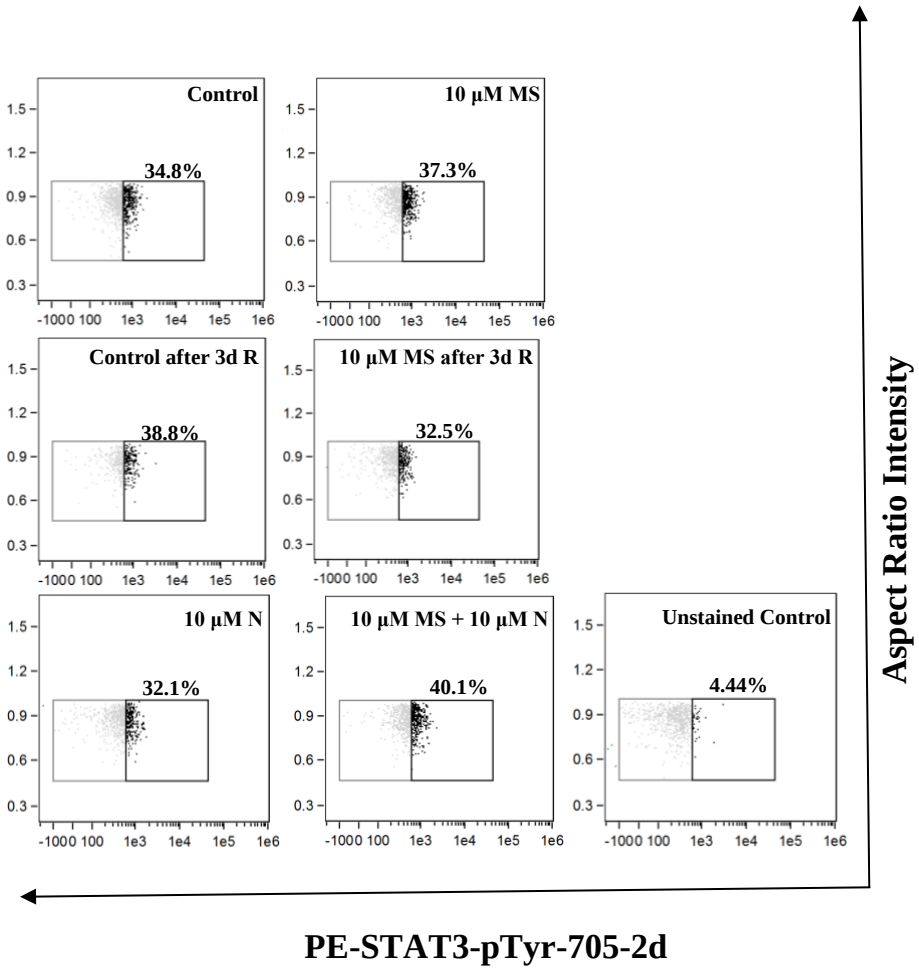

D

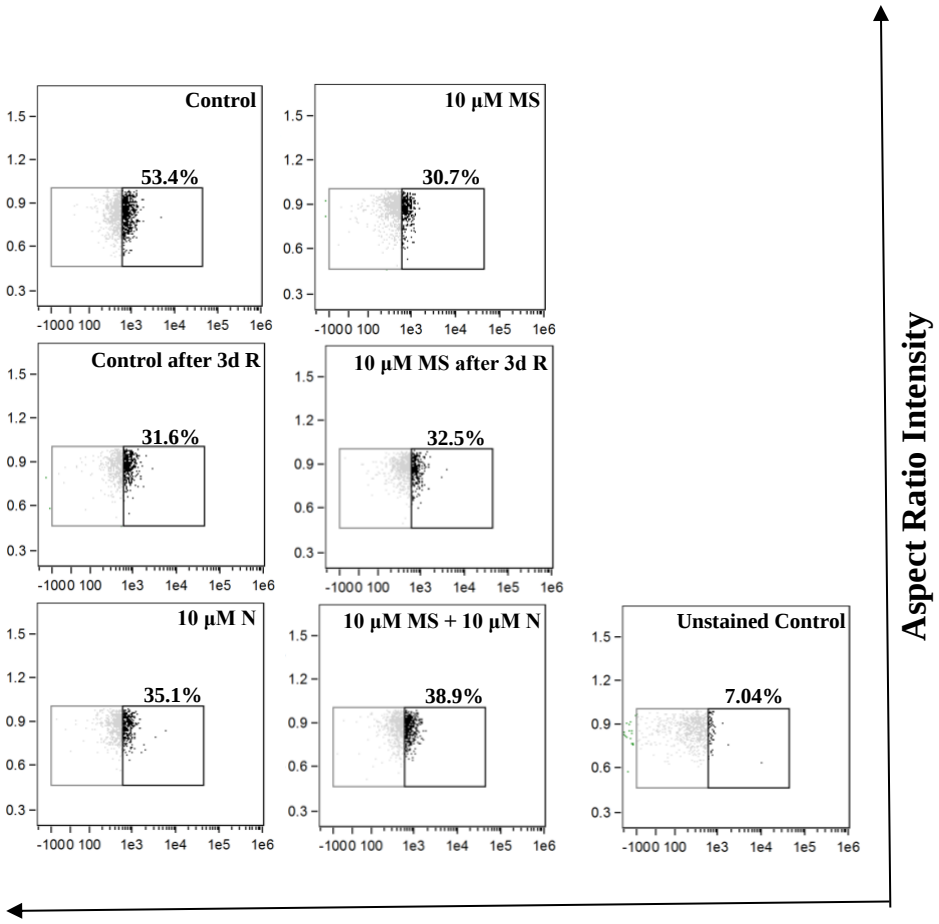

E

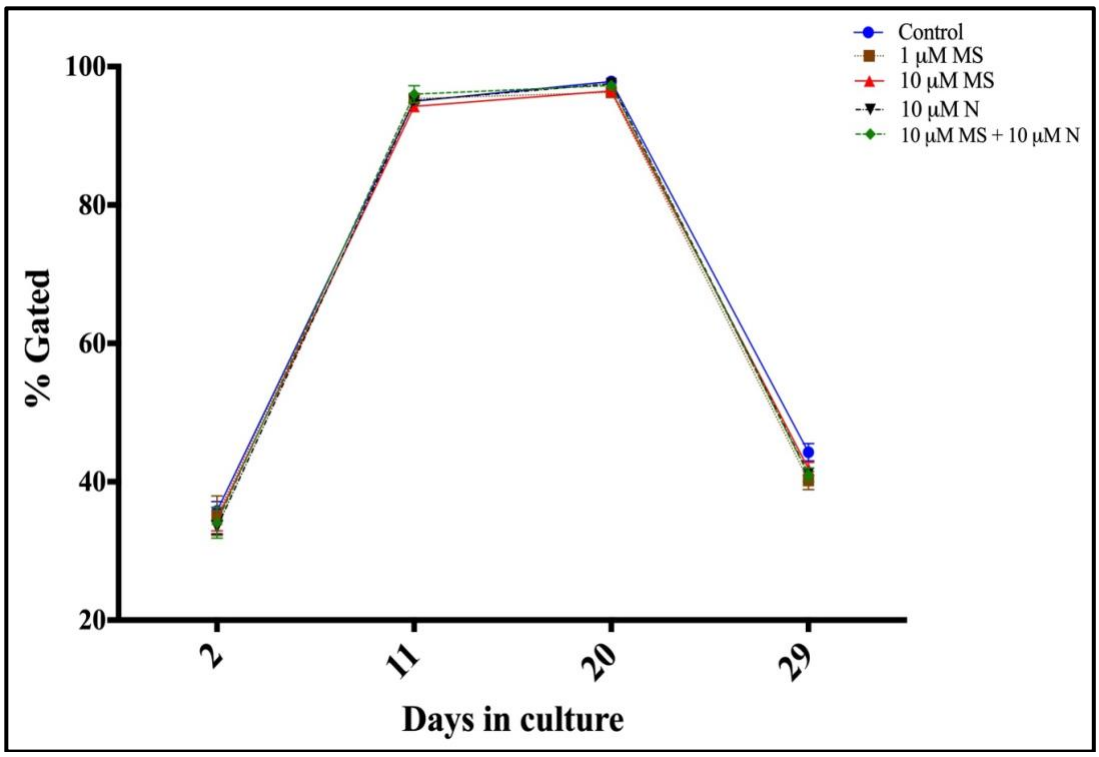

Figure 14. MS induced suppression in levels of STAT3-pSer-727.
Figures A and B show FC mediated analysis of STAT3 protein levels from control-, MS exposed-, MS exposed and recovered- (R), pre-exposed to N followed by exposure to equimolar concentrations of MS and N-, and N exposed- samples of iPSC.
Two-way ANOVA followed by Bonferroni's post-hoc test. Experiment was performed 3 independent times with 3 replicates. $^{**}p<0.01$, and $^{***}p<0.001$ relative to control. Data represented as %Gated ± SEM. (A) STAT3-pSer-727, 2d MS exposure (B) STAT3-pSer-727, 5d MS exposure. AlexaFluor-647-STAT3-pSer-727-2d (Panel 14C) and AlexaFluor-647-STAT3-pSer-727-5d (Panel 14D). Panel's 14C and 14D show one representative FC scatter plot of each sample following 2- and 5-day MS exposure, respectively. FC aided pattern analyses of changes in phosphorylated protein levels of STAT3-pSer-727 (E) protein levels on days 2, 11, 20 and 29, respectively. Experiment was performed 3 independent times with 3 replicates. $^{*}p<0.05$, $^{**}p<0.01$, and $^{***}p<0.001$ relative to control; two-way ANOVA followed by Bonferroni's post-hoc test was used for statistical analyses (Refer table 8).

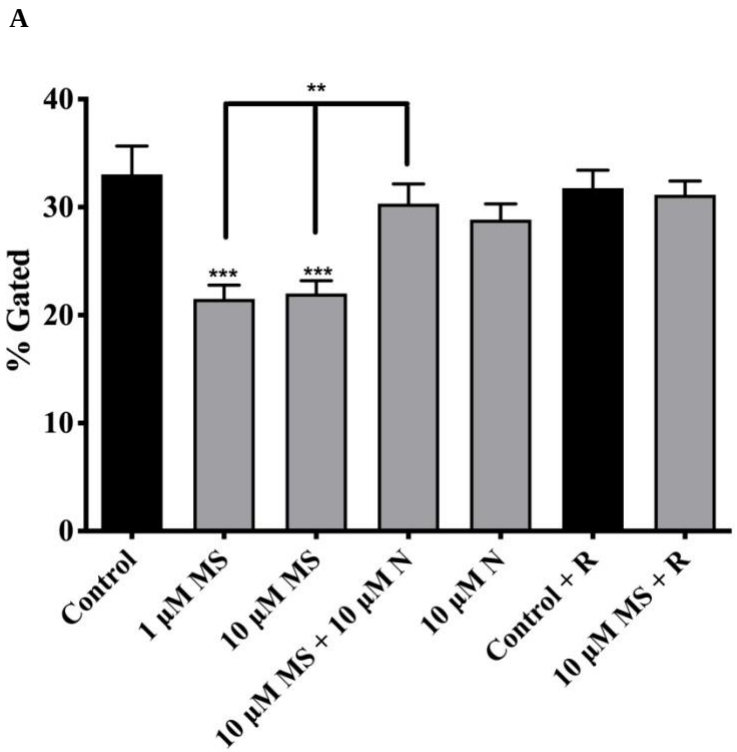

B

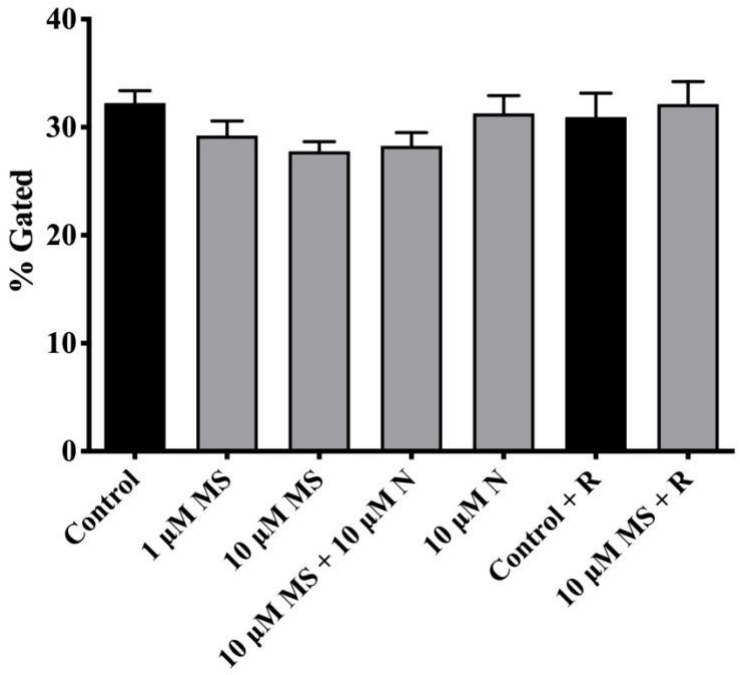

C

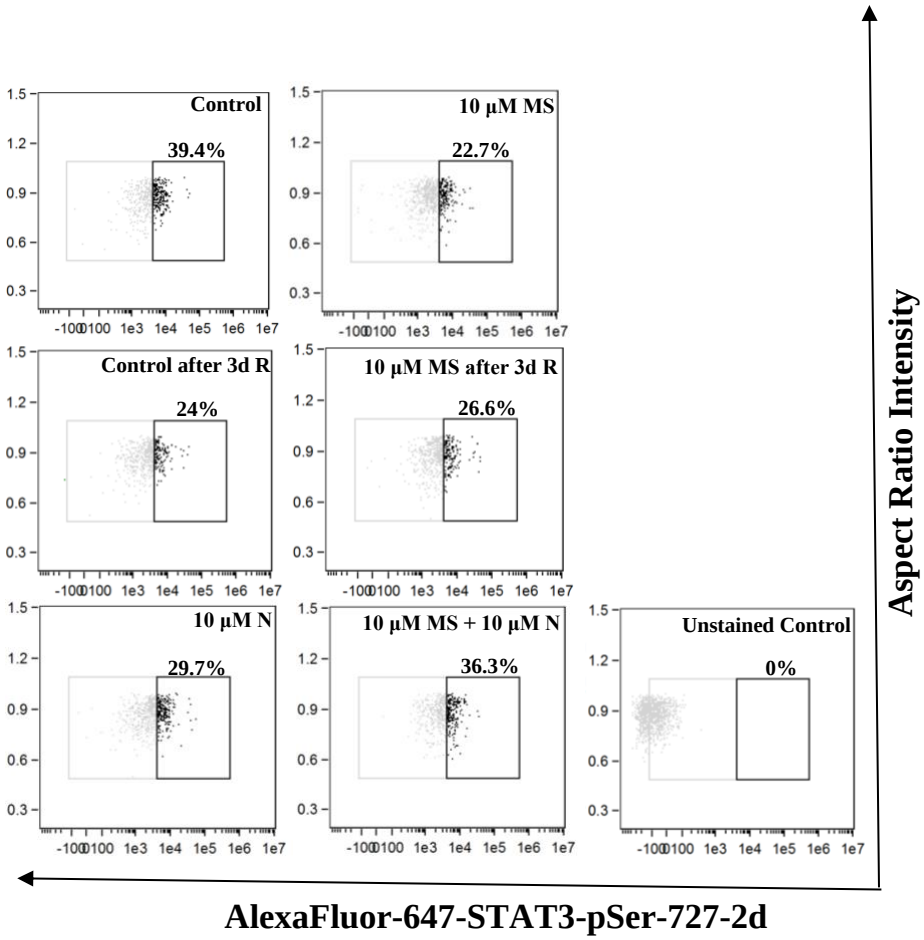

D

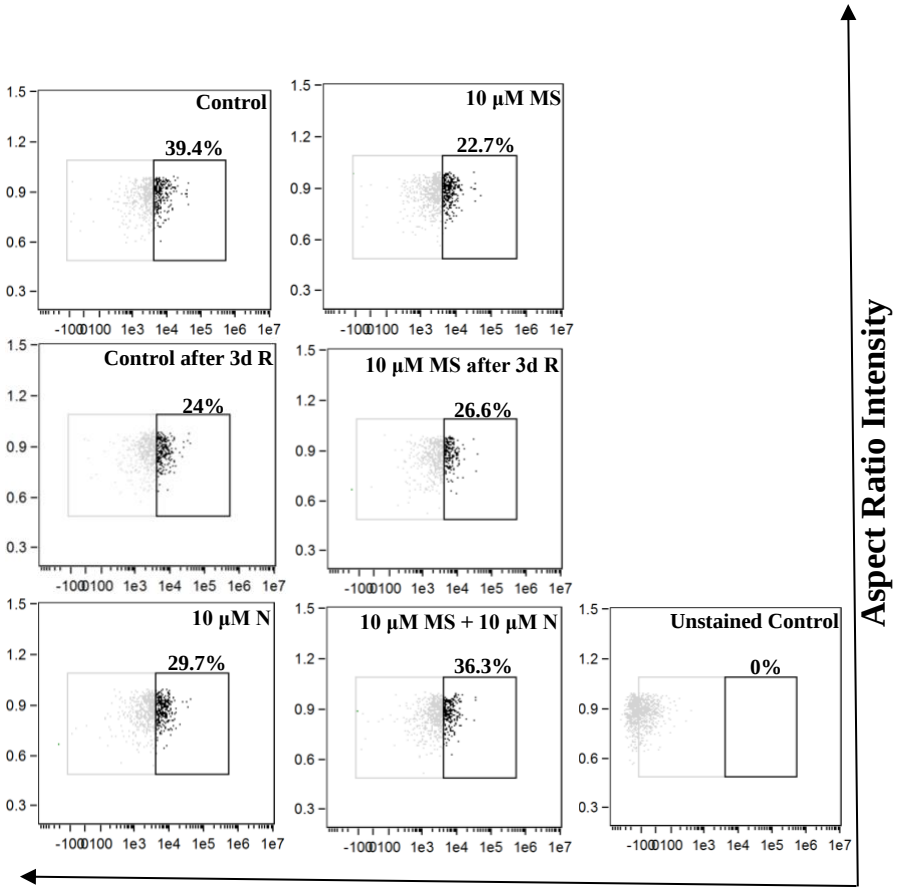

E

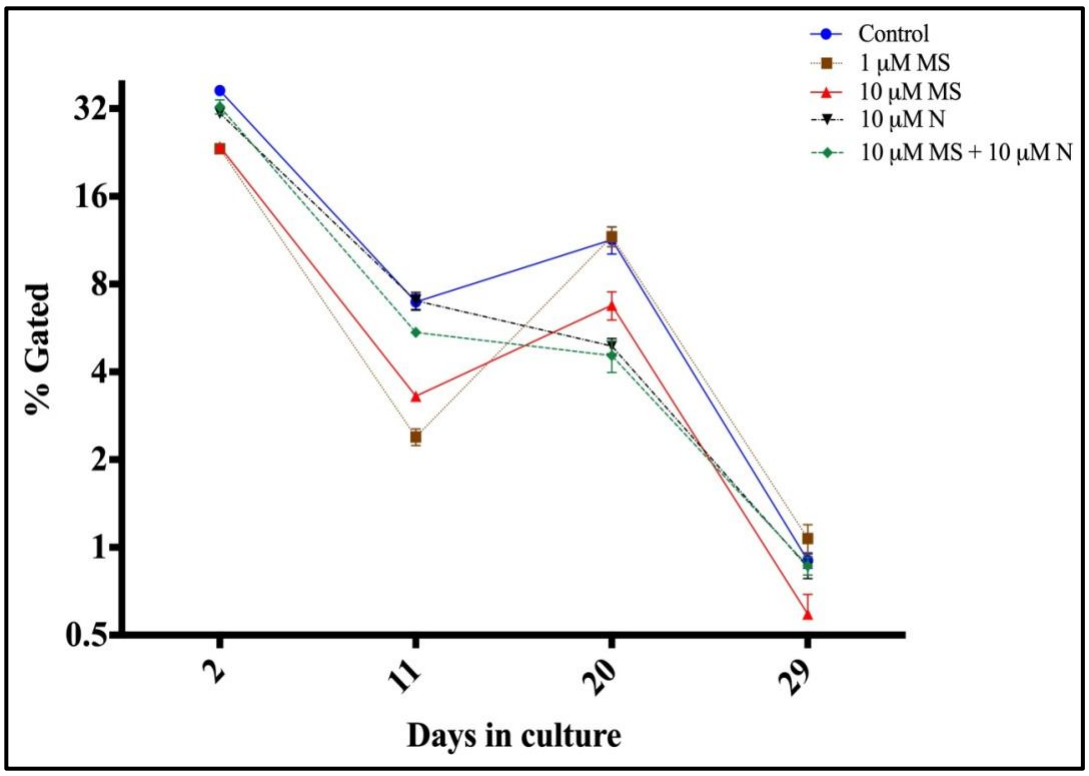

Figure 15. Opioid receptor genes expression changes following continuous exposure of MS to iPSC. Genes (A) *OPRM1*, (B) *OPRD1*, and (C) *OPRK1*.
OPRM1 demonstrated highest suppression in mRNA level following MS exposure. Transcriptional down-regulation followed by up-regulation of ORs genes as determined by RT-qPCR. Experiment was performed 3 independent times with 3 replicates. Data represent up/down-regulation ± SEM of normalized fold change mean relative to 18s rRNA, mRNA levels, followed by one-way ANOVA and Tukey's multiple comparisons post-hoc test (Refer table 9).

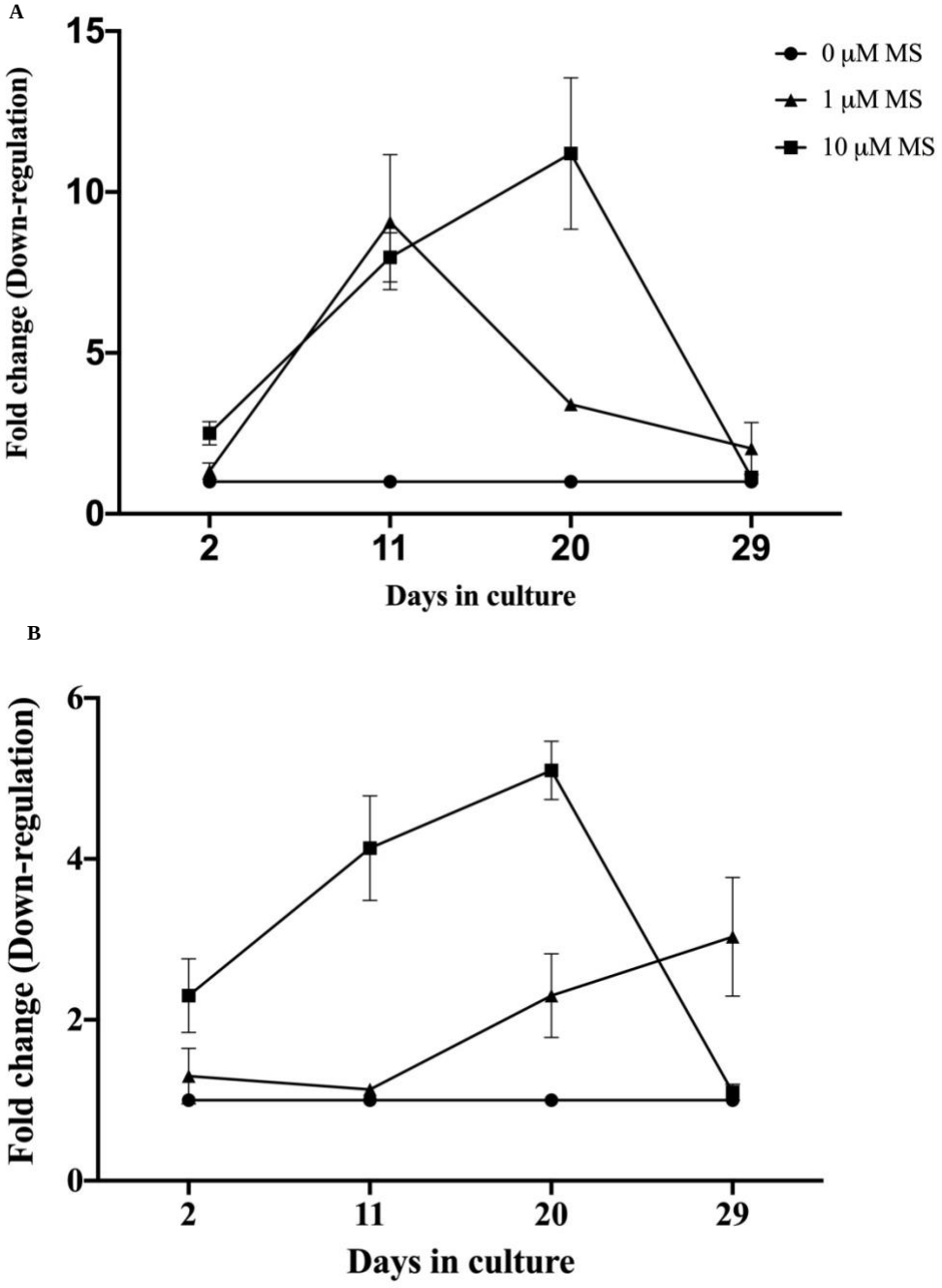

c

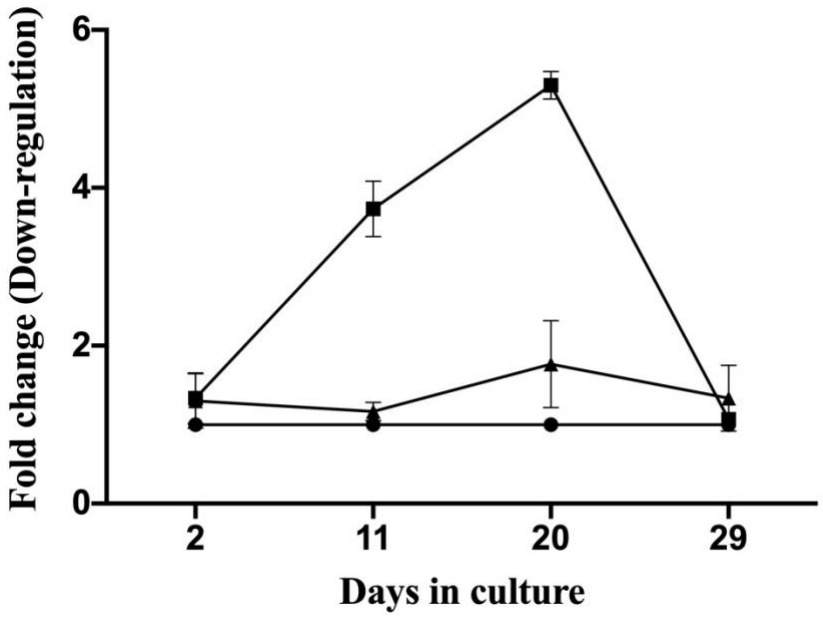

Figure 16. Effects of MS exposure on levels of pluripotency markers in iPSC. FC analyses of changes in (A) OCT4, (B) and TRA-1-60 protein levels on days 2, 11, 20, and 29 respectively. Two-way ANOVA followed by Bonferroni's post-hoc test was used for statistical analyses. Experiment was performed 3 independent times with 3 replicates. Data represented as %Gated ± SEM (Refer tables 10 and 11).

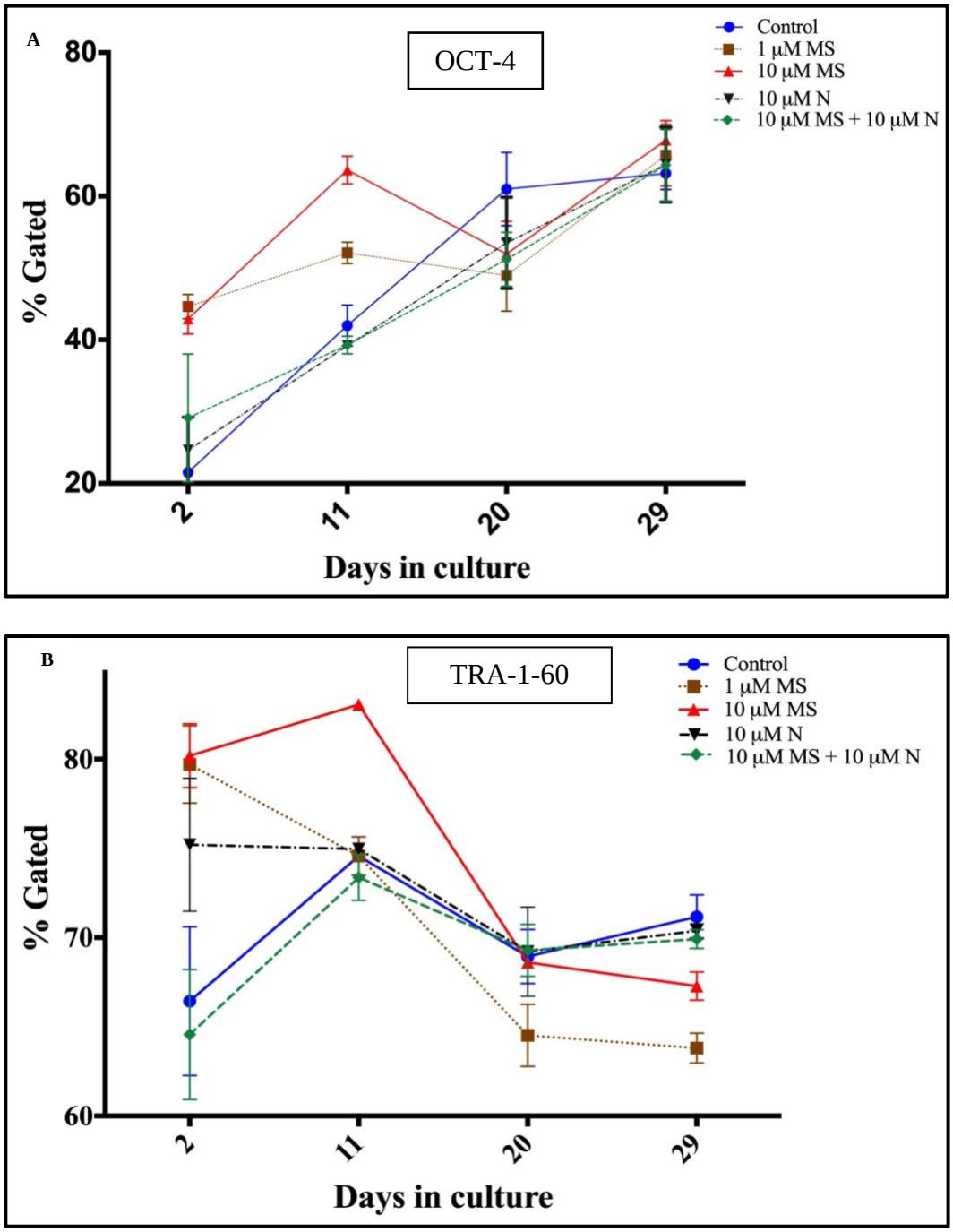

Table 1. Opiates,opioids, and their classification with respective compounds in each class.

Category	Compound
Natural Opiates	Morphine Codeine Narcotine Thebaine Papaverine Narceine
Natural Endogenous Opioids	β-endorphin Enkephelin Dynorphin
Semi-synthetic Opioids	Oxycodone Hydrocodone Hydromorphone Heroin
Fully Synthetic Opioids	Fentanyl Pethidine Levorphenol Methadone Tramadol Dextropropoxyphene

Table 2. Durations of MS exposure to iPSC after which the cell samples were collected for downstream analyses.

Target measured- Method	**Days in culture with MS exposure followed by cell sample collection for these days listed**
H3K9me1-**ELISA**	2;8;11;14;17;20;23;26;29
H3K27me3-**ELISA**	2;5;8;11;14;17;20;23;26;29
Levels of STAT3; STAT3-pSer-727; STAT3-pTyr-705- **FC**	2;11;20;29
Gene expression analyses of 44 stem cell transcription regulation genes and *OPRM1*, *OPRD1*, *OPRK1*, and *STAT3*- **RT-qPCR**	2;11;20;29
Levels of Oct-4 and TRA-1-60- **FC**	2;11;20;29

Table 3. H3-PTMs measured using ELISA-based multiplex assay, following exposure to MS, nicotine and ethanol in iPSC. UR: up-regulation; DR: down-regulation.

H3-PTM	10 µM MS- 2d	10 µM MS- 5d	10 µM Nicotine- 5d	1% Ethanol-5d
Total H3	-	-	-	-
H3K9ac	-	-	-	-
H3K14ac	-	-	-	-
H3K18ac	-	-	UR	-
H3K56ac	-	-	-	-
H3ser10P	-	-	UR	-
H3ser28P	-	-	DR	-
H3K4me1	-	-	-	-
H3K4me2	-	-	-	-
H3K4me3	-	-	-	-
H3K9me1	DR	-	-	-
H3K9me2	-	-	-	-
H3K9me3	-	-	-	-
H3K27me1	-	-	-	-
H3K27me2	-	-	-	-
H3K27me3	-	DR	-	-
H3K36me1	-	-	-	-
H3K36me2	-	-	-	-
H3K36me3	-	-	-	-
H3K79me1	-	-	-	-
H3K79me2	-	-	UR	-
H3K79me3	-	-	-	-

Table 4. Stem cell transcriptional regulatory network genes whose expression changes were measured using RT-qPCR, following exposure to MS, nicotine, and ethanol in iPSC.

Well Position	Gene	Function of the protein encoded by corresponding gene:	Reference
A01	*18S*	Endogenous control	(Kuchipudi *et al.*, 2012)
A02	*GAPDH*	Endogenous control	(Toegel *et al.*, 2007)
A03	*HPRT1*	Endogenous control	(Fu et al., 2009)
A04	*GUSB*	Endogenous control	(Gubern *et al.*, 2009)
A05	*CALB1*	Member of the calcium-binding protein superfamily that includes calmodulin and troponin	(O. Li *et al.*, 2007)
A06	*CDX2*	Regulates early embryonic development of intestinal tract	(Bernardo *et al.*, 2011)
B01	*CDYL*	Reader protein of H3K9- and H3K27-methylation marks (Escamilla-Del-Arenal et al., 2013)(Escamilla-Del-Arenal et al., 2013)	(Mulligan *et al.*, 2008)
B02	*EOMES*	Transcription factor crucial for development of embryonic mesoderm and CNS in vertebrates (Pfeiffer et al., 2018)(Pfeiffer et al., 2018)	(Pfeiffer *et al.*, 2018)
B03	*ESX1*	Participates in transcriptional regulatory network in embryonic stem cells	(Fohn & Behringer, 2001)
B04	*FOXC1*	Encodes protein that binds to specific regions of DNA and modulate the activities of other genes	(Berry *et al.*, 2006)
B05	*FOXD3*	Maintenance of mammalian embryonic stem cell pluripotency and regulation of Nanog signaling pathway	(Guo *et al.*, 2002)
B06	*GATA4*	Regulates genes involved in embryogenesis and myocardial differentiation	(Shi *et al.*, 2017)
C01	*GATA6*	Family of zinc finger transcription factors involved in regulation of cellular differentiation and organogenesis	(Guye *et al.*, 2016)
C02	*GBX2*	Involved in neural crest differentiation and dopaminergic neurogenesis	*(*Chapman *et al.*, 1997)
C03	*GJD2*	Gap junction protein forming gap junction inter-cellular channel	(Green *et al.*, 2018)
C04	*GRIN1*	A critical subunit of N-methyl-D-aspartate receptors essential in formation of synaptic plasticity critical for memory and learning processes	(Cantley *et al.*, 2018)
C05	*GSX2*	Significant role in development of telencephalic region of the brain	(Qin *et al.*, 2017)

C06	*HAND1*	Member of helix-loop-helix family of transcription factor; participate in cardiac morphogenesis	(Fujita *et al.*, 2019)
D01	*HESX1*	Transcription factor involved in regulation and coordination of early embryonic development	(Pozzi *et al.*, 2019)
D02	*HNF4A*	Nuclear transcription factor which binds DNA as a homodimer; controls the expression of several genes, including hepatocyte nuclear factor 1 alpha, a transcription factor which regulates the expression of several hepatic genes	(Ng *et al.*, 2019)
D03	*HOXB1*	Transcription factor involved in morphogenesis in all multicellular organisms	(Zhou *et al.*, 2019)
D04	*ISL1*	DNA-binding transcriptional activator; recognizes and binds to the consensus octamer binding site 5'-ATAATTAA-3' in promoter of target genes	(Xiang *et al.*, 2018)
D05	*JARID2*	Regulation of histone methyltransferase complex recruitment essential for embryonic development	(Landeira *et al.*, 2010)
D06	*LHX5*	regulation of neuronal differentiation and migration during development of the central nervous system	(Sigova *et al.*, 2013)
E01	*MEIS1*	Homeobox protein belonging to the TALE ('three amino acid loop extension') family of homeodomain-containing proteins; required for hematopoiesis, megakaryocyte lineage development and vascular patterning	(H. Wang *et al.*, 2018)
E02	*MYF5*	Transcriptional activation of muscle-specific target genes and their differentiation	(J. Wu *et al.*, 2016)
E03	*MYST3*	The protein is composed of a nuclear localization domain, a double C2H2 zinc finger domain that binds to acetylated histone tails, a histone acetyl-transferase domain, a glutamate/aspartate-rich region, and a serine- and methionine-rich transactivation domain	(Y.-C. Wang *et al.*, 2015)
E04	*NANOG*	Transcriptional activation and repression involved in regulation of embryonic stem cells and inner cell mass; regulation of SMAD transcriptional complexes	(Z. Wang *et al.*, 2012)
E05	*NEUROD1*	Acts as a transcriptional activator mediating transcriptional activation by binding to E box-containing promoter consensus core sequences 5'-CANNTG-3'	(Borromeo *et al.*, 2016)
E06	*NEUROG1*	Transcription factor essential for neuronal differentiation	(Boisvert *et al.*, 2015)
F01	*ONECUT1*	Transcriptional activation of hepatic genes	(Sapkota et al., 2014)

F02	*OTX1*	Essential role in embryonic brain and sense organs development	(Larsen et al., 2010)
F03	*PAX6*	Transcription factors essential for maintenance cell functions at embryonic stage, and development of brain, spinal cord and pancreas	(X. Zhang *et al.*, 2010)
F04	*POU5F1*	Transcription factor that forms a trimeric complex with SOX2 on DNA and controls the expression of a genes essential for early embryogenesis and for embryonic stem cell pluripotency	(Gao *et al.*, 2013)
F05	*REST*	Transcriptional repression of neuronal genes in non-neuronal tissues	(Charbord *et al.*, 2013)
F06	*RFX4*	Transcriptional factor rendering transcriptional activation and essential for early brain development	(La Manno *et al.*, 2016)
G01	*RIF1*	Participates in DNA repair mechanisms	(Dan *et al.*, 2014)
G02	*SALL1*	Transcription factors essential for embryonic development	(J. Yang *et al.*, 2010)
G03	*SET*	Inhibition of histone acetylases, particularly to histone H4 causing transcriptional repression	(Kaliman *et al.*, 2014)
G04	*SIX3*	Transcription factor essential for development of forebrain and eyes	(Lavado & Oliver, 2011)
G05	*SKIL*	Actively participates in embryonic stem cell differentiation	(Roson-Burgo *et al.*, 2014)
G06	*SMARCAD1*	Transcription factor promoting transcription initiation of several genes	(Xiao *et al.*, 2017)
H01	*SOX2*	Essential role in formation of several tissues and organs during embryonic development	(Pevny & Nicolis, 2010)
H02	*STAT3*	Refer introduction	Refer introduction
H03	*TCF7L1*	Essential for terminal differentiation of epidermal cells and involved in WNT signaling pathway	(Sierra *et al.*, 2018)
H04	*TRIM24*	Protein localizes in the nucleus and interacts with nuclear receptor signaling	(L.-H. Zhang *et al.*, 2015)
H05	*ZFHX3*	Transcriptional modulator regulating myogenic and neuronal differentiation	(D. Weber *et al.*, 2015)
H06	*ZIC3*	Transcriptional activator involved in embryonic left-right body axis formation	(Kumar *et al.*, 2012)

Table 5. Statistical analysis of *STAT3* gene expression following 2, 11, 20, and 29d MS exposure.

GENE	TWO-WAY ANOVA Bonferroni post tests (d vs d)	Statistical significance- Concentration of MS(µM), P value
STAT-3	2d vs 11d	1, P<0.001;10, P<0.001
	2d vs 20d	1, P<0.001;10, P<0.001
	2d vs 29d	1, P<0.001;10, P<0.001
	11d vs 20d	ns
	11d vs 29d	10, P<0.01
	20d vs 29d	10, P<0.001

Table 6. Statistical analysis of STAT3 protein levels following 2, 11, 20, and 29d MS exposure.

MARKER	DAY	TWO-WAY ANOVA Bonferroni post tests (d vs d)	Statistical significance- P value
STAT3	2d	C vs 1 μM MS	P<0.01
		C vs 10 μM MS	P<0.01
		C vs 10 μM N	ns
		C vs 10 μM MS + 10 μM N	ns
		1 μM MS vs 10 μM MS	ns
		1 μM MS vs 10 μM N	P<0.01
		1 μM MS vs 10 μM MS + 10 μM N	P<0.05
		10 μM MS vs 10 μM N	P<0.05
		10 μM MS vs 10 μM MS + 10 μM N	ns
		10 μM N vs 10 μM MS + 10 μM N	ns
	11d	C vs 1 μM MS	ns
		C vs 10 μM MS	P<0.01
		C vs 10 μM N	ns
		C vs 10 μM MS + 10 μM N	ns
		1 μM MS vs 10 μM MS	ns
		1 μM MS vs 10 μM N	ns
		1 μM MS vs 10 μM MS + 10 μM N	ns
		10 μM MS vs 10 μM N	P<0.001
		10 μM MS vs 10 μM MS + 10 μM N	ns
		10 μM N vs 10 μM MS + 10 μM N	ns
	20d	C vs 1 μM MS	ns
		C vs 10 μM MS	ns
		C vs 10 μM N	ns
		C vs 10 μM MS + 10 μM N	ns
		1 μM MS vs 10 μM MS	ns
		1 μM MS vs 10 μM N	ns
		1 μM MS vs 10 μM MS + 10 μM N	ns
		10 μM MS vs 10 μM N	ns
		10 μM MS vs 10 μM MS + 10 μM N	ns
		10 μM N vs 10 μM MS + 10 μM N	ns
	29d	C vs 1 μM MS	ns
		C vs 10 μM MS	ns
		C vs 10 μM N	ns
		C vs 10 μM MS + 10 μM N	ns
		1 μM MS vs 10 μM MS	ns
		1 μM MS vs 10 μM N	ns
		1 μM MS vs 10 μM MS + 10 μM N	ns
		10 μM MS vs 10 μM N	ns
		10 μM MS vs 10 μM MS + 10 μM N	ns
		10 μM N vs 10 μM MS + 10 μM N	ns

Table 7. Statistical analysis of STAT3-pTyr-705 protein levels following 2, 11, 20, and 29d MS exposure.

MARKER	DAY	TWO-WAY ANOVA Bonferroni post tests (d vs d)	Statistical significance-P value
STAT3-pTyr-705	2d	C vs 1 μM MS	ns
		C vs 10 μM MS	ns
		C vs 10 μM N	ns
		C vs 10 μM MS + 10 μM N	ns
		1 μM MS vs 10 μM MS	ns
		1 μM MS vs 10 μM N	ns
		1 μM MS vs 10 μM MS + 10 μM N	ns
		10 μM MS vs 10 μM N	ns
		10 μM MS vs 10 μM MS + 10 μM N	ns
		10 μM N vs 10 μM MS + 10 μM N	ns
	11d	C vs 1 μM MS	ns
		C vs 10 μM MS	ns
		C vs 10 μM N	ns
		C vs 10 μM MS + 10 μM N	ns
		1 μM MS vs 10 μM MS	ns
		1 μM MS vs 10 μM N	ns
		1 μM MS vs 10 μM MS + 10 μM N	ns
		10 μM MS vs 10 μM N	ns
		10 μM MS vs 10 μM MS + 10 μM N	ns
		10 μM N vs 10 μM MS + 10 μM N	ns
	20d	C vs 1 μM MS	ns
		C vs 10 μM MS	ns
		C vs 10 μM N	ns
		C vs 10 μM MS + 10 μM N	ns
		1 μM MS vs 10 μM MS	ns
		1 μM MS vs 10 μM N	ns
		1 μM MS vs 10 μM MS + 10 μM N	ns
		10 μM MS vs 10 μM N	ns
		10 μM MS vs 10 μM MS + 10 μM N	ns
		10 μM N vs 10 μM MS + 10 μM N	ns
	29d	C vs 1 μM MS	ns
		C vs 10 μM MS	ns
		C vs 10 μM N	ns
		C vs 10 μM MS + 10 μM N	ns
		1 μM MS vs 10 μM MS	ns
		1 μM MS vs 10 μM N	ns
		1 μM MS vs 10 μM MS + 10 μM N	ns
		10 μM MS vs 10 μM N	ns
		10 μM MS vs 10 μM MS + 10 μM N	ns
		10 μM N vs 10 μM MS + 10 μM N	ns

Table 8. Statistical analysis of STAT3-pSer-727 protein levels following 2, 11, 20, and 29d MS exposure.

MARKER	DAY	TWO-WAY ANOVA Bonferroni post tests (d vs d)	Statistical significance-P value
STAT3-pSer-727	2d	C vs 1 μM MS	P<0.01
		C vs 10 μM MS	P<0.01
		C vs 10 μM N	ns
		C vs 10 μM MS + 10 μM N	ns
		1 μM MS vs 10 μM MS	ns
		1 μM MS vs 10 μM N	P<0.01
		1 μM MS vs 10 μM MS + 10 μM N	P<0.05
		10 μM MS vs 10 μM N	P<0.05
		10 μM MS vs 10 μM MS + 10 μM N	ns
		10 μM N vs 10 μM MS + 10 μM N	ns
	11d	C vs 1 μM MS	ns
		C vs 10 μM MS	P<0.01
		C vs 10 μM N	ns
		C vs 10 μM MS + 10 μM N	ns
		1 μM MS vs 10 μM MS	ns
		1 μM MS vs 10 μM N	ns
		1 μM MS vs 10 μM MS + 10 μM N	ns
		10 μM MS vs 10 μM N	P<0.001
		10 μM MS vs 10 μM MS + 10 μM N	P<0.001
		10 μM N vs 10 μM MS + 10 μM N	ns
	20d	C vs 1 μM MS	ns
		C vs 10 μM MS	ns
		C vs 10 μM N	ns
		C vs 10 μM MS + 10 μM N	ns
		1 μM MS vs 10 μM MS	ns
		1 μM MS vs 10 μM N	ns
		1 μM MS vs 10 μM MS + 10 μM N	ns
		10 μM MS vs 10 μM N	ns
		10 μM MS vs 10 μM MS + 10 μM N	ns
		10 μM N vs 10 μM MS + 10 μM N	ns
	29d	C vs 1 μM MS	ns
		C vs 10 μM MS	ns
		C vs 10 μM N	ns
		C vs 10 μM MS + 10 μM N	ns
		1 μM MS vs 10 μM MS	ns
		1 μM MS vs 10 μM N	ns
		1 μM MS vs 10 μM MS + 10 μM N	ns
		10 μM MS vs 10 μM N	ns
		10 μM MS vs 10 μM MS + 10 μM N	ns
		10 μM N vs 10 μM MS + 10 μM N	ns

Table 9. Statistical analysis of *OPRMI, OPRD1,* and *OPRK1* gene expressions following 2, 11, 20, and 29d MS exposure.

GENE	ONE-WAY ANOVA Bonferroni post tests (d vs d)	Statistical significance- Concentration of MS(μM), P value
OPRM1	2d vs 11d	1, P<0.001;10, P<0.001
	2d vs 20d	1, P<0.05;10, P<0.001
	2d vs 29d	ns
	11d vs 20d	1, P<0.001;10, P<0.01
	11d vs 29d	1, P<0.001;10, P<0.001
	20d vs 29d	10, P<0.001
OPRD1	2d vs 11d	10, P<0.001
	2d vs 20d	1, P<0.05;10, P<0.001
	2d vs 29d	1, P<0.001;10, P<0.01
	11d vs 20d	1, P<0.01;10, P<0.05
	11d vs 29d	1.P<0.001, P<0.001
	20d vs 29d	10, P<0.001
OPRK1	2d vs 11d	10, P<0.001
	2d vs 20d	10, P<0.001
	2d vs 29d	ns
	11d vs 20d	1, P<0.05;10, P<0.001
	11d vs 29d	10, P<0.001
	20d vs 29d	10, P<0.001

Table 10. Statistical analysis of OCT4 protein levels following 2, 11, 20, and 29d MS exposure.

MARKER	DAY	TWO-WAY ANOVA Bonferroni post tests (d vs d)	Statistical significance- P value
OCT-4	2d	C vs 1 μM MS	P<0.01
		C vs 10 μM MS	P<0.01
		C vs 10 μM N	ns
		C vs 10 μM MS + 10 μM N	ns
		1 μM MS vs 10 μM MS	ns
		1 μM MS vs 10 μM N	P<0.01
		1 μM MS vs 10 μM MS + 10 μM N	P<0.05
		10 μM MS vs 10 μM N	P<0.05
		10 μM MS vs 10 μM MS + 10 μM N	ns
		10 μM N vs 10 μM MS + 10 μM N	ns
	11d	C vs 1 μM MS	ns
		C vs 10 μM MS	P<0.01
		C vs 10 μM N	ns
		C vs 10 μM MS + 10 μM N	ns
		1 μM MS vs 10 μM MS	ns
		1 μM MS vs 10 μM N	ns
		1 μM MS vs 10 μM MS + 10 μM N	ns
		10 μM MS vs 10 μM N	P<0.001
		10 μM MS vs 10 μM MS + 10 μM N	P<0.001
		10 μM N vs 10 μM MS + 10 μM N	ns
	20d	C vs 1 μM MS	ns
		C vs 10 μM MS	ns
		C vs 10 μM N	ns
		C vs 10 μM MS + 10 μM N	ns
		1 μM MS vs 10 μM MS	ns
		1 μM MS vs 10 μM N	ns
		1 μM MS vs 10 μM MS + 10 μM N	ns
		10 μM MS vs 10 μM N	ns
		10 μM MS vs 10 μM MS + 10 μM N	ns
		10 μM N vs 10 μM MS + 10 μM N	ns
	29d	C vs 1 μM MS	ns
		C vs 10 μM MS	ns
		C vs 10 μM N	ns
		C vs 10 μM MS + 10 μM N	ns
		1 μM MS vs 10 μM MS	ns
		1 μM MS vs 10 μM N	ns
		1 μM MS vs 10 μM MS + 10 μM N	ns
		10 μM MS vs 10 μM N	ns
		10 μM MS vs 10 μM MS + 10 μM N	ns
		10 μM N vs 10 μM MS + 10 μM N	ns

Table 11. Statistical analysis of TRA-1-60 protein levels following 2, 11, 20, and 29d MS exposure.

MARKER	DAY	TWO-WAY ANOVA Bonferroni post tests (d vs d)	Statistical significance- P value
TRA-1-60	2d	C vs 1 μM MS	ns
		C vs 10 μM MS	ns
		C vs 10 μM N	ns
		C vs 10 μM MS + 10 μM N	ns
		1 μM MS vs 10 μM MS	ns
		1 μM MS vs 10 μM N	ns
		1 μM MS vs 10 μM MS + 10 μM N	ns
		10 μM MS vs 10 μM N	ns
		10 μM MS vs 10 μM MS + 10 μM N	ns
		10 μM N vs 10 μM MS + 10 μM N	ns
	11d	C vs 1 μM MS	ns
		C vs 10 μM MS	ns
		C vs 10 μM N	ns
		C vs 10 μM MS + 10 μM N	ns
		1 μM MS vs 10 μM MS	ns
		1 μM MS vs 10 μM N	ns
		1 μM MS vs 10 μM MS + 10 μM N	ns
		10 μM MS vs 10 μM N	P<0.001
		10 μM MS vs 10 μM MS + 10 μM N	ns
		10 μM N vs 10 μM MS + 10 μM N	ns
	20d	C vs 1 μM MS	ns
		C vs 10 μM MS	ns
		C vs 10 μM N	ns
		C vs 10 μM MS + 10 μM N	ns
		1 μM MS vs 10 μM MS	ns
		1 μM MS vs 10 μM N	ns
		1 μM MS vs 10 μM MS + 10 μM N	ns
		10 μM MS vs 10 μM N	ns
		10 μM MS vs 10 μM MS + 10 μM N	ns
		10 μM N vs 10 μM MS + 10 μM N	ns
	29d	C vs 1 μM MS	ns
		C vs 10 μM MS	ns
		C vs 10 μM N	ns
		C vs 10 μM MS + 10 μM N	ns
		1 μM MS vs 10 μM MS	ns
		1 μM MS vs 10 μM N	ns
		1 μM MS vs 10 μM MS + 10 μM N	ns
		10 μM MS vs 10 μM N	ns
		10 μM MS vs 10 μM MS + 10 μM N	ns
		10 μM N vs 10 μM MS + 10 μM N	ns

4. DISCUSSION

Biomarkers, once validated, can serve as correlations to illicit drug use, addiction, and their relative prognosis (Chintalapati & Barile, 2019). Until recently, a majority of studies have focused on opioid-induced EG changes related to malformations in neuronal circuitry (Browne *et al*., 2020; Farris *et al*., 2015; Heller *et al*., 2016; Kenny, 2014). Consequently there has been limited attention to the EG mechanisms at the cellular level following opioid exposure (Liang *et al*., 2013; Oertel *et al*., 2012; Wachman *et al*., 2014). In this study, human-iPSC were used to study changes in genomic H3-PTM following prolonged periods of MS exposure. The data demonstrate a decrease in genomic H3K9me1 and H3K27me3 levels which was not antagonized by N. Interestingly, levels of transcriptionally repressive genomic H3K9me1 and H3K27me3 decrease over time followed by a rise, suggesting an initial accumulation of these modifications in chromatin. This is then shadowed by innate compensatory repair mechanisms or acquired resistance to continuous MS exposure *in vitro*. In addition, recovery with regular media post-MS exposure shifted H3-PTM levels to that of control effectively demonstrating the ability of iPSC to recover from MS-mediated EG insult. Studies examining EG effects of nicotine and ethanol are limited, but indicate that nicotine promotes acetylation of H3 and H4 HP, creating a transcriptionally permissive chromatin environment. Nicotine exposure to mouse primary cortical neuronal culture and lymphocyte culture resulted in decreased genomic levels of transcriptionally repressive H3K9me2 (Chase & Sharma, 2013). Our study demonstrates an increase in genomic levels of H3K18ac, H3ser10P, and H3K79me2 and concurrent decrease in H3ser28P following 5d nicotine exposure. Further quantitative analysis of these modifications and their association with gene promoter

regions is necessary to understand the biological significance of nicotine induced H3-PTM.

For stem cells to maintain a defined pluripotent state, it is necessary for controlled expression of genes involved in regulation of the transcriptional regulatory network in iPSC (Kunarso *et al*., 2010; Neph *et al*., 2012). STAT3, an acute phase response factor, is considered a key biological regulator of cellular proliferation, survival, and angiogenesis (Haghikia *et al*., 2014; Siveen *et al*., 2014). Expression array analyses of genes involved in transcription regulatory network in stem cells revealed an initial transcription up-regulation followed by subsequent downregulation of *STAT3* gene. Furthermore, phosphorylation of STAT3 is essential for its activation, and intrinsic biological activity. Evidence exists that nuclear translocation of STAT3 can occur despite its phosphorylation (Haghikia *et al*., 2014; Siveen *et al*., 2014; Yu *et al*., 2014). Previous studies have demonstrated that MS causes STAT3 activation and phosphorylation in mouse retinal endothelial cells and mesangial cells via OPRK1 receptors (Weber *et al*., 2013).

Our data demonstrate an inverse relationship between *STAT3* transcription and translation with MS exposure for shorter durations; continuous exposure to MS however, resulted in a shift of both transcription and translation relative to control. Hence, *STAT3* gene expression disruption occurs via distinct alterations to transcription and translation. These findings were further bolstered by observing the levels of STAT3-pTyr-705 and STAT3-pSer-727; namely -pTyr-705 was down-regulated with 5d MS exposure while -pSer-727 was suppressed with 2d MS exposure suggesting the influence of duration of MS exposure and consequent suppression of phosphorylated STAT3. Interestingly,

protein levels of STAT3, STAT3-pTyr-705 and -pSer-727 were not different from control following 3d recovery. Also, exposing cells to N prior to MS exposure reversed the MS-induced down-regulation of STAT3 and its phosphorylated forms, suggesting an OR-mediated effect.

OR genes *OPRM1*, *OPRD1* and *OPRK1* are expressed in all types of stem cells and their stimulation by endogenous and exogenous ligands is linked to several sub-cellular alterations (Carlo *et al*., 2003; Narita *et al*., 2006). Our results support down-regulation in mRNA levels of OR's. Moreover, the suppression of *OPRM1* mRNA was identified as most pronounced following MS exposure, compared to *OPRD1*, and *OPRK1*. However, suppression in ORs mRNA was more evident during early durations of MS exposure, followed by subsequent equalization in ORs mRNA levels to that of control. These results demonstrate that MS induced transcriptional suppression of ORs is related to both duration of exposure and concentration of MS. It is reasonable to apply these results to mimic the differences in clinical applications of opioids, depending on whether the drugs are used for short-term pain relief or longer-term dependency.

Non-differentiation and continual maintenance of pluripotency phenotype are critical to ensure survival and perpetuation of iPSC (Humphrey *et al*., 2004; James *et al*., 2005). Previous studies in our lab involving mES cells exposed to MS caused inhibition of neuronal differentiation via mu-opioid receptor activation (Dholakiya *et al*., 2016). In our current study, we observed MS-induced stimulation of pluripotency markers in iPSC with 2d and 11d MS exposure. The level of stem cell nuclear transcription factor OCT4 was lower but statistically insignificant from control on day 20 and not different from control on day 29. Cell surface stem cell marker TRA-1-60 was increased with 2d MS

exposure followed by a continuous decrease on days 11, 20, and 29 respectively, suggesting an apparent stimulation (or maintenance) of stem cell phenotype with shorter duration of MS exposure and reversing for longer durations. Interestingly, levels of observed markers were effectively blocked by pre-treating cells with N, signifying an OR-dependent pluripotent perturbation.

In conclusion, our study addresses the plausible potential of opioids to cause aberrations in EG H3-PTM and gene expression perturbations of *STAT3* in iPSC *in vitro*. The genotypic and phenotypic characteristics of iPSC involving substantial EG reprogramming with dynamic chromatin remodeling guiding their ability to differentiate into any cells of the three embryonic layers—ectoderm, endoderm and mesoderm—render them ideal for EG mechanistic studies (Goodnight *et al*., 2019; Ming-Tao *et al*., 2017). Interestingly, all sub-cellular effects identified in this study were not different from that of control following recovery, and in general, during prolonged periods of MS exposure, portending innate molecular compensatory repair mechanisms in iPSC that are yet to be delineated. Future studies may concentrate on mechanistic correlations between opioid receptor pathways and MS induced EG perturbations, and their heritable nature, further solidifying the biomarker premise.

REFERENCES

Baust, J. G., Snyder, K. K., Van Buskirk, R., & Baust, J. M. (2017). Integrating Molecular Control to Improve Cryopreservation Outcome. *Biopreservation and Biobanking*, *15*(2), 134–141. https://doi.org/10.1089/bio.2016.0119

Bernardo, A. S., Faial, T., Gardner, L., Niakan, K. K., Ortmann, D., Senner, C. E., Callery, E. M., Trotter, M. W., Hemberger, M., Smith, J. C., Bardwell, L., Moffett, A., & Pedersen, R. A. (2011). BRACHYURY and CDX2 Mediate BMP-Induced Differentiation of Human and Mouse Pluripotent Stem Cells into Embryonic and Extraembryonic Lineages. *Cell Stem Cell*, *9*(2), 144–155. https://doi.org/https://doi.org/10.1016/j.stem.2011.06.015

Berry, F. B., Lines, M. A., Oas, J. M., Footz, T., Underhill, D. A., Gage, P. J., & Walter, M. A. (2006). Functional interactions between FOXC1 and PITX2 underlie the sensitivity to FOXC1 gene dose in Axenfeld–Rieger syndrome and anterior segment dysgenesis. *Human Molecular Genetics*, *15*(6), 905–919. https://doi.org/10.1093/hmg/ddl008

Betts, B. C., Sagatys, E. M., Veerapathran, A., Lloyd, M. C., Beato, F., Lawrence, H. R., Yue, B., Kim, J., Sebti, S. M., Anasetti, C., & Pidala, J. (2015). CD4+ T cell STAT3 phosphorylation precedes acute GVHD, and subsequent Th17 tissue invasion correlates with GVHD severity and therapeutic response. *Journal of Leukocyte Biology*, *97*(4), 807–819. https://doi.org/10.1189/jlb.5A1114-532RR

Biswas, S., & Rao, C. M. (2018). Epigenetic tools (The Writers, The Readers and The Erasers) and their implications in cancer therapy. *European Journal of Pharmacology*, *837*, 8–24. https://doi.org/https://doi.org/10.1016/j.ejphar.2018.08.021

Boisvert, E. M., Engle, S. J., Hallowell, S. E., Liu, P., Wang, Z.-W., & Li, X.-J. (2015). The Specification and Maturation of Nociceptive Neurons from Human Embryonic Stem Cells. *Scientific Reports*, *5*(1), 16821. https://doi.org/10.1038/srep16821

Borromeo, M. D., Savage, T. K., Kollipara, R. K., He, M., Augustyn, A., Osborne, J. K., Girard, L., Minna, J. D., Gazdar, A. F., Cobb, M. H., & Johnson, J. E. (2016). ASCL1 and NEUROD1 Reveal Heterogeneity in Pulmonary Neuroendocrine Tumors and Regulate Distinct Genetic Programs. *Cell Reports*, *16*(5), 1259–1272. https://doi.org/https://doi.org/10.1016/j.celrep.2016.06.081

Browne, C. J., Godino, A., Salery, M., & Nestler, E. J. (2020). Epigenetic Mechanisms of Opioid Addiction. *Biological Psychiatry*, *87*(1), 22–33. https://doi.org/https://doi.org/10.1016/j.biopsych.2019.06.027

Cadet, J. L., McCoy, M. T., & Jayanthi, S. (2016). Epigenetics and addiction. *Clinical Pharmacology & Therapeutics*, *99*(5), 502–511. https://doi.org/10.1002/cpt.345

Cantley, W. L., Du, C., Lomoio, S., DePalma, T., Peirent, E., Kleinknecht, D., Hunter, M., Tang-Schomer, M. D., Tesco, G., & Kaplan, D. L. (2018). Functional and Sustainable 3D Human Neural Network Models from Pluripotent Stem Cells. *ACS Biomaterials Science & Engineering*, *4*(12), 4278–4288. https://doi.org/10.1021/acsbiomaterials.8b00622

Carlo, V., Elisabetta, Z., Emiliana, M., Marina, F., & Margherita, M. (2003). Protein Kinase C Signaling Transduces Endorphin-Primed Cardiogenesis in GTR1 Embryonic Stem Cells. *Circulation Research*, *92*(6), 617–622. https://doi.org/10.1161/01.RES.0000065168.31147.5B

Chapman, G., Remiszewski, J. L., Webb, G. C., Schulz, T. C., Bottema, C. D. K., & Rathjen, P. D. (1997). The Mouse Homeobox Gene,Gbx2:Genomic Organization and Expression in Pluripotent Cellsin Vitroandin Vivo. *Genomics*, *46*(2), 223–233. https://doi.org/https://doi.org/10.1006/geno.1997.4969

Charbord, J., Poydenot, P., Bonnefond, C., Feyeux, M., Casagrande, F., Brinon, B., Francelle, L., Aurégan, G., Guillermier, M., Cailleret, M., Viegas, P., Nicoleau, C., Martinat, C., Brouillet, E., Cattaneo, E., Peschanski, M., Lechuga, M., & Perrier, A. L. (2013). High throughput screening for inhibitors of REST in neural derivatives of human embryonic stem cells reveals a chemical compound that promotes expression of neuronal genes. *STEM CELLS*, *31*(9), 1816–1828. https://doi.org/10.1002/stem.1430

Chase, K. A., & Sharma, R. P. (2013). Nicotine induces chromatin remodelling through decreases in the methyltransferases GLP, G9a, Setdb1 and levels of H3K9me2. *International Journal of Neuropsychopharmacology*, *16*(5), 1129–1138. https://doi.org/10.1017/S1461145712001101

Chintalapati, A. J., & Barile, F. A. (2019). *Chapter 45 - Epigenetic Biomarkers in Toxicology* (R. C. B. T.-B. in T. (Second E. Gupta (ed.); pp. 823–839). Academic Press. https://doi.org/https://doi.org/10.1016/B978-0-12-814655-2.00045-1

Dan, J., Liu, Y., Liu, N., Chiourea, M., Okuka, M., Wu, T., Ye, X., Mou, C., Wang, L., Wang, L., Yin, Y., Yuan, J., Zuo, B., Wang, F., Li, Z., Pan, X., Yin, Z., Chen, L., Keefe, D. L., … Liu, L. (2014). Rif1 Maintains Telomere Length Homeostasis of ESCs by Mediating Heterochromatin Silencing. *Developmental Cell*, *29*(1), 7–19. https://doi.org/https://doi.org/10.1016/j.devcel.2014.03.004

Dholakiya, S. L., Aliberti, A., & Barile, F. A. (2016). Morphine sulfate concomitantly decreases neuronal differentiation and opioid receptor expression in mouse embryonic stem cells. *Toxicology Letters*, *247*, 45–55. https://doi.org/https://doi.org/10.1016/j.toxlet.2016.01.010

Eckmann-Scholz, C., Bens, S., Kolarova, J., Schneppenheim, S., Caliebe, A., Heidemann, S., von Kaisenberg, C., Kautza, M., Jonat, W., Siebert, R., & Ammerpohl, O. (2012). DNA-methylation profiling of fetal tissues reveals marked epigenetic differences between chorionic and amniotic samples. *PloS One*, *7*(6), e39014–e39014. https://doi.org/10.1371/journal.pone.0039014

Escamilla-Del-Arenal, M., da Rocha, S. T., Spruijt, C. G., Masui, O., Renaud, O., Smits, A. H., Margueron, R., Vermeulen, M., & Heard, E. (2013). Cdyl, a new partner of the inactive X chromosome and potential reader of H3K27me3 and H3K9me2. *Molecular and Cellular Biology*, *33*(24), 5005–5020. https://doi.org/10.1128/MCB.00866-13

Farris, S. P., Harris, R. A., & Ponomarev, I. (2015). Epigenetic modulation of brain gene networks for cocaine and alcohol abuse . In *Frontiers in Neuroscience* (Vol. 9, p. 176). https://www.frontiersin.org/article/10.3389/fnins.2015.00176

Fohn, L. E., & Behringer, R. R. (2001). ESX1L, a Novel X Chromosome-Linked Human Homeobox Gene Expressed in the Placenta and Testis. *Genomics*, *74*(1), 105–108. https://doi.org/https://doi.org/10.1006/geno.2001.6532

Fu, L.-Y., Jia, H.-L., Dong, Q.-Z., Wu, J.-C., Zhao, Y., Zhou, H.-J., Ren, N., Ye, Q.-H., & Qin, L.-X. (2009). Suitable reference genes for real-time PCR in human HBV-related hepatocellular carcinoma with different clinical prognoses. *BMC Cancer*, *9*(1), 49. https://doi.org/10.1186/1471-2407-9-49

Fujita, J., Tohyama, S., Kishino, Y., Okada, M., & Morita, Y. (2019). Concise Review: Genetic and Epigenetic Regulation of Cardiac Differentiation from Human Pluripotent Stem Cells. *STEM CELLS*, *37*(8), 992–1002. https://doi.org/10.1002/stem.3027

Gadhia, S. R., O'Brien, D., & Barile, F. A. (2015). Cadmium affects mitotically inherited histone modification pathways in mouse embryonic stem cells. *Toxicology in Vitro*, *30*(1, Part B), 583–592. https://doi.org/https://doi.org/10.1016/j.tiv.2015.11.001

Gao, F., Wei, Z., An, W., Wang, K., & Lu, W. (2013). The interactomes of POU5F1 and SOX2 enhancers in human embryonic stem cells. *Scientific Reports*, *3*(1), 1588. https://doi.org/10.1038/srep01588

Goodnight, A. V, Kremsky, I., Khampang, S., Jung, Y. H., Billingsley, J. M., Bosinger, S. E., Corces, V. G., & Chan, A. W. S. (2019). Chromatin accessibility and transcription dynamics during in vitro astrocyte differentiation of Huntington's Disease Monkey pluripotent stem cells. *Epigenetics & Chromatin*, *12*(1), 67. https://doi.org/10.1186/s13072-019-0313-6

Green, A. D., Vasu, S., & Flatt, P. R. (2018). Cellular models for beta-cell function and diabetes gene therapy. *Acta Physiologica*, *222*(3), 1. https://jerome.stjohns.edu/login?url=https://search.ebscohost.com/login.aspx?direct=true&db=s3h&AN=127900323&site=ehost-live

Gubern, C., Hurtado, O., Rodríguez, R., Morales, J. R., Romera, V. G., Moro, M. A., Lizasoain, I., Serena, J., & Mallolas, J. (2009). Validation of housekeeping genes for quantitative real-time PCR in in-vivo and in-vitro models of cerebral ischaemia. *BMC Molecular Biology*, *10*(1), 57. https://doi.org/10.1186/1471-2199-10-57

Guo, Y., Costa, R., Ramsey, H., Starnes, T., Vance, G., Robertson, K., Kelley, M., Reinbold, R., Scholer, H., & Hromas, R. (2002). The embryonic stem cell transcription factors Oct-4 and FoxD3 interact to regulate endodermal-specific promoter expression. *Proceedings of the National Academy of Sciences*, *99*(6), 3663 LP – 3667. https://doi.org/10.1073/pnas.062041099

Guye, P., Ebrahimkhani, M. R., Kipniss, N., Velazquez, J. J., Schoenfeld, E., Kiani, S., Griffith, L. G., & Weiss, R. (2016). Genetically engineering self-organization of human pluripotent stem cells into a liver bud-like tissue using Gata6. *Nature Communications*, *7*(1), 10243. https://doi.org/10.1038/ncomms10243

Haghikia, A., Ricke-Hoch, M., Stapel, B., Gorst, I., & Hilfiker-Kleiner, D. (2014). STAT3, a key regulator of cell-to-cell communication in the heart. *Cardiovascular Research*, *102*(2), 281–289. https://doi.org/10.1093/cvr/cvu034

Heard, E., & Martienssen, R. A. (2014). Transgenerational Epigenetic Inheritance: Myths and Mechanisms. *Cell*, *157*(1), 95–109. https://doi.org/https://doi.org/10.1016/j.cell.2014.02.045

Heller, E. A., Hamilton, P. J., Burek, D. D., Lombroso, S. I., Peña, C. J., Neve, R. L., & Nestler, E. J. (2016). Targeted Epigenetic Remodeling of the Cdk5 Gene in Nucleus Accumbens Regulates Cocaine- and Stress-Evoked Behavior. *The Journal of Neuroscience*, *36*(17), 4690 LP – 4697. https://doi.org/10.1523/JNEUROSCI.0013-16.2016

Herz, H.-M., Morgan, M., Gao, X., Jackson, J., Rickels, R., Swanson, S. K., Florens, L., Washburn, M. P., Eissenberg, J. C., & Shilatifard, A. (2014). Histone H3 lysine-to-methionine mutants as a paradigm to study chromatin signaling. *Science*, *345*(6200), 1065 LP – 1070. https://doi.org/10.1126/science.1255104

Humphrey, R. K., Beattie, G. M., Lopez, A. D., Bucay, N., King, C. C., Firpo, M. T., Rose-John, S., & Hayek, A. (2004). Maintenance of Pluripotency in Human Embryonic Stem Cells Is STAT3 Independent. *STEM CELLS*, *22*(4), 522–530. https://doi.org/10.1634/stemcells.22-4-522

Hyun, K., Jeon, J., Park, K., & Kim, J. (2017). Writing, erasing and reading histone lysine methylations. *Experimental & Molecular Medicine*, *49*(4), e324–e324. https://doi.org/10.1038/emm.2017.11

James, D., Levine, A. J., Besser, D., & Hemmati-Brivanlou, A. (2005). TGFβ/activin/nodal signaling is necessary for the maintenance of pluripotency in human embryonic stem cells. *Development*, *132*(6), 1273 LP – 1282. https://doi.org/10.1242/dev.01706

Kaliman, P., Álvarez-López, M. J., Cosín-Tomás, M., Rosenkranz, M. A., Lutz, A., & Davidson, R. J. (2014). Rapid changes in histone deacetylases and inflammatory gene expression in expert meditators. *Psychoneuroendocrinology*, *40*, 96–107. https://doi.org/https://doi.org/10.1016/j.psyneuen.2013.11.004

Kenny, P. J. (2014). Epigenetics, microRNA, and addiction. *Dialogues in Clinical Neuroscience*, *16*(3), 335–344. https://www.ncbi.nlm.nih.gov/pubmed/25364284

Kreek, M. J. (1996). Opiates, opioids and addiction. *Molecular Psychiatry*, *1*(3), 232–254.

Kuchipudi, S. V, Tellabati, M., Nelli, R. K., White, G. A., Perez, B. B., Sebastian, S., Slomka, M. J., Brookes, S. M., Brown, I. H., Dunham, S. P., & Chang, K.-C. (2012). 18S rRNAis a reliable normalisation gene for real time PCR based on influenza virus infected cells. *Virology Journal*, *9*(1), 230. https://doi.org/10.1186/1743-422X-9-230

Kumar, A., Declercq, J., Eggermont, K., Agirre, X., Prosper, F., & Verfaillie, C. M. (2012). Zic3 induces conversion of human fibroblasts to stable neural progenitor-like cells. *Journal of Molecular Cell Biology*, *4*(4), 252–255. https://doi.org/10.1093/jmcb/mjs015

Kumarswamy, R., Volkmann, I., & Thum, T. (2011). Regulation and function of miRNA-21 in health and disease. *RNA Biology*, *8*(5), 706–713. https://doi.org/10.4161/rna.8.5.16154

Kunarso, G., Chia, N.-Y., Jeyakani, J., Hwang, C., Lu, X., Chan, Y.-S., Ng, H.-H., & Bourque, G. (2010). Transposable elements have rewired the core regulatory network of human embryonic stem cells. *Nature Genetics*, *42*(7), 631–634. https://doi.org/10.1038/ng.600

La Manno, G., Gyllborg, D., Codeluppi, S., Nishimura, K., Salto, C., Zeisel, A., Borm, L. E., Stott, S. R. W., Toledo, E. M., Villaescusa, J. C., Lönnerberg, P., Ryge, J., Barker, R. A., Arenas, E., & Linnarsson, S. (2016). Molecular Diversity of Midbrain Development in Mouse, Human, and Stem Cells. *Cell*, *167*(2), 566-580.e19. https://doi.org/https://doi.org/10.1016/j.cell.2016.09.027

Landeira, D., Sauer, S., Poot, R., Dvorkina, M., Mazzarella, L., Jørgensen, H. F., Pereira, C. F., Leleu, M., Piccolo, F. M., Spivakov, M., Brookes, E., Pombo, A., Fisher, C., Skarnes, W. C., Snoek, T., Bezstarosti, K., Demmers, J., Klose, R. J., Casanova, M., … Fisher, A. G. (2010). Jarid2 is a PRC2 component in embryonic stem cells required for multi-lineage differentiation and recruitment of PRC1 and RNA Polymerase II to developmental regulators. *Nature Cell Biology*, *12*(6), 618–624. https://doi.org/10.1038/ncb2065

Lankenau, S. E., Teti, M., Silva, K., Bloom, J. J., Harocopos, A., & Treese, M. (2012). Initiation into prescription opioid misuse amongst young injection drug users. *International Journal of Drug Policy*, *23*(1), 37–44. https://doi.org/https://doi.org/10.1016/j.drugpo.2011.05.014

Larsen, K. B., Lutterodt, M. C., Møllgård, K., & Møller, M. (2010). Expression of the Homeobox Genes OTX2 and OTX1 in the Early Developing Human Brain. *Journal of Histochemistry & Cytochemistry*, *58*(7), 669–678. https://doi.org/10.1369/jhc.2010.955757

Lavado, A., & Oliver, G. (2011). Six3 is required for ependymal cell maturation. *Development*, *138*(24), 5291 LP – 5300. https://doi.org/10.1242/dev.067470

Lawrence, M., Daujat, S., & Schneider, R. (2016). Lateral Thinking: How Histone Modifications Regulate Gene Expression. *Trends in Genetics*, *32*(1), 42–56. https://doi.org/https://doi.org/10.1016/j.tig.2015.10.007

Lester, B. M., Tronick, E., Nestler, E., Abel, T., Kosofsky, B., Kuzawa, C. W., Marsit, C. J., Maze, I., Meaney, M. J., Monteggia, L. M., Reul, J. M. H. M., Skuse, D. H., Sweatt, J. D., & Wood, M. A. (2011). Behavioral epigenetics. *Annals of the New York Academy of Sciences*, *1226*, 14–33. https://doi.org/10.1111/j.1749-6632.2011.06037.x

Li, B.-Z., Huang, Z., Cui, Q.-Y., Song, X.-H., Du, L., Jeltsch, A., Chen, P., Li, G., Li, E., & Xu, G.-L. (2011). Histone tails regulate DNA methylation by allosterically activating de novo methyltransferase. *Cell Research*, *21*(8), 1172–1181. https://doi.org/10.1038/cr.2011.92

Li, O., Li, J., & Dröge, P. (2007). DNA architectural factor and proto-oncogene HMGA2 regulates key developmental genes in pluripotent human embryonic stem cells. *FEBS Letters*, *581*(18), 3533–3537. https://doi.org/https://doi.org/10.1016/j.febslet.2007.06.072

Liang, D.-Y., Li, X., & Clark, J. D. (2013). Epigenetic Regulation of Opioid-Induced Hyperalgesia, Dependence, and Tolerance in Mice. *The Journal of Pain*, *14*(1), 36–47. https://doi.org/https://doi.org/10.1016/j.jpain.2012.10.005

Ming-Tao, Z., Ning-Yi, S., Shijun, H., Ning, M., Rajini, S., Fereshteh, J., Jaecheol, L., L., Z. S., P., S. M., & C., W. J. (2017). Cell Type-Specific Chromatin Signatures Underline Regulatory DNA Elements in Human Induced Pluripotent Stem Cells and Somatic Cells. *Circulation Research*, *121*(11), 1237–1250. https://doi.org/10.1161/CIRCRESAHA.117.311367

Mohn, F., & Schübeler, D. (2009). Genetics and epigenetics: stability and plasticity during cellular differentiation. *Trends in Genetics*, *25*(3), 129–136. https://doi.org/https://doi.org/10.1016/j.tig.2008.12.005

Mosmann, T. (1983). Rapid colorimetric assay for cellular growth and survival: Application to proliferation and cytotoxicity assays. *Journal of Immunological Methods*, *65*(1), 55–63. https://doi.org/https://doi.org/10.1016/0022-1759(83)90303-4

Mulligan, P., Westbrook, T. F., Ottinger, M., Pavlova, N., Chang, B., Macia, E., Shi, Y.-J., Barretina, J., Liu, J., Howley, P. M., Elledge, S. J., & Shi, Y. (2008). CDYL Bridges REST and Histone Methyltransferases for Gene Repression and Suppression of Cellular Transformation. *Molecular Cell*, *32*(5), 718–726. https://doi.org/https://doi.org/10.1016/j.molcel.2008.10.025

Narita, M., Kuzumaki, N., Miyatake, M., Sato, F., Wachi, H., Seyama, Y., & Suzuki, T. (2006). Role of δ-opioid receptor function in neurogenesis and neuroprotection. *Journal of Neurochemistry*, *97*(5), 1494–1505. https://doi.org/10.1111/j.1471-4159.2006.03849.x

Neph, S., Stergachis, A. B., Reynolds, A., Sandstrom, R., Borenstein, E., & Stamatoyannopoulos, J. A. (2012). Circuitry and Dynamics of Human Transcription Factor Regulatory Networks. *Cell*, *150*(6), 1274–1286. https://doi.org/https://doi.org/10.1016/j.cell.2012.04.040

Ng, N. H. J., Jasmen, J. B., Lim, C. S., Lau, H. H., Krishnan, V. G., Kadiwala, J., Kulkarni, R. N., Ræder, H., Vallier, L., Hoon, S., & Teo, A. K. K. (2019). HNF4A Haploinsufficiency in MODY1 Abrogates Liver and Pancreas Differentiation from Patient-Derived Induced Pluripotent Stem Cells. *IScience*, *16*, 192–205. https://doi.org/https://doi.org/10.1016/j.isci.2019.05.032

Nguyen, L. X. T., Raval, A., Garcia, J. S., & Mitchell, B. S. (2015). Regulation of Ribosomal Gene Expression in Cancer. *Journal of Cellular Physiology*, *230*(6), 1181–1188. https://doi.org/10.1002/jcp.24854

Oertel, B. G., Doehring, A., Roskam, B., Kettner, M., Hackmann, N., Ferreirós, N., Schmidt, P. H., & Lötsch, J. (2012). Genetic–epigenetic interaction modulates μ-opioid receptor regulation. *Human Molecular Genetics*, *21*(21), 4751–4760. https://doi.org/10.1093/hmg/dds314

Pevny, L. H., & Nicolis, S. K. (2010). Sox2 roles in neural stem cells. *The International Journal of Biochemistry & Cell Biology*, *42*(3), 421–424. https://doi.org/https://doi.org/10.1016/j.biocel.2009.08.018

Pfeiffer, M. J., Quaranta, R., Piccini, I., Fell, J., Rao, J., Röpke, A., Seebohm, G., & Greber, B. (2018). Cardiogenic programming of human pluripotent stem cells by dose-controlled activation of EOMES. *Nature Communications*, *9*(1), 440. https://doi.org/10.1038/s41467-017-02812-6

Powell, D., Pacula, R. L., & Taylor, E. (2020). How increasing medical access to opioids contributes to the opioid epidemic: Evidence from Medicare Part D. *Journal of Health Economics*, *71*, 102286. https://doi.org/https://doi.org/10.1016/j.jhealeco.2019.102286

Pozzi, S., Bowling, S., Apps, J., Brickman, J. M., Rodriguez, T. A., & Martinez-Barbera, J. P. (2019). Genetic Deletion of Hesx1 Promotes Exit from the Pluripotent State and Impairs Developmental Diapause. *Stem Cell Reports*, *13*(6), 970–979. https://doi.org/https://doi.org/10.1016/j.stemcr.2019.10.014

Qin, S., Ware, S. M., Waclaw, R. R., & Campbell, K. (2017). Septal contributions to olfactory bulb interneuron diversity in the embryonic mouse telencephalon: role of the homeobox gene Gsx2. *Neural Development*, *12*(1), 13. https://doi.org/10.1186/s13064-017-0090-5

Quinn, J. J., & Chang, H. Y. (2016). Unique features of long non-coding RNA biogenesis and function. *Nature Reviews Genetics*, *17*(1), 47–62. https://doi.org/10.1038/nrg.2015.10

Rao, X., Huang, X., Zhou, Z., & Lin, X. (2013). An improvement of the 2ˆ(-delta delta CT) method for quantitative real-time polymerase chain reaction data analysis. *Biostatistics, Bioinformatics and Biomathematics*, *3*(3), 71–85. https://www.ncbi.nlm.nih.gov/pubmed/25558171

Roson-Burgo, B., Sanchez-Guijo, F., Del Cañizo, C., & De Las Rivas, J. (2014). Transcriptomic portrait of human Mesenchymal Stromal/Stem cells isolated from bone marrow and placenta. *BMC Genomics*, *15*(1), 910. https://doi.org/10.1186/1471-2164-15-910

Sapkota, D., Chintala, H., Wu, F., Fliesler, S. J., Hu, Z., & Mu, X. (2014). Onecut1 and Onecut2 redundantly regulate early retinal cell fates during development. *Proceedings of the National Academy of Sciences*, *111*(39), E4086 LP-E4095. https://doi.org/10.1073/pnas.1405354111

Schvartzman, J. M., Thompson, C. B., & Finley, L. W. S. (2018). Metabolic regulation of chromatin modifications and gene expression. *Journal of Cell Biology*, *217*(7), 2247–2259. https://doi.org/10.1083/jcb.201803061

Sharma, A. (2017). Transgenerational epigenetics: Integrating soma to germline communication with gametic inheritance. *Mechanisms of Ageing and Development*, *163*, 15–22. https://doi.org/https://doi.org/10.1016/j.mad.2016.12.015

Shenoy, S. S., & Lui, F. (2019). *Biochemistry, Endogenous Opioids*. StatPearls Publishing, Treasure Island (FL).

Shi, Z.-D., Lee, K., Yang, D., Amin, S., Verma, N., Li, Q. V, Zhu, Z., Soh, C.-L., Kumar, R., Evans, T., Chen, S., & Huangfu, D. (2017). Genome Editing in hPSCs Reveals GATA6 Haploinsufficiency and a Genetic Interaction with GATA4 in Human Pancreatic Development. *Cell Stem Cell*, *20*(5), 675-688.e6. https://doi.org/https://doi.org/10.1016/j.stem.2017.01.001

Sierra, R. A., Hoverter, N. P., Ramirez, R. N., Vuong, L. M., Mortazavi, A., Merrill, B. J., Waterman, M. L., & Donovan, P. J. (2018). TCF7L1 suppresses primitive streak gene expression to support human embryonic stem cell pluripotency. *Development*, *145*(4), dev161075. https://doi.org/10.1242/dev.161075

Sigova, A. A., Mullen, A. C., Molinie, B., Gupta, S., Orlando, D. A., Guenther, M. G., Almada, A. E., Lin, C., Sharp, P. A., Giallourakis, C. C., & Young, R. A. (2013). Divergent transcription of long noncoding RNA/mRNA gene pairs in embryonic stem cells. *Proceedings of the National Academy of Sciences*, *110*(8), 2876 LP – 2881. https://doi.org/10.1073/pnas.1221904110

Siveen, K. S., Sikka, S., Surana, R., Dai, X., Zhang, J., Kumar, A. P., Tan, B. K. H., Sethi, G., & Bishayee, A. (2014). Targeting the STAT3 signaling pathway in cancer: Role of synthetic and natural inhibitors. *Biochimica et Biophysica Acta (BBA) - Reviews on Cancer*, *1845*(2), 136–154. https://doi.org/https://doi.org/10.1016/j.bbcan.2013.12.005

Skolnick, P. (2018). The Opioid Epidemic: Crisis and Solutions. *Annual Review of Pharmacology and Toxicology*, *58*(1), 143–159. https://doi.org/10.1146/annurev-pharmtox-010617-052534

Smith, Z. D., & Meissner, A. (2013). DNA methylation: roles in mammalian development. *Nature Reviews Genetics*, *14*(3), 204–220. https://doi.org/10.1038/nrg3354

Takahashi, K., Tanabe, K., Ohnuki, M., Narita, M., Ichisaka, T., Tomoda, K., & Yamanaka, S. (2007). Induction of Pluripotent Stem Cells from Adult Human Fibroblasts by Defined Factors. *Cell*, *131*(5), 861–872. https://doi.org/https://doi.org/10.1016/j.cell.2007.11.019

Toegel, S., Huang, W., Piana, C., Unger, F. M., Wirth, M., Goldring, M. B., Gabor, F., & Viernstein, H. (2007). Selection of reliable reference genes for qPCR studies on chondroprotective action. *BMC Molecular Biology*, *8*(1), 13.

https://doi.org/10.1186/1471-2199-8-13
Toth, A. R., Possidente, C. J., Sawyer, L. M., DiParlo, M. A., & Fanciullo, G. J. (2016). National and Northern New England Opioid Prescribing Patterns, 2013–2014. *Pain Medicine*, *18*(9), 1706–1714. https://doi.org/10.1093/pm/pnw231

Wachman, E. M., Hayes, M. J., Lester, B. M., Terrin, N., Brown, M. S., Nielsen, D. A., & Davis, J. M. (2014). Epigenetic Variation in the Mu-Opioid Receptor Gene in Infants with Neonatal Abstinence Syndrome. *The Journal of Pediatrics*, *165*(3), 472–478. https://doi.org/https://doi.org/10.1016/j.jpeds.2014.05.040

Wang, H., Liu, C., Liu, X., Wang, M., Wu, D., Gao, J., Su, P., Nakahata, T., Zhou, W., Xu, Y., Shi, L., Ma, F., & Zhou, J. (2018). MEIS1 Regulates Hemogenic Endothelial Generation, Megakaryopoiesis, and Thrombopoiesis in Human Pluripotent Stem Cells by Targeting TAL1 and FLI1. *Stem Cell Reports*, *10*(2), 447–460. https://doi.org/https://doi.org/10.1016/j.stemcr.2017.12.017

Wang, Y.-C., Stein, J. W., Lynch, C. L., Tran, H. T., Lee, C.-Y., Coleman, R., Hatch, A., Antontsev, V. G., Chy, H. S., O'Brien, C. M., Murthy, S. K., Laslett, A. L., Peterson, S. E., & Loring, J. F. (2015). Glycosyltransferase ST6GAL1 contributes to the regulation of pluripotency in human pluripotent stem cells. *Scientific Reports*, *5*(1), 13317. https://doi.org/10.1038/srep13317

Wang, Z., Oron, E., Nelson, B., Razis, S., & Ivanova, N. (2012). Distinct Lineage Specification Roles for NANOG, OCT4, and SOX2 in Human Embryonic Stem Cells. *Cell Stem Cell*, *10*(4), 440–454. https://doi.org/https://doi.org/10.1016/j.stem.2012.02.016

Weber, D., Heisig, J., Kneitz, S., Wolf, E., Eilers, M., & Gessler, M. (2015). Mechanisms of epigenetic and cell-type specific regulation of Hey target genes in ES cells and cardiomyocytes. *Journal of Molecular and Cellular Cardiology*, *79*, 79–88. https://doi.org/https://doi.org/10.1016/j.yjmcc.2014.11.004

Weber, M. L., Chen, C., Li, Y., Farooqui, M., Nguyen, J., Poonawala, T., Hebbel, R. P., & Gupta, K. (2013). Morphine stimulates platelet-derived growth factor receptor-β signalling in mesangial cells in vitro and transgenic sickle mouse kidney in vivo. *BJA: British Journal of Anaesthesia*, *111*(6), 1004–1012. https://doi.org/10.1093/bja/aet221

Wu, J., Hunt, S. D., Xue, H., Liu, Y., & Darabi, R. (2016). Generation and Characterization of a MYF5 Reporter Human iPS Cell Line Using CRISPR/Cas9 Mediated Homologous Recombination. *Scientific Reports*, *6*(1), 18759. https://doi.org/10.1038/srep18759

Wu, W., Bhagat, T. D., Yang, X., Song, J. H., Cheng, Y., Agarwal, R., Abraham, J. M., Ibrahim, S., Bartenstein, M., Hussain, Z., Suzuki, M., Yu, Y., Chen, W., Eng, C., Greally, J., Verma, A., & Meltzer, S. J. (2013). Hypomethylation of Noncoding

DNA Regions and Overexpression of the Long Noncoding RNA, AFAP1-AS1, in Barrett's Esophagus and Esophageal Adenocarcinoma. *Gastroenterology*, *144*(5), 956-966.e4. https://doi.org/10.1053/j.gastro.2013.01.019

Xiang, Q., Liao, Y., Chao, H., Huang, W., Liu, J., Chen, H., Hong, D., Zou, Z., Xiang, A. P., & Li, W. (2018). ISL1 overexpression enhances the survival of transplanted human mesenchymal stem cells in a murine myocardial infarction model. *Stem Cell Research & Therapy*, *9*(1), 51. https://doi.org/10.1186/s13287-018-0803-7

Xiao, S., Lu, J., Sridhar, B., Cao, X., Yu, P., Zhao, T., Chen, C.-C., McDee, D., Sloofman, L., Wang, Y., Rivas-Astroza, M., Telugu, B. P. V. L., Levasseur, D., Zhang, K., Liang, H., Zhao, J. C., Tanaka, T. S., Stormo, G., & Zhong, S. (2017). SMARCAD1 Contributes to the Regulation of Naive Pluripotency by Interacting with Histone Citrullination. *Cell Reports*, *18*(13), 3117–3128. https://doi.org/https://doi.org/10.1016/j.celrep.2017.02.070

Yang, A. Y., Kim, H., Li, W., & Kong, A.-N. T. (2016). Natural compound-derived epigenetic regulators targeting epigenetic readers, writers and erasers. *Current Topics in Medicinal Chemistry*, *16*(7), 697–713. https://doi.org/10.2174/1568026615666150826114359

Yang, J., Gao, C., Chai, L., & Ma, Y. (2010). A Novel SALL4/OCT4 Transcriptional Feedback Network for Pluripotency of Embryonic Stem Cells. *PLOS ONE*, *5*(5), e10766. https://doi.org/10.1371/journal.pone.0010766

Yang, W., Xia, Y., Hawke, D., Li, X., Liang, J., Xing, D., Aldape, K., Hunter, T., Alfred Yung, W. K., & Lu, Z. (2012). PKM2 Phosphorylates Histone H3 and Promotes Gene Transcription and Tumorigenesis. *Cell*, *150*(4), 685–696. https://doi.org/https://doi.org/10.1016/j.cell.2012.07.018

Yu, H., Lee, H., Herrmann, A., Buettner, R., & Jove, R. (2014). Revisiting STAT3 signalling in cancer: new and unexpected biological functions. *Nature Reviews Cancer*, *14*(11), 736–746. https://doi.org/10.1038/nrc3818

Zhang, L.-H., Yin, A.-A., Cheng, J.-X., Huang, H.-Y., Li, X.-M., Zhang, Y.-Q., Han, N., & Zhang, X. (2015). TRIM24 promotes glioma progression and enhances chemoresistance through activation of the PI3K/Akt signaling pathway. *Oncogene*, *34*(5), 600–610. https://doi.org/10.1038/onc.2013.593

Zhang, Q.-J., & Liu, Z.-P. (2015). Histone methylations in heart development, congenital and adult heart diseases. *Epigenomics*, *7*(2), 321–330. https://doi.org/10.2217/epi.14.60

Zhang, X., Huang, C. T., Chen, J., Pankratz, M. T., Xi, J., Li, J., Yang, Y., LaVaute, T. M., Li, X.-J., Ayala, M., Bondarenko, G. I., Du, Z.-W., Jin, Y., Golos, T. G., & Zhang, S.-C. (2010). Pax6 Is a Human Neuroectoderm Cell Fate Determinant. *Cell*

Stem Cell, *7*(1), 90–100. https://doi.org/https://doi.org/10.1016/j.stem.2010.04.017

Zhang, Z. H., Li, M. Y., Wang, Z., Zuo, H. X., Wang, J. Y., Xing, Y., Jin, C., Xu, G., Piao, L., Piao, H., Ma, J., & Jin, X. (2020). Convallatoxin promotes apoptosis and inhibits proliferation and angiogenesis through crosstalk between JAK2/STAT3 (T705) and mTOR/STAT3 (S727) signaling pathways in colorectal cancer. *Phytomedicine*, *68*, 153172. https://doi.org/https://doi.org/10.1016/j.phymed.2020.153172

Zhou, J.-L., Deng, S., Fang, H.-S., Yu, G., & Peng, H. (2019). Hsa-let-7g promotes osteosarcoma by reducing HOXB1 to activate NF-kB pathway. *Biomedicine & Pharmacotherapy*, *109*, 2335–2341. https://doi.org/https://doi.org/10.1016/j.biopha.2018.11.026

VITA

Name:	Anirudh J. Chintalapati
Elementary School:	Bhashyam Public School, Andhra Pradesh, India
High School:	Sri Chaitanya Junior college, Andhra Pradesh, India
Date Graduated:	March 2009
Baccalaureate Degree:	PharmD., Andhra University, Andhra Pradesh, India
Date Graduated:	December 2015
Other Degrees:	Master of Science, Pharmaceutical Sciences, St. John's University College of Pharmacy and Health Sciences, Queens, NY, USA
Date Graduated:	November 2017